Oxidative conversion of lower alkanes to olefins

László Leveles

Leden van de promotiecommissie:

Voorzitter/Secretaris:	Prof. dr. ir. J.H.A. de Smit
Promotor:	Prof. dr. ir. L. Lefferts
Promotor:	Prof. dr. J.A. Lercher
Co-Promotor:	Dr. K Seshan
Leden:	Prof. dr. ir. G.F. Versteeg
	Prof. dr. ir. J.A.M. Kuipers
	Prof. dr. ir. G. Marin
	Prof. dr. ir. A. Bliek
	Dr. E. Grotendorst
Deskundige:	Prof dr. ir. F. Dautzenberg

This work has been carried out under the auspices of the Netherlands Institute for Catalysis Research (NIOK) and the Process-technology Institute Twente (PIT). The work was financially supported by STW/NWO under project nr. 349-4428.

ISBN 90-365-1744-3

© László Leveles, Enschede, The Netherlands, 2002

Printed by PrintPartners Ipskamp, Enschede

OXIDATIVE CONVERSION OF LOWER ALKANES TO OLEFINS

PROEFSCHRIFT

ter verkrijging van
de graad van doctor aan de Universiteit Twente,
op gezag van de rector magnificus,
prof.dr. F.A. van Vught,
volgens besluit van het College voor Promoties
in het openbaar te verdedigen
op donderdag 30 mei 2002 te 13:15 uur

door
László Leveles
geboren op 1 april 1972
te Csíkkarcfalva/Cîrța, Roemenië

Dit proefschrift is goedgekeurd door de promotors
Prof. dr. ir. L. Lefferts en *Prof. dr. J. A. Lercher*
en de assistent promotor
dr. K. Seshan

Nothing is created or destroyed… only the shape can change

to all my family: present and passed

Acknowledgements

It is prime time to look back over the four nice years spent in the Netherlands, and it is the place here to say thanks to those who contributed to making my stay here as pleasant and meaningful as possible. To make it a bit chronological, I would like to express my sincere gratitude to all members of the Faculty of Chemistry and Chemical Engineering of the Babeş-Bolyai University, namely Jenő Bódis, Csaba Bolla, Csaba Muzsnay, Liviu Oniciu and others who helped me with information or supported me otherwise in order to be able to do this study abroad.

This four years experience, or rather call it adventure, was just an elusive dream, had Prof. dr. J.A. Lercher not offered me a place in the pool of his PhD students. Thank you, Johannes for having trusted in me, even though I had little experience in catalysis before coming here, and thanks for the clear arguments and ideas during our discussions.

If this thesis can be considered by any means a success, that has to do a lot with Prof. dr. ir. Leon Lefferts, his leadership, his bird-eye view on the subject and application oriented critical approach that helped me to summarize only the relevant information in this work. Thank you Leon for your guidance and, why not recognize, your smart, human influence of my work and of the project pathway.

It would not have been possible or would have been very difficult to finish these four years without the helpfulness and patience of dr. K. Seshan, who managed to be a work-leader and become a friend at the same time. Thank you Seshan for proving me that life is ultimately a very simple thing and we should not worry too much about certain things.

Having been accepted in a this colorful group four years ago, it is needless to say that it was a fine feeling to be the colleague of people from so many countries, so many cultures. I have to say that the Netherlands was a window to the world for me, and that has to do a lot with the composition of our group. At the beginning while staying apart from my family I had a flashback to my student times, it was nice to go out to the city for a couple of beer or race on bicycle for a movie, then dance on the table or go to a party or other social event somewhere. Thank you for embracing me with friendship. I cannot go further without mentioning a couple of people both related to the work and the social aspects of my life: Gerhard, László, Gautam, Sergio, Andre, Laurent, J.P., Martijn, Martin, Viktor, Sheila, Katia, Cristina, Olivier, Javier and others for things like introducing me to the lab(irinth), for improving my show-up skills, for the various parties and dinners, for a common interest in downloading as much music as possible, for sharing the room and chicken-pox for a while, for the nasty e-mail jokes, etc.; thank you all as well as the people of Munich and everybody whose name is not on this "blacklist". I owe a special thanks to dr. Stefan Fuchs whose contribution added to the content and value of my thesis.

I should not forget the countless number of students that kept the mood of the group high for short times, especially the three students that worked with me, I think they deserve a very special thanks as they have contributed an awful lot to this thesis: David, whose ambition made it possible to screen through the periodic system, Itziar, whose loyalty gave me the freedom to only plan experiments and seldom look after, and Heike, whose discipline and ambition made me feel I have the extension of my own hands working in the lab with unbelievable efficiency.

And let me thank finally my present colleagues: Marco for being the most lasting colleague of mine and for the various (lengthy) discussions about all imaginable subjects, Valer for having the same east-Carpathian-basin heritage and discussing the issues back home, Igor for sharing a room and a number of scientific and technical problems for a while, Nabil for his efforts to make me become tax-advisor, Mujeebur and Zhu for their trying to inherit the experience in measurements automation and CSW, further Li, Jiang, Sepp, Dejan, Thomas, Anna and everybody once more for the company by the coffee table and by the borrels, offering me a sharp insight to the various cultures they come from during the discussions we had. The members of the permanent staff deserve a special thanks: Bert for being the voodoo of all known and unknown problems, Cis for being the nicest and at the same time the most efficient secretary I've ever seen, Karin for her enthusiasm for letting me know what was allowed in the lab and what not, Vilmos for being always ready to exchange a bottle, Barbara for the struggle to make this group socially disciplined and Jan for never letting the fire of any discussion to extinct by having always the last word. I would like to express my sincere gratitude to Ulrich K., whose edgy comments, declined slightly towards negativity, represented the first critical look on my work. Thanks for the technicians of the CT, especially Henk Jan and Benno, and thank everybody from the university who contributed the slightest bit to this work.

The contribution of the project's user-committee constituted probably the most relevant feedback from the outside. I would like to thank everybody who has been part of the user-committee for his or her interest and help.

Outside work I happened to find a cordial friend circle partially related to my home country and also formed through our children and other contacts. Friends in Enschede, surroundings and the whole Netherlands thank you to let me feel home in this country. Vrienden in Enschede, omgeving en door het hele Nederland bedankt voor jullie gezelschap en voor de thuisgevoel in dit land.

And now I would like to express my deep gratitude for my parents and parents-in-low for their unconditional support and love in whatever I was going to do, and their understanding and not trying to hold me back from going to abroad.

And last, but most importantly, there are no words that can express my feelings for my wife Ibolya and my children Boriska and Péter. Without you, your support and understanding, this work not only could not have been fulfilled properly, but it would also not make sense for me!

László Leveles

May 2002

Table of contents

1 Introduction *11*

1.1 Objectives and justification 11

1.2 Current methods of olefin production 12
1.2.1 Steam cracking 12
1.2.1.1 Mechanism of cracking 14
1.2.2 Catalytic cracking 16
1.2.3 Catalytic dehydrogenation 18

1.3 Oxidative methods for olefin production 19
1.3.1 Oxidative dehydrogenation (ODH) 20
1.3.1.1 Redox catalysis 20
1.3.1.2 Non-redox catalysis 20
1.3.1.3 Noble metal catalysis 21
1.3.1.4 Non-catalytic reactions 21
1.3.2 Oxidative coupling 21

2 Experimental details *23*

2.1 Introduction 23

2.2 Materials used 23

2.3 Catalyst preparation 23

2.4 Catalytic measurements 24
2.4.1 Kinetic setup 24
2.4.2 Evaluation of kinetic data 25

2.5 Characterization 26
2.5.1 Bulk characterization 26
2.5.1.1 Elemental analysis 26
2.5.1.2 XRD measurements 26
2.5.2 Surface characterization 26
2.5.2.1 Surface area and porosity measurements 26
2.5.2.2 TPD measurements 26
2.5.2.3 TGA measurements 27
2.5.2.4 XPS measurements 27

3 Oxidative conversion of light alkanes to olefins over alkali promoted oxide catalysts *29*

3.1 Introduction 29

3.2 Experimental 29
3.2.1 Catalyst preparation 29
3.2.2 Catalytic measurements 30
3.2.3 Catalyst characterization 30

3.3 Results **31**
3.3.1 Influence of support 31
3.3.2 Catalytic functions of Li, Dy and Cl 33
3.3.3 Temperature programmed desorption (TPD) 34

3.4 Discussion **35**
3.4.1 Influence of support on catalytic performance in n-butane oxidative conversion 35
3.4.2 Catalytic functions of Li, Dy and Cl 35
3.4.3 Reaction pathways 36
3.4.4 Performance comparison with industrial routes to olefins 37

3.5 Conclusions **38**

4 Promoter effect in the oxidative dehydrogenation and cracking of ethane and propane over Li-Dy-Mg mixed oxides ***41***

4.1 Introduction **41**

4.2 Experimental **42**
4.2.1 Catalyst preparation 42
4.2.2 Temperature programmed desorption (TPD) 42
4.2.3 Kinetic measurements 42

4.3 Results and Discussion **43**
4.3.1 Acid-base characterization of the materials 43
4.3.1.1 TPD of ammonia 43
4.3.1.2 TPD of carbon dioxide 44
4.3.2 Kinetic measurements 45
4.3.2.1 The influence of the chloride content 45
4.3.2.2 The influence of the Li content 46
4.3.2.3 The reaction network 47
4.3.2.4 Influence of the reaction conditions 48

4.4 Conclusions **48**

5 Kinetics and mechanism of the oxidative conversion of propane over lithium promoted magnesia catalyst ***51***

5.1 Introduction **51**

5.2 Experimental **52**

5.3 Results **52**
5.3.1 Propane partial pressure variation 52
5.3.2 Oxygen partial pressure variation 53
5.3.3 Gas phase reactions 53
5.3.4 Effect of reaction products on the reaction rates 55
5.3.5 Reactions of propene 56

5.4 Discussion **57**
5.4.1 Catalytic vs. homogeneous activation of propane 57
5.4.2 The role of oxygen and the reaction mechanism 59
5.4.3 Mechanism in the absence of oxygen 60

5.4.4 Mechanism in the presence of oxygen 61
5.4.5 Effects of byproducts on the catalytic performance 62
5.4.6 Importance of secondary reactions 63

5.5 Conclusions 64

6 Factors that influence catalytic activation, hetero-homogeneous reactions and the selectivity of C-C bond vs. C-H bond scission during the oxidative conversion of lower alkanes to olefins 65

6.1 Introduction 65

6.2 Experimental 66

6.3 Results 67
6.3.1 Catalytic performance of Li/MgO catalysts with varying Li content 67
6.3.2 Interaction of reactants and products on Li/MgO 69
6.3.3 Influence of the deoxygenation degree in hydrocarbon activation 70
6.3.4 Influence of the surface area on catalytic performance 71
6.3.5 Influence of temperature on catalytic activity and selectivity 72
6.3.6 Influence of the reactant on the product distribution 72

6.4 Discussion 73
6.4.1 Role of Li in creating the active site and the removable oxygen 73
6.4.2 Reaction mechanism of propane activation 76
6.4.3 C-C vs. C-H bond breaking 77

6.5 Conclusions 78

7 General discussion and recommendations: criteria for oxidative conversion of alkanes to olefins 81

7.1 The relative importance of catalytic and gas-phase reactions 81

7.2 Active site and mechanism 82

7.3 Catalyst criteria for alkane conversion to olefins 83

7.4 Process conditions criteria 84

7.5 Concluding remarks 85

8 References 87

9 Summary 91

9.1 Samenvatting 93

9.2 Összefoglaló 95

9.3 Rezumat 97

Chapter 1

1 Introduction

1.1 Objectives and justification

In our rapidly developing world the production of new synthetic materials is flourishing, consequently, the demand for bulk chemicals like olefins is increasing tremendously. The present industrial capacity for lower olefins including ethene, propene, and butenes is expected to be insufficient, as the demand grows for these important intermediates of the modern petrochemical industry [1-3]. These light olefins (along with methane and aromatics) are, e.g., obtained from catalytic or steam cracking of naphtha and natural gas and from fluid catalytic cracking (FCC) of vacuum gas oil. While these two routes are very well developed, increasing the capacity of these processes is only possible to some extent, as the changing regulation limits the use of byproducts (notably aromatic molecules) in fuels. The rate at which refineries can increase their olefin production is also limited by the complexity of refinery processes, thus for satisfactory olefin production, industry needs dedicated olefin producing processes.

Catalytic dehydrogenation of alkanes, as an alternative route to light olefins, shows some major disadvantages, i.e., thermodynamic limitations, a high tendency to coking and consequently short catalyst lifetime [4]. A conceptually interesting way to overcome thermodynamic limitation in the direct dehydrogenation reaction is to couple it with hydrogen oxidation. Moreover, the presence of oxygen limits coking and extends, therefore, catalyst lifetime. This new concept of olefin production, generically called oxidative dehydrogenation (ODH), has been thoroughly studied in the literature, motivated by the prospective of a new alternative process with the above-mentioned advantages [4,5]. Despite the research efforts invested, industrial scale application of ODH reaction has not been realized to date, due to the low olefin selectivities shown by the catalysts employed. The main problem with most of the catalysts studied in ODH is that olefin yields do not exceed typically 30%. Conventional transition metal oxides with pronounced redox properties such as supported vanadia catalysts have been explored [6-11], but have not been seen promising, as readsorption of olefins (leading to total oxidation) appears to limit the olefin yield [5,12,13].

In contrast, Lunsford *et al.* [14-16] reported that magnesia based catalysts containing rare-earth oxides, promoted with alkali halide (mainly chlorides) show high activity and selectivity for forming olefins in comparison to other mixed oxides. Over 70% ethene selectivity was reported at 75% conversion of ethane at 570°C. Somewhat later Landau et al.

[17,18] reported on the oxidative conversion of LPG. The composition of the studied catalysts resembled those studied for methane oxidative coupling [19] and contained a basic oxide (such as MgO) mixed with rare-earth oxide (e.g. Dy_2O_3) and promoted by alkali metal (Li, Na) oxide and halogen (Cl, Br) [18]. Chlorine was claimed to be essential to achieve high conversions. The yield of total olefins reached 50% at 585°C at 62% conversion [17]. While the catalysts showed only a minor tendency to form carbon oxides, catalyst stability was still not satisfactory.

The goal of this thesis is to formulate a catalyst composition, based on this new approach, which is selective towards olefin production, to describe the kinetics of the reaction in order to be used in reactor modeling, and to investigate the reaction mechanism in order to understand the various reaction routes leading to the various reaction products. Chapter 2 will describe the experimental methods, Chapters 3 and 4 are dedicated to explore the effects of the catalysts composition, in Chapter 5 full description of the reaction kinetics and the mechanism is given on a chosen catalyst, and Chapter 6 will deal with the characterization of the active site and the mechanism of the hydrocarbon activation step.

1.2 Current methods of olefin production

Most of the low olefins produced are converted directly or indirectly to polymers and other synthetic materials. As the demand for these new synthetic materials is steadily increasing, the need for low olefins, especially for ethene and propene follows this demand.

The entire capacity of C_2-C_4 olefins worldwide is produced by three commercial processes: thermal cracking (pyrolysis or steam cracking), catalytic cracking and catalytic dehydrogenation. A brief description of these processes is given here based mainly on review literature [20-22]. More detailed description is available in the mentioned references.

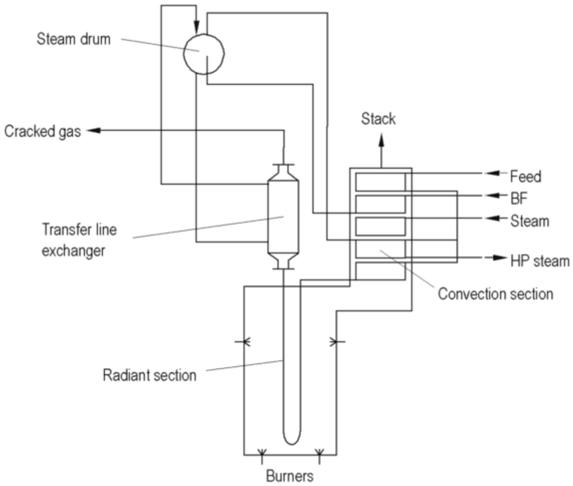

Figure 1.1 Principal arrangement of a cracking furnace

1.2.1 Steam cracking

The majority of today's olefin production comes from thermal cracking of various petroleum hydrocarbon, most often LPG and naphtha, with steam; the process is commonly called pyrolysis or steam cracking. The main product of steam cracking is ethene; propene and limited amounts of higher olefins are byproducts from this process.

The schematics of a steam cracking reactor is shown in Figure 1.1. A hydrocarbon stream is heated by heat exchange against flue gas in the convection section, mixed with steam, and further heated to incipient cracking temperature (500–680 °C, depending on the feedstock). The stream then enters a fired tubular reactor (radiant tube or radiant coil) where, under controlled residence time, temperature profile, and partial pressure, it is heated from 500–650 to 750–875 °C for 0.1–0.5 s. During this short reaction time hydrocarbons in the feedstock are cracked into smaller molecules; ethylene, other olefins, and diolefins are the major products. Since the conversion of saturated hydrocarbons to olefins in the radiant tube is highly endothermic, high energy input rates are needed. The reaction products leaving the radiant tube at 800–850 °C are cooled to 550–650 °C within 0.02–0.1 s to prevent degradation of the highly reactive products by secondary reactions.

The resulting product mixtures, which can vary widely, depending on feedstock and severity of the cracking operation, are then separated into the desired products by using a complex sequence of separation and chemical-treatment steps.

Table 1.1 Yields from propane cracking with various residence times (wt%)

Conversion, kg/kg	90.020	90.035	89.926	89.983
Steam dilution, kg/kg	0.3	0.3	0.3	0.3
Residence time, s	0.4450	0.3337	0.1761	0.1099
H_2	1.51	1.55	1.61	1.68
CO	0.04	0.04	0.03	0.04
CO_2	0.01	0.01	0.01	0.01
H_2S	0.01	0.01	0.01	0.01
CH_4	23.43	23.27	22.82	22.40
C_2H_2	0.46	0.51	0.59	0.82
C_2H_4	37.15	37.51	38.05	38.59
C_2H_6	3.06	2.80	2.37	1.96
C_3H_4	0.52	0.57	0.65	0.89
C_3H_6	14.81	14.82	15.01	15.27
C_3H_8	9.97	9.96	10.07	10.01
C_4H_4	0.08	0.08	0.09	0.11
C_4H_6	2.85	2.9	2.98	2.99
C_4H_8	1.00	1	1.02	1.09
C_4H_{10}	0.04	0.04	0.05	0.05
Benzene	2.15	2.12	2.02	1.80
Toluene	0.43	0.4	0.36	0.28
Xylenes	0.05	0.05	0.04	0.03
Ethylbenzene	0.01	0.01	0.01	0.00
Styrene	0.21	0.2	0.18	0.15
Pyrolysis gasoline	1.27	1.26	1.27	1.24
Pyrolysis fuel oil	0.94	0.89	0.76	0.58
Sum	100.00	100.00	100.00	100.00

A typical commercial product distribution from propane steam cracking is shown in Table 1.1. For very mild propane cracking conditions (70% conversion) yields of propylene show a maximum at 18–19 wt% based on propane feed. The product distribution is strongly influenced by residence time, hydrocarbon partial pressure, steam-to-oil ratio, and coil outlet pressure. Under practical operating conditions, ethylene yield increases with increasing

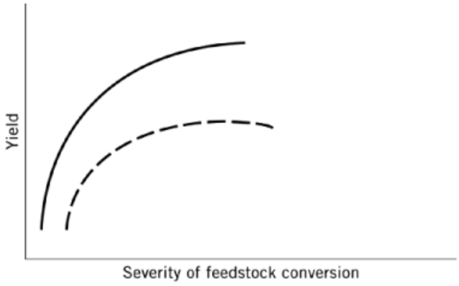

Figure 1.2 Ethylene (—) and propylene (–) yields.

severity of feedstock conversion. Propylene yield passes through a maximum, as shown in Figure 1.2. The economic optimum effluent composition for a furnace usually is beyond the propylene maximum.

Thermal cracking of hydrocarbons is accomplished in tubular reactors commonly known as cracking furnaces, crackers, cracking heaters, etc. Several engineering contractors including ABB Lummus Global, Stone and Webster, Kellogg-Braun & Root, Linde, and KTI offer cracking furnace technology. Usually two cracking furnaces share a common stack, and the height of the heater may vary from 30 to 50 m. Before the 1960s, the cracking tubes were arranged in horizontal rows in a radiant chamber leading to low ethylene capacity (<20,000 t/yr). Modern designs use tubes arranged in vertical rows, providing superior mechanical performance and higher capacity. The capacity of a single furnace is well over 130,000 t/yr.

1.2.1.1 Mechanism of cracking

The thermal cracking of hydrocarbons proceeds via a free-radical mechanism. Since radicals are neutral species with a short life, their concentrations under reaction conditions are extremely small. Much effort has been devoted to mathematical models of pyrolysis reactions for use in designing furnaces and predicting the products obtained from various feedstocks under different furnace conditions.

In recent years, advances have been made in mechanistic modeling of pyrolysis, facilitated by the availability of more accurate thermochemical kinetic and pyrolysis data and of high-speed computers. The major breakthrough in this area, however, has been the development of methods to integrate large systems of differential equations. The accuracy of the models has been improved, driven by the competition between the contractors for ethylene plants. A number of mechanistic models are used today in the ethylene industry, describing the very complex kinetics with hundreds of kinetic equations [Ranzi].

To demonstrate the complexity of the chemical reactions, the cracking of ethane to ethylene is discussed here in detail. A simple reaction equation for ethane cracking is:

$$C_2H_6 \rightarrow C_2H_4 + H_2 \qquad (1)$$

If this were the only reaction, the product at 100% conversion would consist solely of ethylene and hydrogen; at lower conversion, ethylene, hydrogen and ethane would be present. In fact, the cracked gas also contains methane, acetylene, propene, propane, butanes, butenes, benzene, toluene, and heavier components. This reaction (Eq. 1) is clearly not the only reaction occurring.

The free-radical mechanism involves initiation, propagation, and termination steps. Ethane is split into two methyl radicals in the chain initiation step (Eq. 2). The methyl radical reacts with an ethane molecule to produce an ethyl radical (Eq. 3), which decomposes to ethylene and a hydrogen atom (Eq. 4). The hydrogen atom reacts with another ethane molecule to give a molecule of hydrogen and a new ethyl radical (Eq. 5).

Initiation

$$C_2H_6 \rightarrow CH_3\cdot + CH_3\cdot \qquad (2)$$

Propagation

$$CH_3\cdot + C_2H_6 \rightarrow CH_4 + C_2H_5\cdot \qquad (3)$$

$$C_2H_5\cdot \rightarrow C_2H_4 + H\cdot \qquad (4)$$

$$H\cdot + C_2H_6 \rightarrow H_2 + C_2H_5\cdot \qquad (5)$$

If reactions (4) and (5) proceed uninterrupted, the molecular reaction in Equation (1) results. If only reactions (3)–(5) occurred, the cracked gas would contain small amounts of methane (Eq. 3) and equimolar quantities of ethylene and hydrogen with unreacted ethane. This is not observed.

Reactions (3) and (4) terminate if either an ethyl radical or a hydrogen atom reacts with another radical or atom by reactions such as:

Termination

$$H\cdot + H\cdot \rightarrow H_2 \qquad (6)$$

$$CH_3\cdot + H\cdot \rightarrow CH_4 \qquad (7)$$

$$H\cdot + C_2H_5\cdot \rightarrow C_2H_6 \qquad (8)$$

$$C_2H_5\cdot + CH_3\cdot \rightarrow C_3H_8 \qquad (9)$$

$$C_2H_5\cdot + C_2H_5\cdot \rightarrow C_4H_{10} \qquad (10)$$

On termination of chain propagation, new methyl or ethyl radicals or a new hydrogen atom must be generated (Eqs. 2–4) to start a new chain. Thus, every time a new chain is initiated, a molecule of methane is formed (Eq. 3) and a molecule of ethylene is produced (Eq. 4). Other normal and branched-chain alkanes decompose by a similar, but more complex, free-radical mechanism [23]. The number of possible free radicals and reactions increases rapidly as chain length increases.

The free-radical mechanism is generally accepted to explain hydrocarbon pyrolysis at low conversion. As conversion and concentrations of olefins and other products increase, secondary reactions become significant. Partial pressures of olefins and diolefins increase, favoring condensation reactions to produce cyclodiolefins and aromatics. The cracking of heavy feed, such as naphthas or gas oils, often proceeds far enough to exhaust most of the crackable material in the feedstock.

The reaction scheme with heavier feeds is much more complex than with gaseous feedstocks, due to the fact the hundreds of reactants (feed components) react in parallel and some of those components are formed as products during the reaction.

In *propagation* many types of reactions are involved including H · abstraction, addition, radical decomposition, and radical isomerization. In H · abstraction, a hydrogen radical reacts with a molecule (primarily a paraffin) and produces a hydrogen molecule and a radical (Eq 5). In the same way, a methyl radical reacts to produce a radical and methane (Eq 3). Similar reactions with other radicals (ethyl and propyl) can also occur. Radical decomposition is one of the most important types of reaction and it directly produces ethylene according to the following scheme:

Radical decomposition

$$RCH_2CH_2CH_2\cdot \rightarrow RCH_2\cdot + C_2H_4 \qquad (11)$$

This β-scission reaction produces a shorter radical ($RCH_2\cdot$) and ethylene. Radicals normally decompose in the β-position, where the C–C bond is weaker due to electronic effects. Large radicals are more stable than smaller ones and can therefore undergo isomerization.

Radical isomerization frequently occurs for large radicals, and explains to a large extent the observed product distribution.

$$RCH_2CH_2CH_2\cdot \rightarrow RCH_2\dot{C}HCH_3 \qquad (12)$$

The free-radical decomposition of *n*-butane (Eqs. 13–15) results in the molecular equation (Eq. 16):

$$n\text{-}C_4H_{10} + H\cdot \rightarrow n\text{-}C_4H_9\cdot + H_2 \qquad (13)$$

$$n\text{-}C_4H_9\cdot \rightarrow C_2H_4 + C_2H_5\cdot \qquad (14)$$

$$C_2H_5\cdot \rightarrow C_2H_4 + H\cdot \qquad (15)$$

$$n\text{-}C_4H_{10} \rightarrow 2\ C_2H_4 + H_2 \qquad (16)$$

Reactions like (1) and (16) are highly endothermic. Reported values of ΔH at 827 °C are + 145 kJ/mol for Equation (1) and + 232 kJ/mol for Equation (16).

The mathematical description of these complex systems requires special integration algorithms. Based on the pseudo steady state approximation, the chemical reactions can be integrated and the concentration of all components at each location of the reactor (cracking coil) can be computed.

In a generalized and very simplified form the complex kinetics of cracking of hydrocarbons (ethane to gas oil) in steam crackers can be summarized as follows:

		Primary reactions		Secondary reactions
Feedstock	→	ethylene	→	C_4 products
/steam		propylene		C_5 products
		acetylene		C_6 products
		hydrogen		aromatics
		methane		C_7 products
				heavier products

1.2.2 Catalytic cracking

Propylene is formed as a by-product of fluid catalytic cracking (FCC) of gas oils in the refinery. In FCC units, small amounts of ethylene are produced but generally not recovered, except in a few locations where large FCC units are adjacent to petrochemical facilities. This is a refinery process that produces a mixture of butylenes and butanes with very small amounts of butadiene, too. Whereas in Europe, refineries satisfy on average only 20% of the chemical industry's consumption of propene, in the United States they meet more than 40% of the consumption demand. In Western Europe propene demand is predicted to grow faster than that for ethene (3.7% *vs.* 2.4%) in the coming years [3], so additional propene sources are needed.

The conversion reactions of partially vaporized oil distillates in the catalytic cracking process occur mainly in the vapor phase at elevated temperatures in the presence of a cracking catalyst. The acid catalysts first used in catalytic cracking were designated low alumina catalysts; amorphous solids composed of approximately 87% silica, SiO_2, and 13% alumina, Al_2O_3. Later, high alumina catalysts containing 25% alumina and 75% silica were used. However, this type of catalysts have largely been replaced by catalysts containing crystalline aluminosilicates (zeolites) or molecular sieves.

The introduction of powdered catalyst types gave way for the development of fluid-bed catalytic cracking (FCC) in 1942 (United States). Currently, FCC represents the most commonly applied catalytic cracking process. In a lifting gas stream the catalyst powder behaves like a fluid and can be transported in fluidized form through the system. Figure 1.3 shows the principle of an FCC process. The catalyst flowing down from the regenerator is combined with feed and steam, lifted up through the riser into the reactor, where it is fluidized by hydrocarbon vapors. The catalyst then flows down via the stripper to the regenerator, where it is fluidized by combustion gases.

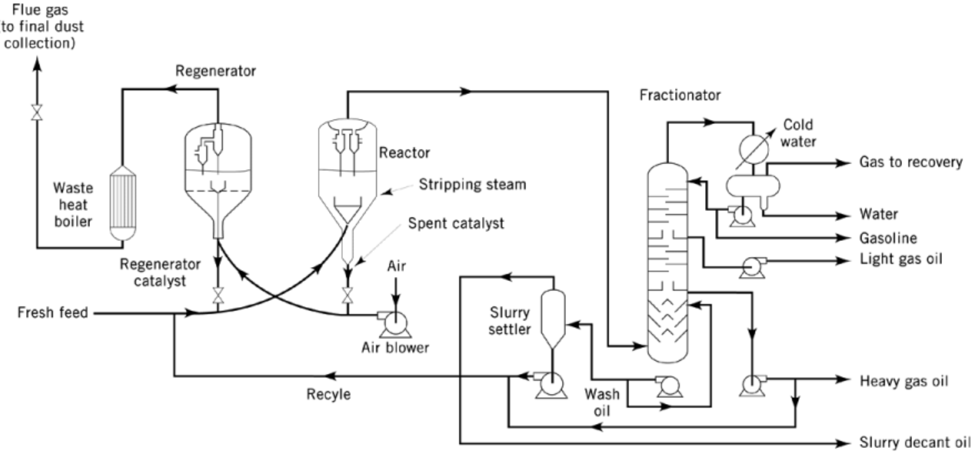
Flue gas (to final dust collection)
Regenerator
Fractionator
Cold water
Reactor
Gas to recovery
Waste heat boiler
Stripping steam
Water
Spent catalyst
Gasoline
Light gas oil
Regenerator catalyst
Air
Fresh feed
Slurry settler
Air blower
Recyle
Wash oil
Heavy gas oil
Slurry decant oil

Figure 1.3 Fluid-bed catalytic cracking with product separation.

The cracking reactions occurring at the active sites of the catalysts proceed via a carbenium ion mechanism that predominantly effects the formation of olefins, isomeric components, and aromatics (the latter *via* intermediate formation of cycloolefins). The formation of low-boiling olefins, branched alkanes, and aromatics favors the production of gasolines with high octane levels.

Converted feedstock forms gasoline-boiling-range hydrocarbons, C_4 and lighter gas, and coke. Gaseous components are separated in a gas plant into fuel gas (containing hydrogen, methane, ethane, ethylene, and hydrogen sulfide) and LPG fractions, i.e., propane−propene and butane−butene. Propylene yield varies, depending on reaction conditions, but yields of 2–5% based on feedstock are common.

1.2.3 Catalytic dehydrogenation

The principal sources of propene are the steam cracking of hydrocarbon feedstocks and refinery conversion processes (e.g., fluid catalytic cracking, visbreaking, and coking). Despite the magnitude of the sources, in these cases propene is a byproduct of the processes for the manufacture of other products, such as ethylene in the case of steam cracking and motor gasoline in the case of catalytic cracking. The availability of propene is thus determined primarily by the demand for the main products, although factors such as feedstock and operating conditions have a significant influence on propene yield. The increasing demand for propene derivatives throughout the 1980s, especially for polypropylene, outstripped the availability from these established sources, and processes for the "on-purpose" production of propene by the dehydrogenation of propane from natural LPG fields were developed commercially.

Catalytic dehydogenation technologies that are aimed for light olefins are developed mainly for propane and isobutane dehydrogenation. While propene production *via* catalytic dehydrogenation increases due to increased demand (mainly for polymerization), environmental concerns on MTBE are expected to slow down isobutene production. Dehydrogenation of ethane over Cr or Pt catalyst allows only very poor yield of ethylene, thus is not competitive with conventional routes.

Dehydrogenation is an endothermic equilibrium reaction that is generally carried out in the presence of a noble- or heavy-metal catalyst such as platinum or chromium.

$$C_3H_8 = C_3H_6 + H_2 \quad \Delta H = 156\ kJ/mol \qquad (17)$$

The process is highly selective; overall yields of propene from propane of ca. 90% are claimed for commercially available processes. As a consequence of thermodynamics, higher temperature and lower pressure increase olefin yield. However, increased process temperature also causes pyrolysis (cracking) of alkane to coke in addition to its dehydrogenation (i.e., reduced selectivity), whereas lower operating pressure increases selectivity. Coke formation wastes feedstock and deactivates the dehydrogenation catalyst. Catalysts coke rapidly and are oxidatively regenerated every 10−100 min. By mixing the catalyst with inert material, much of the heat liberated during coke oxidation can be captured and used to drive the endothermic dehydrogenation. Dehydrogenation processes are operated near atmospheric pressure at around 500−700 °C.

There are four technologies that can be licensed for propane an isobutane dehydrogenation. These are CATOFIN from ABB Lummus, OLEFLEX from UOP, Fluidized Bed Dehydrogenation (FBD) from Snamprogetti, and Steam Active Reforming (STAR) from Phillips Petroleum. These routes differ primarily in the type of catalyst, the reactor design, and the methods used to increase the conversion, eg, the operating pressure, use of diluents, and reaction temperatures.

The CATOFIN process uses a relatively inexpensive and durable chromium oxide–alumina as catalyst. This catalyst can be easily and rapidly regenerated under severe conditions without loss in activity. Dehydrogenation is carried out in the gas phase over fixed beds. Because the catalyst cokes up rapidly, five reactors are typically used. Two are on-stream, while two are being regenerated and one is being purged. The reactors are cycled between the reaction and the reheat/regeneration modes, and the thermal inertia of the catalyst controls the cycle time, which is typically less than 10 minutes. The chromium catalyst is reduced from Cr^{6+} to Cr^{3+} during the dehydrogenation cycle.

The OLEFLEX process uses multiple side-by-side, radial flow, moving-bed reactors connected in series. The heat of reaction is supplied by preheated feed and interstage heaters. The reaction is carried out over platinum supported on alumina, under near isothermal conditions. The catalyst system employs UOP's Continuous Catalyst Regeneration (CCR) technology. The bed of catalyst slowly flows concurrently with the reactants and is removed from the last reactor and regenerated in a separate section. The reconditioned catalyst is then returned to the top of the first reactor.

The Snamprogetti fluidized-bed process uses a chromium catalyst in equipment that resembles conventional fluidized catalytic cracking technology used in the oil refinery. The catalyst is recirculated from the reactor to the regeneration section on a 30–60-min cycle. The process operates under low pressure and has a low pressure drop and uniform temperature profile.

The Phillips Steam Active Reforming (STAR) process uses a noble metal-promoted zinc aluminate spinel catalyst in a fixed-bed reactor. The reaction is carried out with steam in tubes that are packed with catalyst and located in a furnace. The catalyst is a solid, particulate noble metal. Steam is added to the hydrocarbon feed to provide heat to the endothermic reaction, to suppress coke formation, and to increase the equilibrium conversion by lowering partial pressures of hydrogen and propane.

Because propane dehydrogenation is equilibrium-limited and per-pass propylene yield is low, the effluent compression and product purification sections account for nearly 85% of total capital required. Therefore, improvements in the separation section represent the greatest potential for cost reduction. Research efforts are being directed at developing a low cost route to olefins–paraffins separation. Concurrent research is being carried out to remove hydrogen *in situ* in a permeable ceramic reactor. Efforts are also directed at developing high temperature catalytic membrane reactors containing palladium and its alloys in the pores. Another method to remove hydrogen is to oxidize it selectively.

1.3 Oxidative methods for olefin production

Production of olefins through oxidative routes has been recognized as a potentially attractive alternative since the presence of oxygen offers thermodynamic advantages in equilibrium limited processes as catalytic dehydrogenation and limits cokeing on the catalysts.

1.3.1 Oxidative dehydrogenation (ODH)

Because of the limitations of dehydrogenation equilibrium, research has focused on ways to remove one of the products, namely hydrogen, by chemical methods. In this way, hydrogen is oxidized to water and there is no equilibrium limitation.

$$C_3H_8 + O_2 \rightarrow C_3H_6 + H_2O \quad \Delta H = -86\ kJ/mol \tag{18}$$

However, the same oxygen also oxidizes the alkane and alkene to CO_2 and other oxygenated products. Therefore, selectivity to olefins remains a serious problem, as it limits the maximum achievable yield. Despite the research efforts invested maximum yield in propane oxidative dehydrogenation reported in the literature was 30%, unsatisfactory for commercialization [4]. Only the ODH of ethylbenzene to styrene have been commercialized to date. Besides the challenge of finding a selective catalyst to perform the desired reaction, other issues such as safety in handling hydrocarbon-oxygen mixtures, have to be considered.

Several approaches were taken to arrive to a well performing ODH catalyst. Basically three types of catalytic materials were investigated: redox catalysts, non-redox catalysts, nobel metal coated monolith [24]. The reaction mechanism over the different type of catalysts is also supposed to be dependent on the materials used; Baerns *et al.* proposed three types of mechanism being operative over different type of metal oxide materials [25].

1.3.1.1 Redox catalysis

Most literature data is reported over typical transition metal containing redox catalysts. There are excellent reviews that summarize the work done on the ODH of low alkanes [4,5]. Probably, magnesia supported vanadia (VMgO) was the most studied catalyst. The reaction mechanism is typical Mars & van Krevelen description, where the transition metal oxide is reduced by the hydrocarbon in the first step and it is reoxidized by gas-phase oxygen in a subsequent step. The different alkanes showed different conversion, depending on the most labile C-H bond, showing that splitting the carbon-hydrogen bond is the rate-determining step. Over redox catalysts alkenes reacted generally faster than alkanes, except for ethene. Because of the higher activity of alkenes, finding a suitable redox catalyst seems to be an elusive goal [22]. In order to avoid contact of oxygen with the product olefin, reactor operation has been carried out in a cyclic mode, similar to the catalytic dehydrogenation in the CATOFIN process. In one cycle the alkane was oxidatively dehydrogenated with the help of the lattice oxygen, in the subsequent cycle the catalyst was reoxidized with oxygen [26]. A different approach was taken when a good dehydrogenation catalyst (Pt) was used in combination with a selective hydrogen combustion catalyst (Bi_2O_3) in order to perform the oxidative dehydrogenation in a continuous process [27].

1.3.1.2 Non-redox catalysis

Primarily ODH of ethane was studied over non-redox type materials such as alkali promoted alkali-earth oxides and rare-earth oxides [22], often as an extension of the methane oxidative coupling [15,28]. Propane ODH was less studied over non-redox catalysts, but the best propene yields reported in the literature (~30%) involved the use of non-redox materials. Propane ODH over non-redox catalysts does not result propene exclusively, ethene is produced in large amounts as well. Although there are only a few studies of propane oxidative conversion over non-redox type catalysts, it is apparent that gas-phase reactions contribute to olefin formation. However, it is unclear from literature whether catalytic or non-catalytic contributions to propane conversion are more important, unlike in methane oxidative coupling where the role of catalytic and homogeneous reactions is well established [29]. Some authors explain their results of propane conversion to olefins only in terms of catalytic reactions, due to either weakly adsorbed or lattice oxygen, not affected by homogeneous gas-phase contribution [30-32], while others describe their results in terms of radical reactions in the gas-phase initiated on the catalyst, and radical-surface interactions [33,34]. Furthermore, Burch and Crabb compared catalytic and non-catalytic reactions of propane and concluded that the combination of heterogeneous and homogeneous reactions offers better opportunity for obtaining commercially acceptable yields of olefins than purely catalytic reaction [35].

1.3.1.3 Noble metal catalysis

Although noble metals are known to be very good combustion catalyst, under certain conditions, namely limited oxygen concentration and very low contact times, alkanes can be converted to olefins with high selectivity. The product spectrum resembles the one over non-redox catalysts. The mechanism of this process is described by an initial full combustion of alkanes until total oxygen conversion, accompanied by heat generation and further thermal cracking of the remaining alkanes with the heat generated in the first step [36,37]. In practice Pt coated monolith are used under very high flow conditions, contact times are as low as one millisecond [38].

1.3.1.4 Non-catalytic reactions

Several authors studied and compared catalytic ODH with non-catalytic oxidation of propane and concluded that the best performance was achieved when there was no catalyst present in the reactor [16,35,39]. Reaction of alkanes in the gas-phase were studied by a number of groups, they often called the process oxidative pyrolysis or oxycracking [40,41]. The reaction mechanism is described as radical chain reactions similarly to thermal cracking.

1.3.2 Oxidative coupling

Oxidative coupling uses methane as feedstock and results in higher hydrocarbons, mostly ethene. It is difficult to break the C–H bond in methane, therefore relatively severe conditions are needed. The catalyst activates methane while produce methyl radicals that are subsequently released to the gas phase. The methyl radicals combine in the gas phase to give ethane, that further dehydrogenates to ethene. Side reactions of the methyl radical lead to carbon-oxides that reduce selectivity. The process could be economical when methane is available in abundance at extremely low cost, such as in Saudi Arabia and other geographic locations. Since this process does not depend on crude oil for raw feed, research has continued in many countries, and it is possible that it may soon be commercialized.

In the methane oxidative coupling typically non-redox catalysts are employed. It is believed that the active (or activated) lattice oxygen abstracts the hydrogen from the methane molecule while forming a surface hydroxyl. It was first proposed in the methane coupling literature that the active sites of Li promoted magnesia are the oxygen trapped by an electron hole next to a cation defect caused by stoechiometric Li replacement in the magnesia lattice [42]. This active site was commonly noted as $[Li^+O^-]$. When activating a methane molecule this active site transforms to $[Li^+OH^-]$. Regarding the regeneration of the active site there are two principally different propositions; in the mechanism proposed by Ito *et al.* the site is regenerated by dehydroxylation, that implies removal of lattice oxygen [42], while there are alternative propositions that do not require the costly removal of lattice oxygen [43,44].

An important element of the reaction mechanism in methane coupling is the release of radicals from the surface of the catalyst into the gas-phase. There is a vast body of evidence that radicals are released from the catalyst. These include mass-spectrometry, matrix isolation IR and matrix-isolation EPR [45,46]. Furthermore, good correlation has been found between the EPR signal of the [Li^+O^-] sites, the amount of radicals produced [47] and the catalytic activity [42].

The kinetics of the methane coupling reaction has been described by mixed heterogeneous-homogeneous kinetic models [48-50]. These models included heterogeneous generation of radicals and some heterogeneous radical reactions. The kinetic parameters of the gas-phase reactions were generally provided by the extensive literature in the combustion chemistry. The role of homogeneous and heterogeneous reactions was critically discussed and the two contributions were rigorously defined [29].

Computational studies of the [Li^+O^-] active site and the processes occurring on this site are an important tool in studying the methane coupling reaction as the characterization of active sites on oxide materials is difficult. A number of studies computed the optimal geometries of the Li containing defect site [51-53], while the abstraction of hydrogen either from molecular hydrogen or methane on the [Li^+O^-] site was computed as well [54-57], convincingly showing that only homolytic hydrogen abstraction is feasible.

Chapter 2

2 Experimental details

2.1 Introduction

In this chapter the details of experimental measurement procedures, catalyst preparation and materials used in this thesis are given.

2.2 Materials used

In our experiments the following materials have been used: magnesium-hydroxide (Merck, extra pure, 97.8%), magnesium-oxide (Merck, heavy extra pure, 99.6%), zirconium-oxide (Janssen Chimica, 99.5%), niobium-oxide (Niobium Products Company), dysprosium-oxide (Fluka, 99.9%), lithium-nitrate (Merck, >98.0%), ammonium-chloride (Merck, 99.8%), sodium-nitrate (>99.5%), potassium-nitrate (>99.0%), cesium-nitrate (>99.99%), quartz-particles, quartz-wool, butane (Praxair, 3.5), propane (Praxair, Hoek-loos, 3.5), propene (Praxair, 2.5), oxygen (Praxair, 5.0), hydrogen (Praxair, 5.0), carbon-dioxide (Praxair, 4.6), helium (Praxair, 5.0), argon (Hoek-loos 5.0).

2.3 Catalyst preparation

The general catalyst preparation method is given here; the particular details are given in each chapter. All the catalysts were prepared by wet impregnation in slurry. Solid support materials (e.g. magnesia) were impregnated in aqueous solution of the alkali metal and, chloride in particular when chlorine was also added to the catalyst composition. The slurry was mixed at room temperature or at 80°C, then evaporated under vacuum and subsequently dried at 120-130°C. The resulting material was crushed to powder and calcined typically at 750°C for 15-30 hours in flowing air. The resulted catalyst was pressed and crushed, and then sieved to 0.3-0.6 mm particles used in catalytic reaction tests.

2.4 Catalytic measurements

Steady state catalytic measurements were carried out in a quartz microreactor (internal diameter 4 mm) at 1 atm under plug flow conditions. The catalyst bed was packed between two quartz-wool plugs. Before and after the catalyst bed quartz-inserts with 3 mm diameter were introduced to minimize the empty reactor volume. The feed consisted of 5-60% hydrocarbon, 0-22% oxygen, 0-20% CO_2 and balance helium. The total flow rates ranged between 5 and 100 mln/min. Pressure was 1 atm in all cases. Temperatures between 450-700 °C were used. The specific details on the various experiments regarding flow composition and temperatures used will be given in the appropriate chapter.

Catalytic performance was measured under integral conditions in the temperature interval from 450 to 650°C for the case of butane and from 500 to 700°C for propane. The temperature was increased sequentially in steps of 50 °C. Each step consisted of 15 minutes dwell time and 5 minutes heating to the next temperature. Sample injection to the GC took place after 10 minutes dwell at each step. Catalyst stability was tested at 650°C for most of the catalysts with propane as feed after the above-mentioned sequence.

2.4.1 Kinetic setup

The measurement setup consisted of a set of 7 Brooks mass-flow-controllers (S-series), 6 electrically actuated Valco-valves, the reactor oven and heated gas-lines with Eurotherm temperature controllers. The layout of the kinetic setup is presented in Figure 2.1. With the help of the 4-port valves and the bypass line it was possible to measure the feed composition before entering the reactor. The bypass measurements were used to calculate the exact

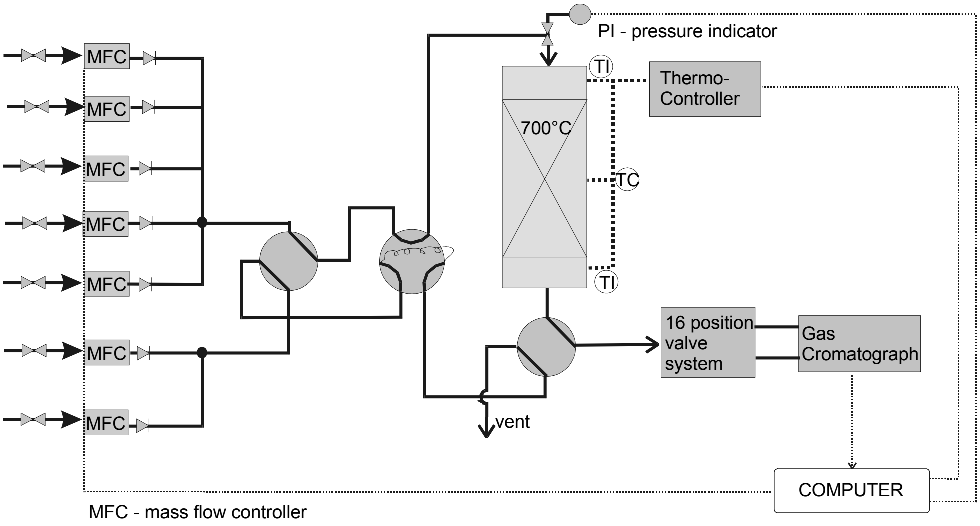

Figure 2.1.The experimental setup used for the kinetic measurements

concentration of the reactants and to assess the carbon balance. A 6-port valve equipped with a loop allowed us to conduct pulsing measurements.

The analysis system consisted of an online GC (Varian, HP) and two 16-position sample storage valves. It was possible to separate all the hydrocarbons up to C_4 on the alumina Plot column with split flow injector, and oxygen, nitrogen, CO, CO_2, water on the Porapak column combined with 13X-Molsieve column. The detector was an FID for hydrocarbons, and TPD for the light gases and water. The layout of the analysis system is shown in Figure 2.2.

The apparatus was fully computer controlled and it was automated by homemade software written under Microsoft Visual Basic 4.0.

During transient measurements quadrupole mass spectrometer (Baltzers OmniStar) was also used and it was connected to the reactor effluent line before the sampling system.

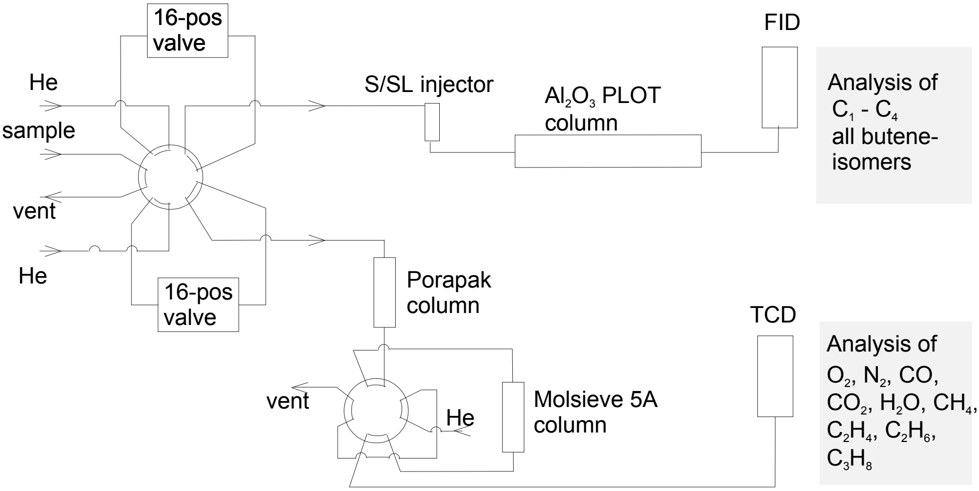
16-pos valve
FID
He
S/SL injector
Al_2O_3 PLOT column
Analysis of C_1 - C_4 all butene-isomers
sample
vent
He
16-pos valve
Porapak column
TCD
Analysis of O_2, N_2, CO, CO_2, H_2O, CH_4, C_2H_4, C_2H_6, C_3H_8
vent
He
Molsieve 5A column

Figure 2.2.Layout of the analysis subsystem

2.4.2 Evaluation of kinetic data

Kinetic data obtained from GC measurements were calculated based on the peak area from the chromatograms. The FID detector measured only relative amounts of hydrocarbons due to the split-flow, while the TCD was calibrated to absolute concentrations. A major compound that was separated and detected on both detectors (usually propane) was used to convert FID peak areas to absolute concentrations. An inert (nitrogen) was used as internal standard in order to account for the volume expansion in the reaction.

Conversion and selectivity to individual products were calculated based on the number of moles of carbon contained in the products divided by the total number of moles carbon in the product mixture (sum of products and reactant not converted). The carbon balance was checked by comparing the total amount of carbon in the measurement to the amount of carbon in the feed.

Reaction rates were determined under differential conditions. The feed for typical measurements consisted of 28% propane, 14% oxygen, 2% carbon-dioxide and balance helium with a total flow of 100 mln/min. Hydrocarbon and oxygen conversions were lower than 5% in all cases.

2.5 Characterization

2.5.1 Bulk characterization

2.5.1.1 Elemental analysis

Determinations of elemental composition of the catalysts tested were performed by X-ray fluorescence spectroscopy (XRF) using a Philips PW1480 apparatus. Lithium and chlorine was determined by atomic adsorption spectroscopy (AAS) on a Unicam Solar system 939 apparatus.

2.5.1.2 XRD measurements

The crystalline phases present in the catalysts were determined by powder X-ray diffraction spectroscopy (XRD) measurements on a Philips PW1830 diffractometer. Peak-width at half-height was used to assess the relative crystallinity of the materials.

2.5.2 Surface characterization

2.5.2.1 Surface area and porosity measurements

BET surface areas of the catalytic materials used were determined by nitrogen physisorption at the liquid nitrogen boiling point and calculation of the surface area according to the BET equation. Pore size distribution and pore volume were determined for some of the catalysts by measuring a full adsorption-desorption cycle. Micrometrics ASAP 2000 apparatus was used for BET measurements.

2.5.2.2 TPD measurements

Temperature programmed desorption studies of ammonia and carbon dioxide were used to determine the acid-basic character of the catalysts. A home made TPD setup connected to a UHV chamber (background pressure 10^{-8} mbar) with a mass spectrometer (BALZERS QMS 200 F) was used. Samples were activated from 50 °C to 600 °C with an increment of 10 °C/min and a final dwell time of 30 minutes. The adsorption temperatures were 50 °C for NH_3 and 100 °C for CO_2, respectively. The time for equilibration was always two hours. Prior to desorption, the samples were evacuated at 10^{-3} mbar for two hours. Then, TPD up to 700 °C was performed with an increment of 10 °C/min.

2.5.2.3 TGA measurements

Adsorption, desorption, oxygen removal, oxygen readsorption measurements were done on a Mettler-Toledo TGA-SDTA apparatus. Argon was used as the carrier gas. Samples were measured in a 70μl alumina sample holder. Sample weight ranged between 50 100 mg, gas flow used was 50 ml/min. Gas composition was made up from 90% Ar and 10% reactive gas, being one of CO_2, O_2, H_2 and propane.

2.5.2.4 XPS measurements

In order have an insight to the surface atomic composition and to exclude any possible contaminant accumulation on the surface, XPS spectra of the most investigated catalysts were taken in a Physical Instruments Φ Quantum 2000 apparatus.

Acknowledgements

Ing. J.A.M. Vrielink for XRF measurements; Ing. A.M. Montanaro-Christenhusz for AAS measurements; Ing. H. Koster for XRD measurements; Ing. V. Skolnik for BET measurements; Ing. A van den Berg for XPS measurements;

Chapter 3

3 Oxidative conversion of light alkanes to olefins over alkali promoted oxide catalysts

Abstract

Alkali promoted mixed oxides were studied as catalysts for the oxidative dehydrogenation (ODH) of butane and propane. Olefin yields as high as 50% were obtained with Li/MgO based catalysts. Magnesia based catalysts showed higher activity for olefin production than catalysts based on zirconia and niobia. Addition of Li to magnesia increases reaction rate normalized to the specific surface area about 7 times and selectivity to olefins from 40% to 70%. Li is an essential ingredient of the catalyst in order to create the catalytic active site. Cl-containing catalysts exhibit slightly higher olefin selectivity, but chloride-free catalysts show superior stability with time on stream. Alkanes show higher conversion rates than alkenes and this surprising observation explains the high selectivity to olefins. It is suggested that Li^+O^- defect sites are the active site for activation of the alkane *via* hydrogen abstraction. Production of olefins *via* this oxidative dehydrogenation/ cracking route may be an attractive alternative to steam cracking.

3.1 Introduction

This chapter describes the function of the catalyst phases and components that determine the catalytic performance. Influence of the support is investigated using materials of varying acidity, a factor which is important in the re-adsorption of olefins and their subsequent conversions. The supports used were magnesia, zirconia and niobia. Furthermore, the function of the various elements (Li, Cl, Dy) in the catalyst is evaluated by analyzing the effect of the catalyst composition on the catalytic performance.

3.2 Experimental

3.2.1 Catalyst preparation

All catalysts were prepared *via* aqueous slurry containing two or more of the following components: a) soluble alkali salt - $LiNO_3$; b) support being one of MgO, ZrO_2 and Nb_2O_5; c)

Dy_2O_3; and d) NH_4Cl when chlorine-containing catalysts were prepared. MgO was freshly prepared from $Mg(OH)_2$ by calcination at 700°C for 3 hours.

Two batches of catalysts were prepared. In the first batch, the catalyst precursor slurry was mixed thoroughly at 80°C, then evaporated under vacuum at 80°C and dried under vacuum at 120°C. The resulting material was crushed and calcined at 750°C two times for 15 hours with intermediate cooling and crushing. In the second batch, thorough mixing of the slurry was carried out at room temperature, evaporation at 80°C and calcination once at 750°C for 15 hours. Composition and basic characterization data are presented in Table 3.1.

Table 3.1 Compositions and characterization data of the catalysts used in this study.

batch	catalyst composition (*nominal wt%*)	BET(m^2/g)	XRD phases present at room temperature
1.	$MgO(\mathit{77.5})-Dy_2O_3(\mathit{7})-Li_2O(\mathit{7})-Cl(\mathit{8.5})$	1.3	Li_2O, $LiDyO_2$, MgO
	$ZrO_2(\mathit{77.5})-Dy_2O_3(\mathit{7})-Li_2O(\mathit{7})-Cl(\mathit{8.5})$	2.1	n.a.
	$Nb_2O_5(\mathit{77.5})-Dy_2O_3(\mathit{7})-Li_2O(\mathit{7})-Cl(\mathit{8.5})$	<1	n.a.
	$MgO(\mathit{84.7})-Dy_2O_3\ (\mathit{7.7})-Li_2O\ (\mathit{7.7})$	1.2	Li2O, LiDyO2, MgO
2.	$MgO(\mathit{77.5})-Dy_2O_3(\mathit{7})-Li_2O(\mathit{7})-Cl(\mathit{8.5})$	6.3	MgO, $LiDyO_2$, $Mg(OH)_2$, Li_2O_2
	$MgO(\mathit{84.7})-Dy_2O_3\ (\mathit{7.7})-Li_2O\ (\mathit{7.7})$	6.1	MgO, $LiDyO_2$, $Mg(OH)_2$, $LiOH.H_2O$
	$MgO(\mathit{91.7})-Li_2O\ (\mathit{8.3})$	6.4	MgO, Li_2CO_3, Li_2O
	MgO	30	MgO, $Mg(OH)_2$

3.2.2 Catalytic measurements

The feed consisted of 5-7% butane, 10-12% oxygen and balance helium when butane was used as alkane, and 10-12% propane, 8-10% oxygen and balance helium for the case of propane as alkane feed.

Typically, a catalyst bed of 100 mg was employed. Weight-hourly-space-velocity ($kg_{hydrocarbon}/kg_{catalyst}$ in 1 hour, noted as WHSV) ranged between 0.2-10 h^{-1}, typically 0.8 h^{-1} for butane and 1.0 h^{-1} for propane was used corresponding to a total gas flow of 10-12 ml/min. Oxygen conversion was below 60% in all cases, unless otherwise noted.

Reaction rates were determined under differential conditions. The feed for typical measurements consisted of 28% propane, 14% oxygen, 2% carbon-dioxide and balance helium with a total flow of 100 mln/min. Hydrocarbon and oxygen conversions were lower than 5% in all cases.

The carbon balance closed within ±5%, except for conversions above 50% in the butane ODH experiments, for which the carbon balance closed within ±10%.

3.2.3 Catalyst characterization

BET surface area measurements, XRD measurements and elemental composition determinations with atomic absorption spectroscopy and X-ray fluorescence were carried out.

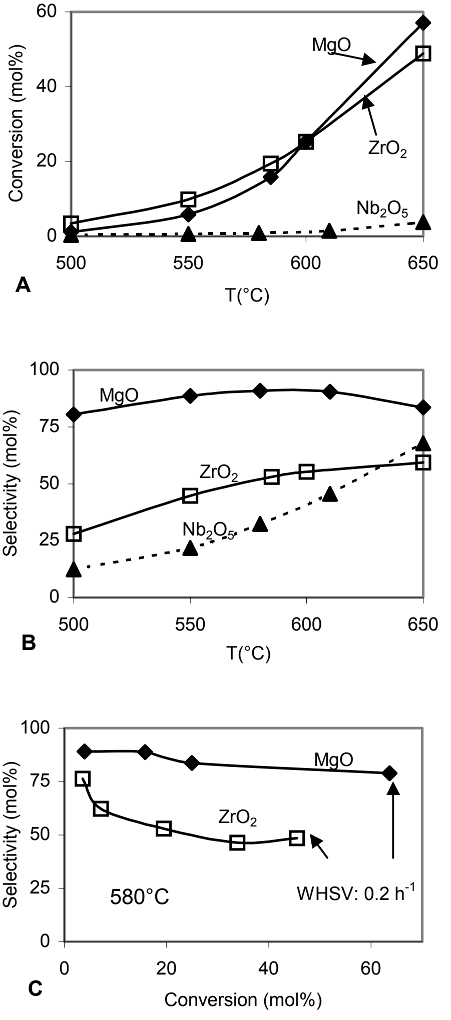

Figure 3.1. Kinetic results with catalysts of the first batch (Table 1), based on the three support materials: MgO (diamonds), ZrO_2 (squares) and Nb_2O_5 (triangles) A: influence of temperature on n-butane conversion; B: selectivity to sum of olefins (ethene, propene and butenes); C: selectivity to sum of olefins vs. conversion at constant temperature (580°C) for the two most active catalysts. Conditions: 5% n-butane, 10% oxygen, balance Helium, WHSV: 0.8 $h^{-1}$for A and B, 0.2-4 $h^{-1}$for C.

The basicity of the catalyst was characterized with temperature programmed desorption (TPD) of carbon dioxide. Details are given in chapter 2.

3.3 Results

3.3.1 Influence of support

In the first series (batch 1), catalysts consisting of the support material (77.5 wt%), dysprosia (7 wt%), Li_2O (7 wt%) and Cl (8.5 wt%) were prepared (Table 1.). The supports used were magnesia, zirconia or niobia. The obtained catalysts have low BET surface area (1.3 m^2/g for magnesia, 2.1 m^2/g for zirconia and <1 m^2/g for niobia). The catalytic performance of the three catalysts in butane oxidative dehydrogenation (ODH) is presented in Figure 3.1

Magnesia and zirconia supported catalysts were more active, leading to a conversion of around 25% at 600°C and space velocity of 0.8 h^{-1} (Figure 3.1 A). Typical performances of these catalysts at 580°C are compiled in Table 3.2. Landau *et.al.* [17] reported 80% selectivity of olefins from LPG at 60% conversion with a similar MgO based catalyst, under comparable conditions, which is in fair agreement with our results. Figure 3.1 A shows that the catalyst based on niobia has very little activity, *i.e.*, close to the activity observed for an empty reactor. Among the catalysts with acceptable catalytic activity, the magnesia-based catalyst was more selective towards olefins than the zirconia based catalyst, over the whole temperature range (see Figure 3.1 B).

The essential differences between MgO and zirconia based catalysts can be observed from the conversion-selectivity graph (Figure 3.1.C). At low conversions the selectivities over the two catalysts were close, but as the conversion increased to 20% the selectivity over ZrO_2 based catalyst dropped significantly (to 50%) while the selectivity over MgO containing catalyst remained relatively unaffected.

Table 3.2. Typical catalytic performance of butane oxidative conversion at 580°C

catalyst composition	WHSV (h^{-1})	conversion (C_4 mol%)	selectivity (C_4 mol%)				olefin yield (C_4 mol%)
			$C_4^{=}$	olefins	$C_4^{==}$	COx	
Mg-Dy-Li-Cl	0.8	15.8	23.4	88.8	1.2	5.8	14.1
	0.2	63.6	14.8	78.9	3.8	12.3	50.2
Zr-Dy-Li-Cl	0.8	19.4	10.0	53.0	0.4	45.9	10.3
Mg-Dy-Li	0.8	21.5	17.5	81.0	1.8	17.2	17.4
	0.2	40.6	13.9	59.5	2.0	33.3	24.2

The results in Figure 3.1C also showed that the zirconia based catalyst led to more deep oxidation than the MgO based catalyst. Oxygen was almost exhausted at higher alkane conversions over zirconia-based catalyst. Therefore, the conversion of alkane did not exceed 50% (due to lack of oxygen) at space velocities where the magnesia based catalyst led to conversions above 60%. Moreover, olefin selectivity remained constant at conversions above 20%, due to the fact that oxygen is almost exhausted.

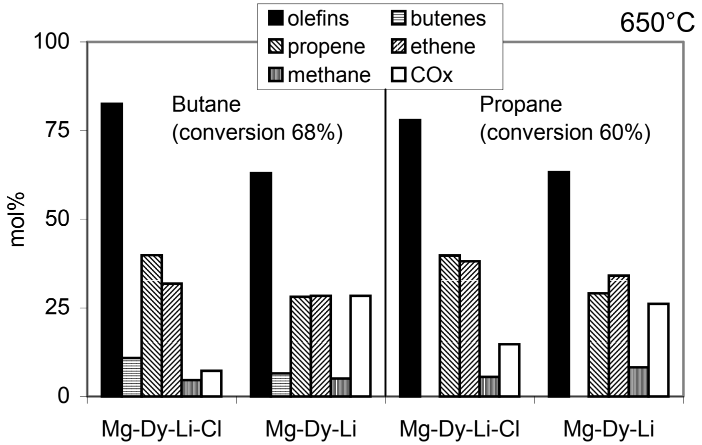

Figure 3.2. Selectivity to products at 650°C using n-butane or propane as hydrocarbon feed on two basic catalysts: Mg-Dy-Li-Cl and Mg-Dy-Li. WHSV: 0.8 h^{-1}

Figure 3.2 compares the catalytic activities of two catalysts prepared in batch 1, i.e., $Li/Cl/MgO/Dy_2O_3$ and one to which chlorine was not added ($Li/MgO/Dy_2O_3$). The selectivities to olefins at similar conversion levels were similar with both hydrocarbons, though, it has to be noted that a considerable amount of the olefins was formed by cracking, especially in case of n-butane. The Cl - free catalyst shows lower selectivity to olefins.

Having shown that the results obtained with propane are comparable to those with n-butane, the rest of the present chapter focuses on an in depth study of the catalytic conversion of propane. The typical catalytic performance of magnesia based catalysts for propane conversion is summarized in Table 3.3.

Table 3.3. Typical catalytic performances in propane oxidative conversion at WHSV: 1/h

T(°C)	catalyst composition	conversion (mol%)	selectivity (mol%)			olefin yield (mol%)
			$C_3^=$	$C_2^=$	COx	
600	Mg-Dy-Li-Cl	20.1	51.6	28.2	17.3	16.0
	Mg-Dy-Li	27.9	42.7	28.8	22.7	19.9
	MgO	19.5	18.8	24.4	54.7	8.4
650	Mg-Dy-Li-Cl	59.8	39.8	38.2	14.7	46.6
	Mg-Dy-Li	59.8	29.1	34.1	26.2	37.8
	MgO	39.1	21.1	33.0	39.9	21.1
700	Mg-Dy-Li-Cl	94.8	16.6	43.3	30.3	56.8
	Mg-Dy-Li	81.0	18.1	35.7	32.3	43.6
	MgO	64.5	20.0	33.9	31.2	34.8

3.3.2 *Catalytic functions of Li, Dy and Cl*

Catalytic performance of MgO, Li/MgO, Li/MgO/Dy_2O_3 and Li/Cl/MgO/Dy_2O_3 (prepared in series 2) was measured, in order to find out which components of the catalyst are responsible for the catalytic activity. An overview of the characteristics of these materials is compiled in Table 3.1. Reducing the calcination time, for the catalyst prepared in series 2, increased the surface area of the catalysts by a factor of 5 compared to the catalysts prepared in series 1.

Rates normalized to the surface area (mol/m^2.s) for MgO and the three catalysts are presented in Figure 3.3 A. Pure magnesia has a relatively high surface area and when Li is added the surface area decreases noticeably (Table 3.1). However, the surface specific

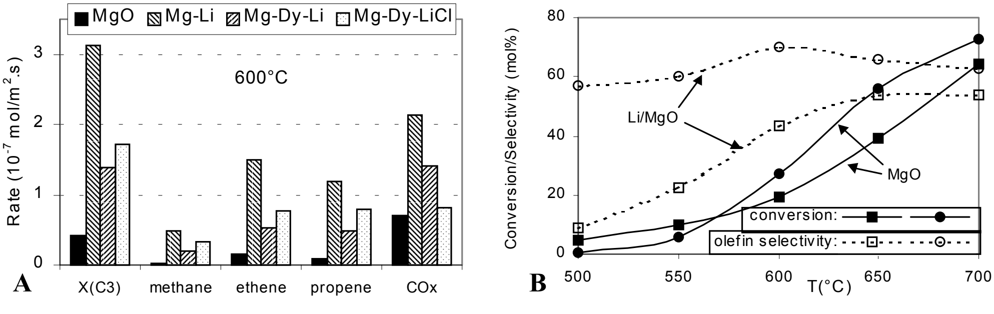

Figure 3.3. Effect of Li addition. A: Surface normalized reaction rates for MgO and three catalysts based on MgO; B: Conversion (filled symbols) and selectivity (open symbols) on MgO (square symbols) and Li-MgO (round symbols). WHSV: 1 h^{-1}.

reactivity increased seven fold (Figure 3.3 A) and thus, conversion obtained with Li/MgO was higher than that for pure magnesia at 600 °C and above (Figure 3.3 B). At the same time the rate of CO_x formation increased three times by the Li addition. This differential increase caused the olefin selectivity to increase from approximately 40% for MgO to about 70% in presence of Li (see Figure 3.3 B). The large activity increase consisted of the remarkable increase in the olefin (both propene and ethylene) and methane formation rates. Figure 3.3 B indicates how the differences between magnesia and the Li/MgO catalyst evolve with temperature. While conversions were rather similar at all temperatures, selectivities to olefins were very different at lower temperatures.

Addition of Dy_2O_3 to the catalyst decreased the activity of the catalyst by about a factor two (third data series in Figure 3.3 A), parallel with only a slight decrease in selectivity.

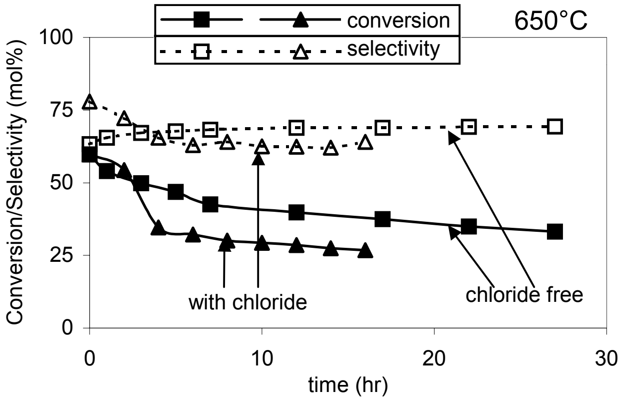

Figure 3.4. Effect of chloride addition on the conversion (filled symbols) and selectivity (open symbols) of the Mg-Dy-Li-Cl (triangle symbols) and Mg-Dy-Li (square symbols) catalysts with time on stream. Feed: propane, WHSV: 1 h^{-1}

Addition of chloride to the Mg-Li-Dy containing catalyst slightly improved activity and selectivity. The combustion rate decreased and the rate of olefin formation increased (fourth data series in Figure 3.3 A). The fresh catalyst containing Cl had a high initial activity and olefin selectivity: about 60% conversion and more than 75% olefin selectivity as shown in Figure 3.4. The chloride-free catalyst had initially somewhat lower selectivity (~65%) and the same conversion as the chloride-containing one. However Cl induces also disadvantages. Figure 3.4 shows the influence of time on stream on conversion and selectivity for both of these catalysts. The activities of the fresh catalysts were identical. Selectivity was only slightly different for the fresh catalysts, 77% olefins for chlorine-containing catalyst and 65% olefins for chloride-free catalyst. The chloride containing catalyst deactivated significantly. The selectivity decreased at the same time. Both conversion and selectivity declined so rapidly that the Cl-free catalysts showed higher activity and selectivity after a few hours time on stream.

3.3.3 Temperature programmed desorption (TPD)

Figure 3.5 shows the result of the CO_2-TPD measurements on the Cl-free catalyst. The catalyst adsorbed relatively large amounts of CO_2, which desorbed at very high temperatures only, as can be seen from the large desorption peak beginning at 550°C and continuing up to the final temperature of the TPD experiment (700°C).

3.4 Discussion

3.4.1 Influence of support on catalytic performance in n-butane oxidative conversion

Figure 3.1.C shows that zirconia based catalysts give more deep oxidation than MgO based catalysts. The most probable explanation for the relatively high oxidation activity is the creation of oxygen vacancies in the ZrO_2 surface [58], which may act as surface-redox sites. However, it cannot be excluded that acid sites are involved, Hoang *et. al.* suggested the formation of catalytically active acid sites on ZrO_2 in the presence of H_2 [46]. A selectivity decrease was also noted, when zirconia was added to the Li/MgO catalyst in methane oxidative coupling [59], which uses similar reaction conditions.

The idea behind trying niobia as a support was the low acidity and surface inertness after calcination at higher temperatures [60, 26]. It was shown that olefin re-adsorption was lower on the niobia support than on magnesia support, thus, secondary olefin combustion decreased, resulting in higher olefin selectivity [61]. Obviously, this feature of niobia was useful only in combination with a very active redox component, such as vanadia, which catalyzes the ODH reaction. However, in case of the alkali promoted catalyst systems employed in this study it appears that the support is essential for the formation of suitable active sites.

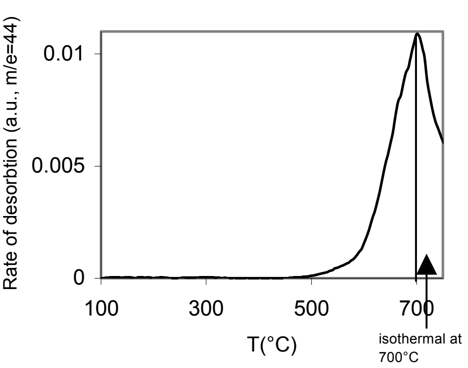

Figure 3.5. Temperature programmed desorption of CO_2 from the Cl-free catalyst, heating rate: 10°C/min

3.4.2 Catalytic functions of Li, Dy and Cl

The increase in selectivity with temperature for pure magnesia compared to Li/MgO (Figure 3.3B) cannot be explained in terms of oxygen conversion. The oxygen conversion was almost identical for MgO and Li/MgO. Therefore, the difference in selectivity must be due to a difference in intrinsic properties of MgO versus Li/MgO. We suggest that the presence of oxygen vacancies is responsible for this effect. Removal of surface hydroxyl groups and generation of oxygen vacancies can be connected with the observed effects. Dehydration of Li/MgO catalyst occurs at a lower temperature than that for pure magnesia [62]. For Li/MgO water desorption takes place between 200-400°C while pure magnesia desorbs water even above 600°C. By dehydration oxygen vacancies are formed [62]. It is generally accepted in the literature, that in the presence of Li, such vacancies are generated on the magnesia surface, and form highly nucleophilic centers *via* dissociative adsorption of O_2. The resulting site is commonly noted as $[Li^+O^-]$ and is considered to be the active site for methane oxidative coupling as well [45,48]. This leads to the hypothesis that a similar active site is responsible for the extraordinary properties of Li/MgO in formation of olefins compared to MgO. However, it cannot be ruled out that other types of oxygen species are involved in the catalytic reactions, e.g. peroxide species adsorbed on the oxygen vacancies.

The XRD patterns of the catalysts containing dysprosia showed presence of bulk $LiDyO_2$ and absence of Dy_2O_3 (Table 3.1.). It is speculated that the formation of a bulk $LiDyO_2$ will limit the amount of Li available in intimate contact with magnesia to form $[Li^+O^-]$. Therefore, the number of active sites and hence the catalytic activity will decrease as observed.

It was stressed by Landau *et al.* [63] that Cl increases the nucleophilicity (basicity) of the surface active oxygen created by the Li doping, by increasing the effective negative charge on it. CO_2 TPD shown in Figure 3.5 shows the strong basic nature of the catalyst. It is reported in Chapter 4 that increasing the amount of Cl in the catalyst results in a smaller CO_2 peak in the TPD spectrum. This is in line with the previous claim that Cl reduces the adsorption of carbon dioxide [64], thereby increasing catalyst activity. However, in Chapter 4 is shown that most of the activity gained by adding Cl to the catalyst could be accounted for by the specific surface area increase caused by chloride addition. As seen from Figure 3.4 the fresh catalyst containing Cl has the same activity as the chlorine-free catalyst – 60% conversion under identical conditions, thus the same conversion rates. For the Cl-containing catalyst conversion decreased to 30% in only five hours. It was demonstrated elsewhere that deactivation is caused by Cl loss from the catalyst during reaction, and its activity can be regenerated by addition of a Cl-containing compound [17].

The Cl-free catalyst in turn maintains activity and selectivity relatively well (Figure 3.4). Under these conditions one notices a slight decrease in the conversion over the Cl-free catalyst as well, but the effect on the olefin yield is partly counterbalanced by the parallel selectivity increase. Thus, it is clear from this experiment, that despite the minor selectivity improvement given by the chloride addition, Cl-free catalysts are more attractive because of their stability and because these catalysts do not cause Cl contaminations. In conclusion, chloride is not found to be significantly important, in disagreement with literature data [63,64].

3.4.3 Reaction pathways

It is difficult to explain the presented product spectrum seen in Figure 3.2 with established catalytic cracking mechanisms [54]. Carbenium ion cracking can be ruled out with certainty. Even in the case a primary carbenium ion would be formed upon activation of the molecule by hydride abstraction from a Lewis acid site, the only fragment that could be cleaved off the primary propylcarbenium ion would be a methyl carbene. Protolytic cracking could occur in principle, but the high propene selectivity compared to ethene and methane is not in agreement with typical protolytic cracking patterns. Moreover, it is highly unlikely that strong Brönsted acid sites exist even in trace quantities on materials such as Li/MgO. It can only be speculated that Li^+ plays similar role to the protons in protolytic cracking. Gas phase generated homogeneous radical cracking cannot prevail under the conditions used, as indicated by the low conversion in the empty reactor.

As noted earlier in this chapter, MgO based catalysts do not show any significant drop in olefin selectivity as conversion increases. In Figure 3.6 reaction rates are compared for two experiments with the same magnesia-based catalysts; in the first experiment propane and oxygen are in the feed while in the second experiment the propane is replaced by propene with identical concentration. During these measurements, no catalyst deactivation was observed. The results obtained are not in line with the general experience in the oxidative dehydrogenation on redox type catalysts, where secondary oxidation of the olefin is always faster than oxidation of the alkane. It also contradicts with predictions that olefin yields from alkanes are theoretically limited due to the fact that olefins are more reactive than alkanes [5]. It is observed that the alkane is more easily converted than the corresponding olefin. That is, the conversion rate of propane is about three times higher than that of propene under the same conditions. It seems that these catalysts have a preference for alkanes though the weakest bond in propene is about 40 kJ/mol weaker than the weakest bond in propane [65]. This might be because propene cannot react any other way than by deep oxidation to CO_x as obsered in Figure 3.6, or to oligomerize which is improbable given the temperatures and pressures used. Deep oxidation requires activation of a significant number of oxygen molecules in contrast to alkene formation out of alkanes. Apparently the Li/MgO oxide catalyst is not very efficient in oxygen activation so that at the end alkenes are converted to CO_x at lower rates than alkanes to alkenes.

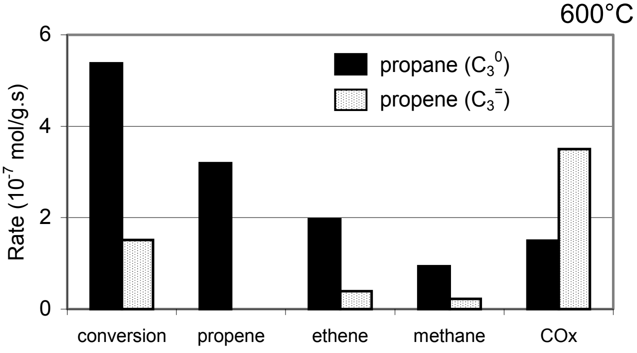

Figure 3.6. Reaction rates of conversion and production of the main reaction products when using propane or propene alternatively over Li/Dy/MgO. Conditions: 28% propane or propene, 14% oxygen, balance He, total flow: 100 ml/min, 0.2 g catalyst.

3.4.4 Performance comparison with industrial routes to olefins

Li-MgO catalysts do not outperform redox catalysts (e.g. VMgO) in dehydrogenation of alkanes. The yield of olefin retaining the same number of carbon atoms as the reacting hydrocarbon (e.g. propene from propane) is limited to 30%, which agrees with the practical barrier found with redox type oxidative dehydrogenation catalysts [4]. However there is a major difference compared to the typical oxidative dehydrogenation catalysts: the total amount of olefins formed is much higher and less hydrocarbon is oxidized to carbon oxides. Olefin yields of 40-60% are obtained; the yields of the various olefins depend on the catalyst and the operating conditions.

In Figure 3.7 the best results of our catalysts with propane are compared with that of steam cracking of propane [21]. It is possible to achieve steam-cracking performance at temperatures as low as 700°C by the Cl-containing catalyst at a space velocity of 1 h^{-1}. Moreover, at 650°C with the same catalyst almost the same yield of olefins is obtained, with a higher ratio of propene at the expense of ethene. This can open the possibility of changing the product pattern according to the actual needs, by only changing the temperature. Furthermore, in chapter 4 it is shown that these catalysts perform well in ethane oxidative dehydrogenation, thus, not only the product spectrum can be varied, but – similarly to steam cracking – also the feed.

At the current state of catalyst development the Cl-containing catalyst is not stable and the outstanding performance is lost within a couple of hours depending also on the operating conditions. Fortunately, the data in Figure 3.7 indicate that a much simpler catalyst without Cl is available. This catalyst shows a very stable performance under relatively severe conditions (temperatures as high as 650-700°C) over 15 hours. Performance is comparable with the original Li/Cl/MgO/Dy_2O_3 catalyst.

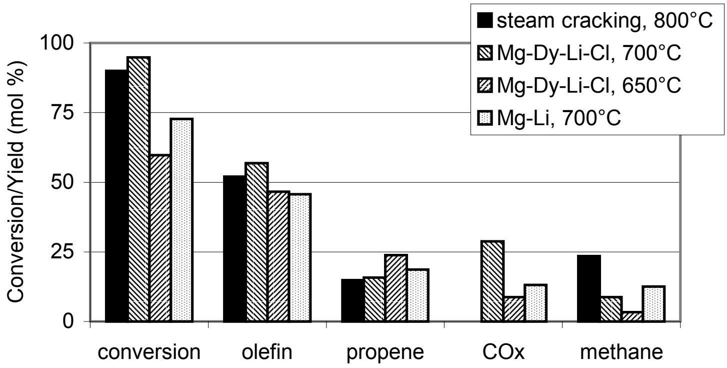

Figure 3.7. The best performance of some of our catalysts compared with industrial steam-cracking performance. Olefin yield is the sum of propene and ethene yields. WHSV: 1 h^{-1}

To summarize, the Li/MgO catalyst seems to be able to compete with steam cracking for production of light olefins. Additional advantage is the fact that the heat is generated internally.

3.5 Conclusions

It is shown that among the three supports tested (magnesia, zirconia and niobia), only magnesia and zirconia gives active catalysts in hydrocarbon oxidative conversion, when combined with Li, Cl and dysprosia. Magnesia-based catalyst had the highest olefin selectivity. Unlike zirconia-based and vanadia-based catalysts, magnesia-based catalysts maintain high olefin selectivity over a large interval of conversions.

We conclude that Li is the only essential addition to magnesia in order to make an active and selective catalyst. Consequently, the essential components for a catalyst which produces olefins with a high yield are a basic oxide support, such as magnesia, and an alkali metal oxide, such as lithia in intimate contact. It is proposed that [Li^+O^-] acts as active site, which is able to split the most active hydrogen from a hydrocarbon.

Olefins proved to be less reactive than alkanes with oxygen over the magnesia based catalyst, allowing high olefin selectivity to be achieved at high conversions. Dysprosium decreases both activity and selectivity because part of the Li is made unavailable *via* the formation of $LiDyO_2$. The addition of chlorine induces only a small improvement in selectivity. However, as Cl^- containing catalysts are unstable, chloride free catalyst may be preferred. Catalysts are about equally active and selective in propane and butane conversion.

The overall productivity suggests that oxidative dehydrogenation and cracking over Li-MgO catalysts may compete with steam cracking leading to similar yields in simpler reactors.

Chapter 4

4 Promoter effect in the oxidative dehydrogenation and cracking of ethane and propane over Li-Dy-Mg mixed oxides

Abstract

The influence of Cl^- and Li^+ on the oxidative dehydrogenation and cracking of ethane and propane over Li-Dy-Mg oxides is reported. Addition of chloride increases the rate of reaction in the ODH of ethane. Selectivity to olefins at isoconversion had a maximum at around 6 wt% chloride. The presence of Li^+ drastically changes the catalytic performance. The catalyst promoted with 1 wt% Li_2O had the highest activity in the propane ODH. Selectivity to olefins at isoconversion showed a maximum at 7 wt% Li_2O. It is speculated that dehydrogenation and cracking involve Li^+ and a rather nucleophilic oxygen site.

4.1 Introduction

In chapter 3 the oxidative dehydrogenation and cracking of butane and propane over mixed oxides based on rare-earth and promoted with Li and Cl was reported to give up to 50% yield of olefins. The catalysts showed only a minor selectivity to carbon oxides but catalyst stability was not satisfactory. The use of Cl-free catalysts was also suggested.

As the key features in these catalysts suggested by the patent literature [18] were the presence of chloride and lithium, the aim of this chapter is to explore the catalytic properties of Li-Dy-Mg mixed oxide catalysts, with varying concentrations of chloride and lithium, for the oxidative dehydrogenation of ethane and propane.

4.2 Experimental

4.2.1 *Catalyst preparation*

The mixed oxide catalysts were prepared according to the method described in chapter 2. Starting chemicals were MgO (Merck), Dy_2O_3 (Aldrich), $LiNO_3$ (Merck), and NH_4Cl (Merck) in the highest purity grade commercially available and used without further purification. Calcination in air was done at 700 °C for 12 hours for the varying Cl-containing catalysts. For the catalysts containing varying amounts of Li calcination was done at 750°C for 20 hours.

Table 4.1. Chemical compositions and specific surface area of the mixed oxide catalysts used

Code	Atomic distribution	MgO (wt%)	Cl (wt%)	Li_2O (wt%)	Dy_2O_3 (wt%)	BET (m^2/g)
L7C0	$Mg_{1.92}Li_{0.47}Dy_{0.04}O_x$	85.0	-	7.7	7.3	2.2
L7C2	$Mg_{1.92}Li_{0.47}Dy_{0.04}Cl_{0.05}O_x$	82.9	2.0	7.5	7.6	4.7
L7C4	$Mg_{1.92}Li_{0.47}Dy_{0.04}Cl_{0.11}O_x$	81.0	4.1	7.4	7.5	5.0
L7C6	$Mg_{1.92}Li_{0.47}Dy_{0.04}Cl_{0.17}O_x$	79.4	6.1	7.2	7.3	4.9
L7C8	$Mg_{1.92}Li_{0.47}Dy_{0.04}Cl_{0.24}O_x$	77.0	8.5	7.0	7.5	5.3
L7C16	$Mg_{1.92}Li_{0.47}Dy_{0.04}Cl_{0.46}O_x$	71.8	15.2	6.5	6.5	6.5
L0C8	$Mg_{1.92}Dy_{0.04}Cl_{0.24}O_x$	84.0	8.5	-	7.5	15.1
x%Li/MgO	MgO	100	-	-	-	75.1
	$MgLi_{0.007}O_x$	99.0	-	1.0	-	11.4
	$MgLi_{0.08}O_x$	97.0	-	3.0	-	2.9
	$MgLi_{0.2}O_x$	93.0	-	7.0	-	1.3
	$MgLi_{0.37}O_x$	88.0	-	12.0	-	<1

Table 4.1 compiles the chemical composition and the BET surface areas of the catalysts used. The lowest specific surface area was observed for the chloride free mixed oxide, while the Li^+ free catalyst L0C8 had the highest BET surface area. XRD analysis suggests that next to the main component MgO, Dy_2O_3 and an unidentified oxide phase containing Li^+ cations was present.

4.2.2 *Temperature programmed desorption (TPD)*

For details see Chapter 2 (Experimental details)

4.2.3 Kinetic measurements

Typically, approximately 300 mg of catalyst were mixed with the same mass of quartz, the rest of the reaction zone being filled with pure quartz. The reaction temperatures were varied from 450 °C to 650 °C. Under the operating conditions used, the empty or quartz filled reactor did not lead to measurable conversion of ethane. The ethane/oxygen molar-ratio was 1:1.2. The propane/oxygen ratio was 1:1. If not otherwise noted the weight hourly space velocity was 0.8 h^{-1}.

The products were analyzed in a Hewlett Packard 6890 Series GC equipped with a FID and a TCD detector operated in parallel. A SUPELCO Carboxen 1010 plot column was used for product separation.

4.3 Results and Discussion

4.3.1 Acid-base characterization of the materials

4.3.1.1 TPD of ammonia

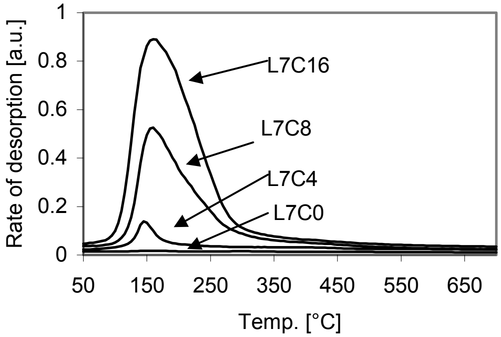

Figure 4.1 TPD curves of ammonia (signals normalized to the BET surface area)

The TPD curves of ammonia after sorption and subsequent evacuation at 50 °C are compiled in Figure 4.1. The total amount of ammonia desorbing from the samples increased sharply with the concentration of chloride in the material. Samples with less than 6 wt.% Cl^- did not show measurable ammonia desorption. The maximum of desorption was at 150 °C for L7C6, at 170 °C for L7C8 and at 180 °C for L7C16 and the peak intensity also increased in this series. This suggests that the strength and the concentration of acid sites increased. As preliminary IR spectroscopic measurements indicate that Brönsted acid sites are not formed on these materials, we tentatively attribute the adsorption sites on the surface to Li^+, Mg^{2+} and /or Dy $^{3+}$ metal cations. Because of the relatively high molar concentration of Li^+ in the materials studied and the method of impregnation, we speculate that accessible Li^+ cations constitute the majority of Lewis acid sites. The asymmetric shape of the desorption curves for L7C8 and L7C16 may suggest also the presence of a second ammonia desorption maximum at approximately 220 °C.

4.3.1.2 TPD of carbon dioxide

The TPD curves for carbon dioxide after equilibration at 150 °C are shown in Figure 4.2. Two groups of TPD peaks were observed one peaking at 700 °C (i.e., the maximum temperature probed) and one at approximately 250 °C. The one at 700°C was only observed with the samples containing less than 4 wt% Cl$^-$, while the samples with more than 6 wt% Cl$^-$ showed the desorption maximum at low temperatures. Note that the peak at 700 °C qualitatively suggests that the stability of the carbonate formed suffices to withstand temperatures lower than 550 °C and that it is rapidly depleted at a constant temperature of 550 °C. Measurements of CO_2 TPD from the individual oxide components, i.e., MgO, Li_2O and Dy_2O_3, showed that the high temperature of the desorption maximum is to be attributed to the Li_2O component and the formation of lithium carbonate (see Figure 4.3). The presence of chloride in the catalysts seems to destabilize the Li carbonate by increasing the overall acid strength of the material or the formation of a LiCl phase. The lack of any evidence in the XRD of the mixed oxides points to the absence of any long range ordered LiCl component. Thus, we tend to attribute the absence of the high temperature desorption maximum of CO_2 to the higher acid strength of the mixed oxide. It should be noted here that L7C6 appears to be the only material of this series that contains a moderate concentration of Lewis acid sites (as detected by ammonia TPD) and some carbonates that are stable up to high temperatures.

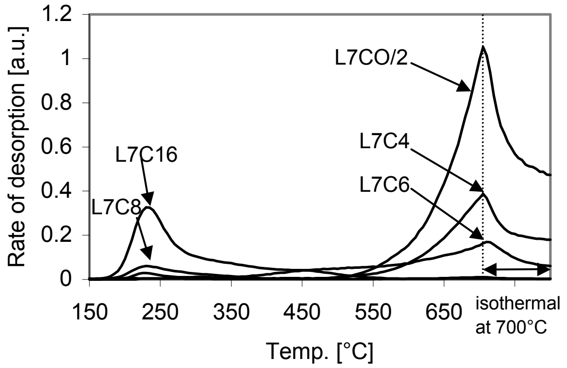

Figure 4.2. TPD curves of carbon dioxide (signals normalized to the BET surface area)

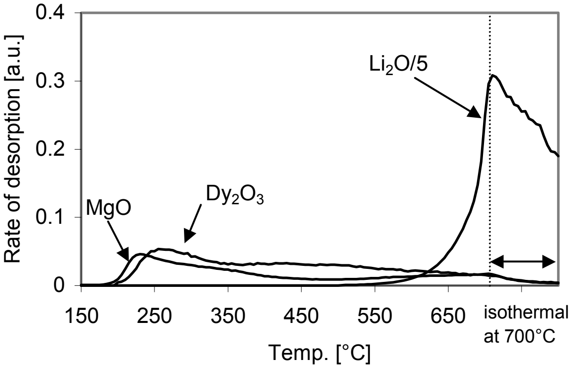

Figure 4.3. TPD curves of carbon dioxide (pure substances; signals normalized to the BET surface area)

4.3.2 Kinetic measurements

4.3.2.1 The influence of the chloride content

Under the reaction conditions employed noteworthy conversion of ethane or oxygen was not observed below 500 °C. Above, primarily ethene, CO and CO_2 were found. Other hydrocarbon products such as methane, acetylene, propane and propene were only formed to a very small extent. The highest ethene yields experimentally reached to 69 mol % realized with L7C8 at 650 °C. It should be emphasized that these values are the highest reported in the open literature to date.

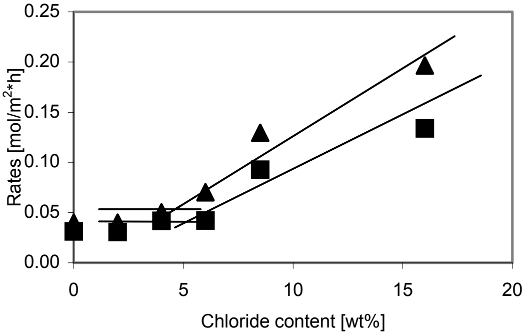

Figure 4.4. Areal rates of ethene formation (■) and ethane conversion (▲) at 580 ℃ for a molar ethane/oxygen ratio of 1:1.2.

In general, at reaction temperatures lower than 550 °C, the selectivity towards combustion was higher than towards ethene. With increasing temperature, however, the selectivity to ethene increased, while the selectivity to carbon oxides decreased. Specifically, at 580 °C the CO_x selectivity varied between 40 (L7C6) and 15 mol % (L7C4), while at 610 °C it varied from 31mol % (L7C6) to 10 mol% (L7C4). The rate of formation of CO_2 was always higher than that the formation of CO.

At the typical reaction temperature of 580 °C and at a space velocity of 0.8 h^{-1} conversions varied from 4 mol % (L7C0) to 47 mol % (L7C16). The maximum conversions were found at 650 °C (89%, L7C8). Up to this temperature, significant conversions of ethane in either a blank or quartz filled reactor were not detected. With all catalysts the conversions at 580 °C were constant for at least 24 hours. Figure 4.4 compiles the rate of ethane conversion and ethene formation at 580 °C for a molar ethane/oxygen ratio of 1:1.2. Up to Li7C6 the rates (normalized to the BET surface areas) did not vary significantly (0.05 +/-0.01 mol/m^2.h) At higher chloride contents the rate increased more than threefold up to 0.2 mol/m^2.h. The apparent energy of activation varied between 120 and 150 kJ/mol without any clear trend.

The catalytic selectivity varied more subtly than the activity. Figure 4.5 shows the catalytic selectivity at 10 mol% conversion for 580 °C. The selectivity to ethene was about 65 mol % for the Cl^- free catalyst. It reached a maximum with L7C6 at approximately 85 mol % and dropped to 58 mol % for L7C16. This indicates that an optimum in the acid-base properties for the selective oxidative dehydrogenation exists. Note that the maximum occurred with the catalyst that showed Lewis acid sites able to retain ammonia up to 200 °C and basic sites that stabilized a (small) portion of carbonates up to 700 °C.

4.3.2.2 The influence of the Li content

The importance of Li^+ for activity and selectivity of the catalysts can be seen by comparing a Li^+ free (L0C8) and a Li^+ containing catalyst (L7C8). L7C8 showed the expected exponential increase of the reaction rate with temperature. L0C8 had a higher activity at lower temperatures than L7C8. At higher temperatures the catalytic activity of L0C8 increased only slightly. This is attributed to the fact that above 580 °C L7C8 converts oxygen almost quantitatively and limits, thus, the conversion of ethane.

The differences between Li^+ containing and Li^+ free catalysts are even more pronounced for the catalytic selectivity. For the Li^+ containing catalysts at 580 °C the ethene selectivities range from 60 mol % (L7C6) to 85 mol % (L7C4). At 610 °C the selectivities to ethene were even higher ranging from 69 mol % (L7C6) to 90% (L7C4). The absence of lithium (L0C8) led to a marked loss in ethene, which did not exceed 25 mol% of the products. The dominant products over this catalyst were carbon oxides.

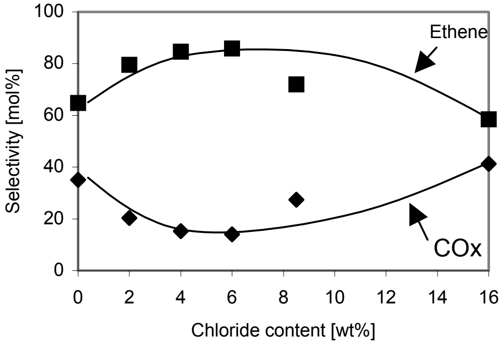

Figure 4.5. Catalytic selectivities at 10 mol % ethane conversion for 580 °C

When we look at the activity of the pure magnesia (0% Li_2O in Figure 4.6; see also chapter 3) it becomes clear that pure the MgO surface could not provide the activity of the L0C8 catalyst, rather it comes from dysprosia. Independent catalytic measurements of dysprosia powder indicated high activity in converting oxygen quantitatively already at 550°C.

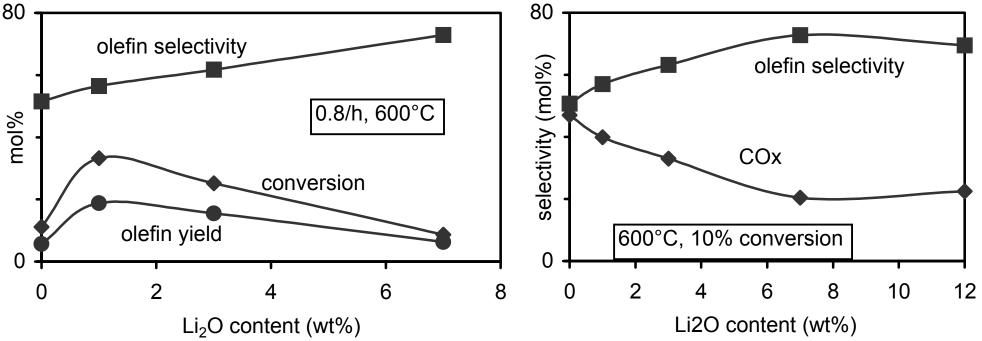

Figure 4.6. Catalytic performance of magnesia with varying amount of Li under typical reaction conditions

Figure 4.7. Selectivity to olefins and carbon oxides at isoconversion vs. Li-content for magnesia with varying amount of Li

At typical reaction conditions conversion of propane over magnesia containing varying amounts of Li showed a maximum at 1 wt% Li_2O content (Figure 4.6) in spite of the fact that surface area was decreased tremendously by the Li addition (Table 4.1). Further addition of Li decreased the conversion parallel with the surface area. Selectivity to olefins increased up to 7% Li_2O/MgO. Strong variation of selectivity with conversion is expected in oxidative dehydrogenation, therefore selectivities were evaluated at constant conversion for the catalysts containing Li in varying amounts (Figure 4.7). Surprisingly, the selectivity trend did not change compared to Figure 4.6. However at 7%Li_2O the selectivity to olefins showed a maximum, parallel with a minimum of carbon-oxides selectivity.

4.3.2.3 The reaction network

One of the key questions to evaluate catalysts for oxidative dehydrogenation is related to the role of the primary and secondary reactions for the formation of the light alkenes and carbon oxides. In order to explore the reaction network (see Figure 4.8), yield conversion relationships are used two of which (for L7C0 and L7C8) are depicted in Figure 4.9.

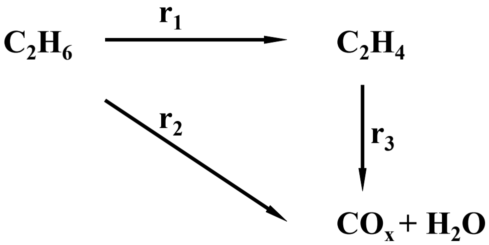

Figure 4.8. The reaction network

The observed linear dependence between conversions and yields for all products and catalysts clearly indicates, that in chloride free and chloride containing catalysts only the rates r_1 and r_2 are of significance, while readsorption of ethene and subsequent oxidation did not occur. Thus, carbon oxides and ethene are concluded to be primary products. Even more strikingly, for a reaction temperature of 580 °C such an inter conversion was not observed up to conversions of more than 60 %. It should be emphasized that for other transition metal oxide catalysts, such as all vanadia-based catalysts, readsorption of the primarily formed olefins and the subsequent oxidation of the olefin was always observed already at very low levels of conversion [4]. These (vanadia containing) catalysts show 100 % selectivity at very low conversions, which drops rapidly above 3-5 mol% conversion. It has been shown that with vanadia type catalysts the selectivity could be somewhat improved by decreasing the readsorption of the olefin *via* decreasing the acidity of the support, increasing the reaction temperature and using lower partial pressures of reactants. None of these factors changes the primary nature of both types of reaction products with the catalysts discussed here. Thus, we have to address the fact that the catalyst activates and dehydrogenates ethane, but that it does not activate ethene, which is a more reactive sorbate for polar surfaces. In the absence of reliable calorimetric data for the chemisorption of ethane and ethene on these surfaces, we would like to speculate that at least one constituent of the active site is so nucleophilic (or repels the π-donor ethene) that this leads to stronger bonding of alkanes than alkenes.

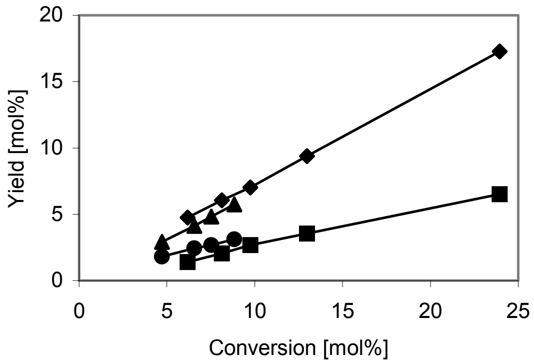

Figure 4.9. Conversion/yield plots for C7L0 (ethene; ▲), (CO$_x$; ●), and C7L8 (ethene; ◆), (CO$_x$; ■) at 580 °C and a molar ethane/oxygen ratio of 1.2:1

4.3.2.4 Influence of the reaction conditions

The influence of the reactions conditions was explored with propene using L7C4 as typical catalyst. Adding up to 8 vol% CO_2 to the reacting mixture led to a marked decrease in the reactivity (see Figure 4.10), while the selectivity did not change. A closer inspection shows that the apparent reaction order is –0.5 which suggests that one carbon dioxide molecule blocks two active sites. This is compatible with the fact that two accessible Li^+ cations are needed to form Li carbonate. It suggests that the active site contains an accessible Li^+ cation. In relation to the stability of the carbonates we can conclude that for the materials with more than 6 wt% chloride the stability of the carbonates will be drastically lower.

4.4 Conclusions

$Li_2O/Dy_2O_3/MgO$ mixed oxides have been shown to be suitable catalysts for the oxidative dehydrogenation and cracking of ethane and propane that did not deactivate during 24 hours time on stream at 580°C. All products were found to be primary with surprising absence of secondary reactions of the olefinic products. Evidence for a marked participation of gas phase processes was not observed for ethane and propane experiments under the conditions tested.

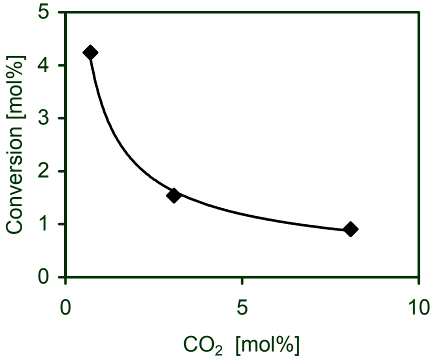

Figure 4.10. Effect of carbon dioxide addition on propane conversion; 600 °C; atmospheric pressure, 28 % propane, 14 % oxygen, balance He, total flow 100 ml/min; catalyst: 100 mg L7C4

The presence of increasing concentrations of chloride in the mixed oxides increases the concentration and strength of the Lewis acid sites above a threshold of 4 wt% Cl^-. Circumstantial evidence (the formation of surface carbonates) suggests that Li^+ cations are preferentially located on the surface of the mixed oxide catalysts. The rate of reaction increased markedly at higher concentration of chloride, which is attributed to the higher acidity of these mixed oxides. In contrast, the selectivity to olefins showed a maximum at approximately 6 wt% chloride in the mixed oxide.

From the experiments with varying the Li content and the poisoning experiments with CO_2 we tentatively conclude that the active sites contain Li^+ cations. The presence of accessible Li^+ appears indispensable for catalytic activity. Under reaction conditions the less acidic mixed oxides are concluded to have a significant abundance of Li_2CO_3 on their surface. The presence of Cl^- anions adjusts that concentration level. The nature and role of the oxygen in the overall process is unclear. The presence if Li^+O^- sites, similar to the proposal for catalysts in oxidative methane coupling, is conceivable as active sites. It is unclear at present, however, if the catalysts act *via* radical sites that react the alkane to an alkyl radical and an ionic surface hydroxyl group to carbenium ions or whether the cleavage of the C-H bond occurs *via* paired electrons (partly ionic intermediates).

As the present catalyst types can be used successfully in their Cl- free form it can be stated that the class of mixed oxides presents a promising route for new materials that will help to satisfy the future olefin demand *via* a combination of dehydrogenation and cracking.

Aknowledgements

Dr. Stefan Fuchs and Heike Borchardt for their help in catalyst preparation and testing.

Chapter 5

5 Kinetics and mechanism of the oxidative conversion of propane over lithium promoted magnesia catalyst

Abstract

Oxidative conversion of lower alkanes over lithium promoted magnesia catalysts offers a viable alternative for propene and ethene production. The catalytic performance of propane oxidative dehydrogenation and cracking shows yields up to 50% of olefin (propene and ethene). The reaction kinetics was studied by means of variation of the partial pressures of the reactant as well as by addition of product species to the reaction mixture. The observations can be qualitatively explained with a mechanism including activation of propane on the catalyst generating propyl radicals that undergo a radical-chain mechanism in the gas phase. Alkane activation is rate determining. Oxygen has two functions in the mechanism. First, the presence of small amounts of oxygen influences the radical gas phase chemistry significantly because the type and concentration of chain propagator radicals is greatly increased. At higher oxygen partial pressures the radical chemistry is only slightly influenced by the increasing oxygen concentration. The second function of oxygen is to facilitate the removal of hydrogen from the surface OH^- species that are formed during the activation of propane on the catalyst. Carbon dioxide has a strong inhibiting effect on the reaction without changing the product distribution, due to strong adsorption on the site that activates propane.

5.1 Introduction

Recently, oxidative conversion of LPG has been reported over Li-Dy-Cl-MgO catalysts: yield of olefins (mixture of butenes, propene and ethene) as high as 50% were obtained [17,63]. While ethane oxidative dehydrogenation and methane oxidative coupling have been studied extensively over alkali promoted magnesia [14,15,66,67], studies of propane oxidative dehydrogenation over these materials are limited [16,35]. In Chapter 3 oxidative conversion of propane and n-butane gave yields of olefins in the range of 50%. Propene and ethene were the major olefin products when propane was used as feed. The ratio of propene to ethene was higher compared to steam cracking at similar conversions, implying a strategic advantage to meet future increased propene demand. From the catalysts reported by Landau *et al.*, (for e.g., Li-Cl-Dy-Mg-O) in Chapter 3 we have shown that lithium was the only essential ingredient for a well performing catalyst, thus providing a Cl free oxidation catalyst.

Cl^- addition gave only marginal improvements in olefin yields, but induced stability problems. A simplified catalyst system Li/Dy/MgO works equally efficiently, the role of each component in this catalyst has also been discussed in detail in Chapters 3 and 4.

In this chapter a detailed study on the reaction kinetics of propane and propene oxidation in the presence of oxygen over Li/Dy/MgO catalyst is reported and a reaction mechanism will be proposed based mainly on the kinetic measurements.

5.2 Experimental

The catalysts was prepared by wet impregnation described in Chapter 2, using aqueous solution of $LiNO_3$ and mixture of MgO and Dy_2O_3 powder with the following target composition of the catalyst: 85 wt% MgO, 7.7 wt% Li_2O and 7.3 wt% Dy_2O_3.

Reaction rates were determined under differential conditions as described in Chapter 2. The feed for typical measurements consisted of 28% propane, 14% oxygen, 2% carbon-dioxide and balance helium. When the kinetics of propene conversion was measured the typical feed consisted of 28% propene, 7% oxygen and 1% carbon-dioxide. Carbon dioxide has been introduced to the feed in order to achieve a constant CO_2 concentration over the whole catalyst bed, as CO_2 has a strong inhibiting effect upon the reaction (for further details see results). The total flow rate was 100 ml/min unless stated otherwise. Propane conversion was less than 10% and oxygen conversions were lower than 15% in all cases unless otherwise noted. The carbon balance closed within ±3% in all experiments where propane conversion was lower than 10%.

Reaction rates were calculated as mol product formed per second per gram of catalyst ($mol.s^{-1}.g^{-1}$). When measurements were done in the absence of a catalyst, rates were calculated in terms of mol product formed per second per ml reactor volume ($mol.s^{-1}.ml^{-1}$). All rates were expressed in terms of reactor volume ($mol.s^{-1}.ml^{-1}$) when rates obtained with catalyst were compared to rates measured in the absence of catalyst, under identical temperature, partial pressures and flow rate conditions.

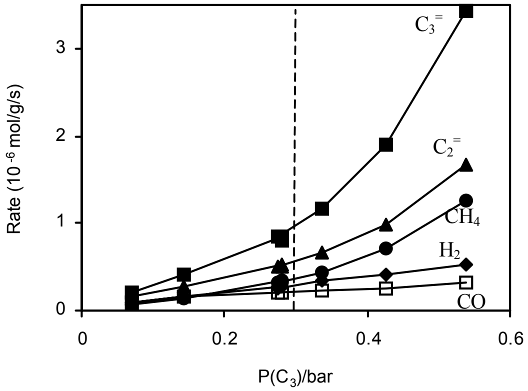

Figure 5.1. Rates of formation vs. *propane partial pressure over the catalyst. Conditions: P(CO_2): 20 mbar; P(O_2): 140 mbar; T: 600°C; total flow: 100 ml/min; 200 mg catalyst.*

Mass transfer and heat transfer limitations were evaluated by calculation. The criteria suggested by Mears indicated the absence of mass- and heat-transfer limitations [68,69].

5.3 Results

5.3.1 Propane partial pressure variation

Rates of formation of products varied linearly with propane partial pressure in the range of 0-0.3 bars (Figure 5.1). This indicates a first order reaction, where propane participates in the rate-determining step. Above 0.3 bars the rate of formation of propene, ethene, and methane showed an exponential increase, while the rate of formation of CO and hydrogen continued to vary linearly.

5.3.2 Oxygen partial pressure variation

The rates of formation of products appear to follow a complex pattern with respect to the oxygen partial pressure (Figure 5.2). The rates of formation of propene, ethene and methane increased steeply at very low oxygen partial pressures, i.e., when increasing oxygen partial pressure from 0 to 5 mbar. It is interesting to note that in the absence of oxygen the molar rates of formation of propene, ethene and methane are nearly equal. Increasing oxygen in the feed from 0 to 5 mbar maintains this 1:1:1 ratio. Further increase of oxygen content in the feed had differing effects on the different products. Propene continued to increase linearly with oxygen partial pressure while ethene remained constant. Rate of methane formation declined with oxygen partial pressure, while at the same time the formation rate of CO increased. By power law fit of these data it was calculated that the formation rate of CO has an apparent order of 0.5 in oxygen partial pressure.

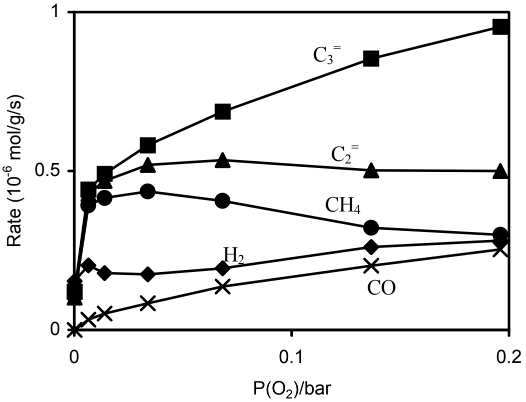

Figure 5.2. Rates of formation over the catalyst vs. *oxygen partial pressure. Conditions: P(CO_2): 20 mbar; P(C_3H_8): 280 mbar; T: 600°C; total flow: 100 ml/min; 200 mg catalyst.*

It is important to note that the sum of production rates of CH_4 and CO equals the formation rate of ethene independent of the partial pressures of both propane and oxygen. This fact seems to indicate that a common C_1 intermediate leads to formation of CH_4 and CO.

5.3.3 Gas phase reactions

The reaction kinetics of propane conversion was also evaluated in an empty reactor in order to assess the extent to which gas phase homogeneous reactions influence the conversion of propane. Propane and oxygen partial pressures have been varied in a manner similar to experiments with catalyst present in the reactor. Care has been taken to avoid any Li contamination of the quartz reactor.

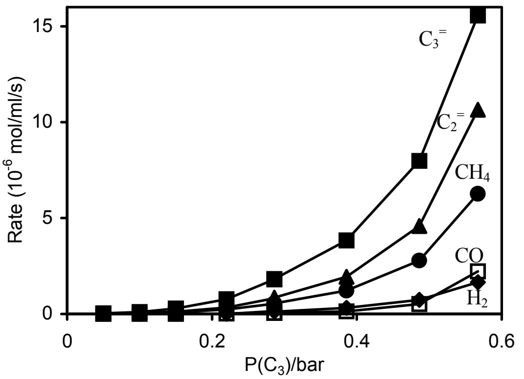

Figure 5.3. Formation rates in the empty reactor vs. *propane partial pressure. Conditions: P(CO_2): 20 mbar; P(O_2): 140 mbar; T: 600°C; total flow: 100 ml/min; 250 µl cylindrical empty volume.*

When the propane partial pressure was varied during reaction in the empty reactor, the formation rates for all products increased exponentially (Figure 5.3). The apparent reaction order increases with propane partial pressure. Formation of CO and H_2 was not detectable below 0.2 bars of propane. Reaction rates varied in a similar fashion with oxygen partial pressure as in the presence of catalyst (Figure 5.4). In both cases a sharp increase at low oxygen pressures was observed. Hydrogen was also formed with a comparable rate. However, the rate of formation of CO was four times lower than that in the presence of catalyst. In the case of the empty reactor the sum of the CO and CH_4 formation rates is not equal to the ethene formation rate (Figure 5.4).

The conversion increased linearly with residence time when catalyst was present. In the empty reactor conversion increased exponentially and followed an S-curve at high residence time due to the exhaustion of oxygen (Figure 5.5). At residence times lower than 0.5 s conversion with the catalyst bed was higher, while at higher residence times (>0.5 s) conversion in the empty reactor was higher than that over the catalyst bed. It has to be mentioned, however, that this experiment was not attempted to be confined to differential conversion and CO_2 was not added to the reaction feed, unlike in all other measurements reported in this chapter. The typical residence time for standard conditions of 28% propane, 14% oxygen, 2% CO_2 and balance helium with 100 ml/min total flow rate at 600°C was 0.15 s in the empty reactor and 0.06 s when the catalyst was present.

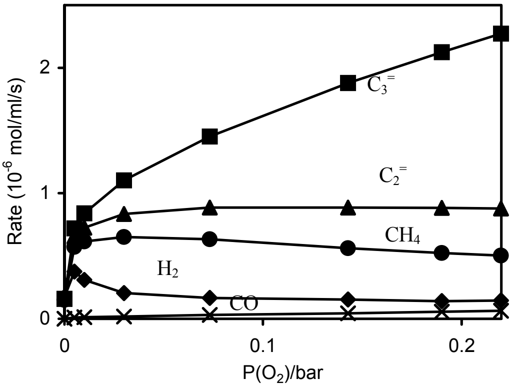

Figure 5.4. Formation rates as a function of oxygen partial pressure in the empty reactor. Conditions: P(CO_2): 20 mbar; P(C_3H_8): 280 mbar; T: 600°C; total flow: 100 ml/min; 250 µl cylindrical empty volume.

The post-catalytic void downstream the catalyst bed was increased by the same volume as the volume of the catalyst bed (e.g. 250 µl) by pulling the inserted quartz bar away from the catalyst bed. This change caused 25% increase in propane conversion at the typical condition of 28% propane, 14% oxygen, 2% CO_2 and balance helium with 100 ml/min total flow rate at 600°C.

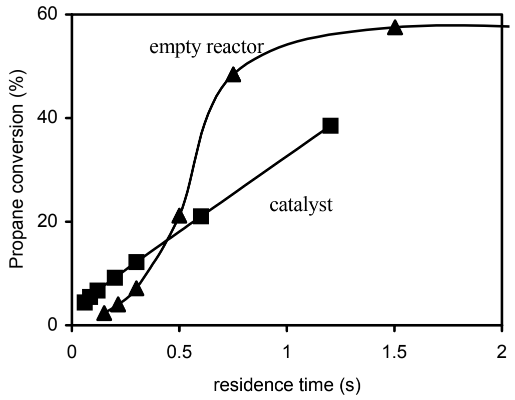

Figure 5.5. Conversion of propane vs. *residence time with and without the catalyst bed. Conditions: $P(C_3H_8)$: 280 mbar; $P(O_2)$: 140 mbar; T: 600°C; total flow: 5-100 ml/min; 250 µl cylindrical empty volume with and without 200 mg catalyst.*

5.3.4 *Effect of reaction products on the reaction rates*

The reaction pathways were investigated by measuring the influence of product species added to the feed on the reaction rates. Product species were added to the reaction mixture, keeping all the conditions including temperature, partial pressures and flow rates constant, except for the partial pressure of He to balance the addition. Figure 5.6 shows the relation between the amount of CO_2 in the feed and the rates of formation of all products. For the sake of clarity, only the rate of propene formation was plotted on the graph, the rates for the other products can be evaluated *via* the selectivities. The rates decreased with a negative order in the CO_2 partial pressure as observed in the methane oxidative coupling also [70], while selectivity to propene and ethene was not significantly affected (Figure 5.6). The strong inhibition caused by the carbon dioxide appears to be reversible, as the activity was restored to its original value, when CO_2 was removed from the feed.

The influence of the CO_2 concentration on the activity is the most significant effect, whereas all other product species showed only minor effects, as will be shown later. Differential measurements result in correct data only when the concentration of all species that influence the reaction rates, are approximately constant. Therefore, it was necessary to add excess CO_2 to the feed in all differential measurements reported here. Addition of CO_2 to the reaction feed did not have any significant influence upon the reaction rates in the absence of catalyst.

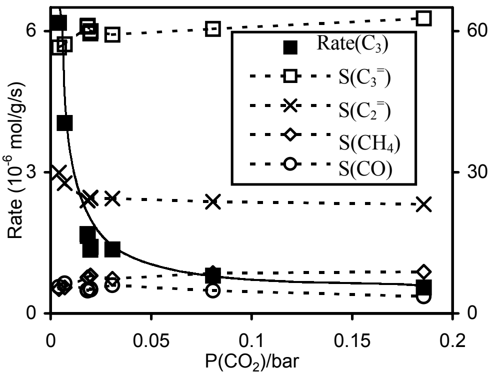

Figure 5.6. Influence of CO_2 over catalytic formation rate of propene and selectivity of the main products. Conditions: $P(C_3H_8)$: 280 mbar; $P(O_2)$: 140 mbar; T: 600°C; total flow: 100 ml/min; 200 mg catalyst.

Adding 5% hydrogen to the reaction mixture influenced the reaction rates only to a marginal extent at 600°C; i.e., the selectivity to CO increased from 9% to 10% and the selectivity to CO_2 decreased from 12% to 11%. Significant conversion of hydrogen was not observed. Addition of water had also no significant influence on the reactions.

The presence CO reduced the reaction rates, however, this inhibiting effect is far smaller than that of CO_2. Adding 5% CO to the reaction stream (which is 10 times more than what is produced in the reaction under the tested conditions) decreased the conversion at 600°C from 7% to 5% and at 650°C from 27.5% to 24%. It was observed that part of the CO was converted to CO_2. Selectivities for the major products were not affected significantly.

5.3.5 Reactions of propene

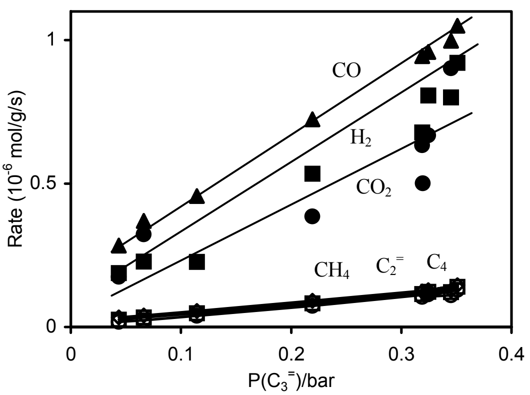

Figure 5.7. Propene partial pressure influence over propene conversion. Conditions: P(CO_2): 10 mbar; P(O_2): 70 mbar; T: 600°C; total flow: 100 ml/min; 200 mg catalyst. CO: triangles, H_2: filled squares, CO_2: filled circles.

The rates of formation of products from the primary product propene were measured as a function of the partial pressures of propene, oxygen and CO_2 in order to assess the reaction kinetics of the secondary reactions. The conditions used were similar to that of propane reaction.

The main products from propene were carbon oxides and hydrogen. The carbon oxides accounted for 70-80% of the products made. Other products include methane, ethene, C_4 (mainly 1-butene), and small amounts of unidentified higher hydrocarbons. The rate of formation of all the measured products varied linearly with the partial pressure of propene (Figure 5.7). The rates of formation of methane, ethene and C_4 were similar over the whole pressure range. The influence of oxygen partial pressure on the propene reaction was clearly different from its effect on the propane conversion. The rates of formation of the main products mentioned above increased linearly with oxygen partial pressure (Figure 5.8). Also in this case the rates of formation of methane, ethene and butene varied similarly.

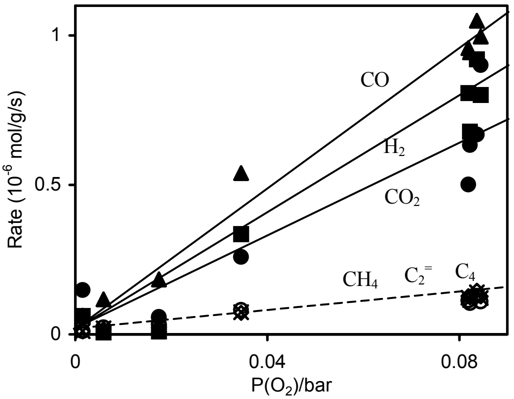

Figure 5.8. Oxygen partial pressure effect over propene catalytic oxidation. Conditions: P(CO_2): 10 mbar; P(C_3H_6): 280 mbar; T: 600°C; total flow: 100 ml/min; 200 mg catalyst. CO: triangles, H_2: filled squares, CO_2: filled circles.

Carbon dioxide had a comparable inhibiting effect on the conversion of propene as on the conversion of propane. Rates of formation of all products decreased with increasing CO_2 partial pressure without markedly changing the product spectrum (Figure 5.9). It can be calculated from these data that the reactions to H_2, CO, CO_2, methane and ethene are order -1 in the CO_2 partial pressure.

Reacting a mixture of propene and hydrogen with oxygen over the catalyst at 600°C, we did not observe preferential combustion of hydrogen. Adding up to 5 vol.% hydrogen did not influence the propene conversion significantly. Upon increasing the hydrogen concentration to 20 vol.%, the conversion rate of propene increased by a factor of 2, and the CO formation rate by a factor 2.4. Under these conditions hydrogenation of propene to propane was not observed.

The propene conversion rate was three times lower than the conversion rate of propane over the catalyst under the same experimental conditions (28% hydrocarbon, 7% oxygen, 2% CO_2 at 600°C). Propene appears to be stable in the gas phase even in the presence of oxygen. The conversion rate of propene was about 40 times lower than the conversion rate of propane under the same conditions (28% hydrocarbon, 7% oxygen at 600°C).

Addition of 2 vol. % propene to the reaction mixture (8 vol. % propane and 10 vol. % oxygen in He) decreased the conversion of propane by 25 to 30% over the catalyst at 600°C. The rate of formation of CO_x from that mixture is equal to the sum of the rates of CO_x formation in the individual reaction of propane and propene. Significant differences in the propene conversion rate were not detected, when it was co-fed with propane, compared to oxidation of propene alone.

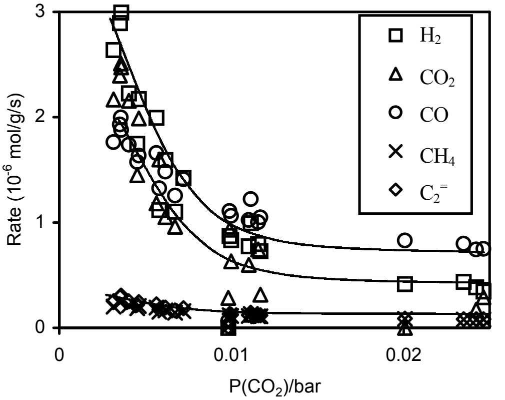

Figure 5.9. Influence of CO_2 over the propene oxidative conversion. Conditions: P(C_3H_6): 280 mbar; P(O_2): 70 mbar; T: 600°C; total flow: 100 ml/min; 200 mg catalyst.

5.4 Discussion

5.4.1 Catalytic vs. homogeneous activation of propane

Under certain conditions the conversion in the empty reactor is higher than the conversion in the reactor containing catalyst (see Figure 5.10). Therefore we will discuss first the question which of the two routes, homogeneous activation or catalytic activation of propane, prevails in the presence of the catalyst.

Activation of propane takes place predominantly on the catalyst as long as the propane partial pressure is below typically 0.3 bar. This is concluded from the strong inhibiting effect of CO_2 on the catalyst activity at 0.28 bars propane (Figure 5.6), while no effect of CO_2 was observed during measurements with the empty reactor. Moreover, a reaction order of one in propane as shown in Figure 5.1, clearly differs form the exponential relation observed in the empty reactor (Figure 5.3), where the reaction order is continuously increasing with propane partial pressure. Furthermore, Figure 5.5 shows a linear relationship between contact time and conversion for the catalyst, whereas the empty reactor shows a sigmoidal relationship. Thus, the activation mechanisms are clearly different in the two cases. The empty reactor shows typical behavior of a radical gas-phase process, during which a pool of radicals needs to be formed to autocatalytically accelerate the reactions [71,72]. In contrast to this, experiments with the catalyst show behavior typical for a catalytic reaction with propane taking part in the rate-determining step. The rates of propane conversion expressed in terms of mols per reactor volume per second with the catalyst and in the empty reactor are compared in Figure 5.10. In the same plot, the rate over the catalyst corrected to the same residence time as in the empty reactor, with the dense volume of the catalyst bed, is also shown. In the correction procedure it was assumed that all reactions take place in the volume of the reactor where the catalyst bed is located, small contributions to the residence time from the entry and exit zones were neglected.

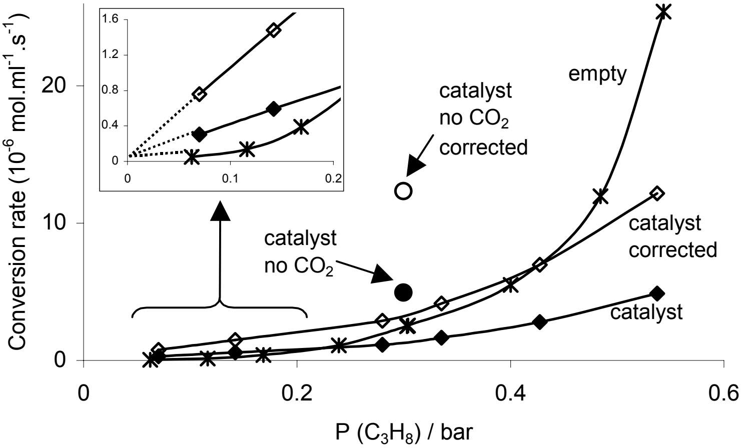

Figure 5.10. Volumetric reaction rate of propane conversion vs. *propane partial pressure: over the catalyst (filled diamonds), over the catalyst corrected for the same residence time as in the empty reactor (open diamonds) and in the empty reactor (stars). Conditions: P(CO_2): 20 mbar, except where noted; P(O_2): 140 mbar; T: 600°C; total flow: 100 ml/min; 200 mg catalyst or 250 μl cylindrical empty volume.*

It follows from these observations that the contribution of alkane activation in the gas phase is much smaller when the catalyst is present than in the empty reactor. In Figure 5.11 the rates over the catalyst bed (from Figure 5.1) are separated into contributions from catalytic activation and homogeneous gas phase activation. Extrapolating the linear increase at low partial pressures to the high partial pressures the contribution of the catalyst is tentatively obtained (continuous line in Figure 5.11). The second contribution is obtained by subtracting the extrapolated line from the measured data (dashed line in Figure 5.11). The resulting curve strongly resembles the dependence of the conversion rate upon pressure in the empty reactor. Therefore, this contribution is attributed to homogeneous gas-phase reactions. The rate of the homogeneous gas-phase reaction estimated in this way is one order of magnitude lower than the rates observed in the empty reactor. The decrease in contact time caused by the volume occupied by the catalyst cannot account for this decrease. Apparently, quenching of gas-phase radicals takes place, similarly to the process observed during methane oxidative coupling [29,50,73], limiting the formation of a pool of radicals to accelerate the reaction.

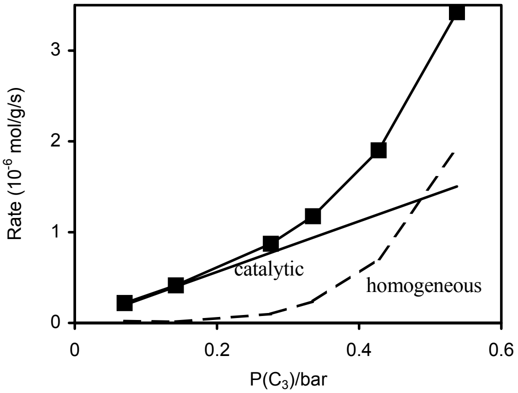

Figure 5.11. Decomposition of the rate of propene formation into catalytic and homogeneous contributions. Data from Figure 5.1.

In conclusion, it appears that the rate-determining step in the reaction pathways to propene, ethene and methane involves activation of propane on the catalyst surface, provided that the propane concentration is below typically 0.3 bars, despite the fact that catalyst activity in this study is significantly suppressed by addition of CO_2. At the typical reaction condition of 28% propane, 14% oxygen and 2% CO_2, total flow rate of 100 ml/min with the catalyst present, the homogeneous activation is insignificant according to the estimation shown in Figure 5.11. However, at the highest propane partial pressure employed (0.5 bar) the contributions of homogeneous gas phase reactions and catalyzed reactions are approximately equal in the presence of catalyst.

The rate of formation of hydrogen and CO remain linear up to very high propane partial pressures, indicating that these products are mainly formed through catalysis on the solid surface. The comparatively low formation rates of H_2 and CO in the homogeneous reaction support this conclusion.

5.4.2 The role of oxygen and the reaction mechanism

The role of oxygen in activating propane is complex. The presence of oxygen opens a fast reaction pathway, shown by the marked increase of the rates of hydrocarbon product formation upon increasing the oxygen concentration from 0 to 5 mbar (Figure 5.2). This very significant increase is not due to shifting the chemical equilibrium, as the gas composition at the reactor exit is far from the equilibrium even in the absence of oxygen. A stepwise increase of the rates in the empty reactor is also noted (Figure 5.4) pointing out the role of gas-phase oxygen in the reaction pathways to the products. However, oxygen does not participate in the rate determining step at pressures above 5 mbar, as the apparent reaction order in oxygen observed is below 0.2 for propene, ethene and methane. Oxygen possibly reacts fast with an activated intermediate and this reaction step is rate determining at extremely low oxygen partial pressures only.

The mechanism proposed to be operative under our conditions here is based on homogeneous radical chain propagation reactions, similar to thermal pyrolysis. Thus, we need to introduce the terminology for radical chain reactions. The term “activation” used so far should be understood as “initiation” in the terminology of radical chemistry. We propose that the initiation takes place mainly on the catalyst at low propane partial pressures, while at the highest partial pressures both on the catalysts and in the gas phase. The catalyst influences the radical concentration in two ways, as it not only generates radicals but also quenches them. The place of initiation is speculated to be a Li^+O^- site [67, Chapter 3]. Let us examine first the situation without oxygen.

5.4.3 Mechanism in the absence of oxygen

When propane is activated on the catalyst a propyl radical is formed by a hydrogen abstraction. Hydrogen is transferred to the O^- and forms OH^-. *In situ* DSC studies of methane activation over Li/MgO catalysts at 650°C showed heat evolution due to surface OH^- formation on the Li^+O^- active site [74]. *In situ* DRIFTS studies of Li/MgO catalyst under methane oxidative coupling conditions (at 690°C) showed the presence of strongly bound OH^- [75]. In analogy, we conclude, therefore, that in the presence of catalyst propane will form a propyl radical and surface OH^-.

Two different propyl radicals can be formed depending on whether primary or secondary hydrogen is abstracted. Based on bond energies we tempt to conclude that predominantly iso-propyl radicals are formed on the catalyst (i.e. C-H bond energy on a secondary carbon atom is 3 kcal/mol lower than on the primary one), however, there is no experimental evidence to confirm this. The two radicals have different decomposition routes: i-propyl can only undergo β-scission of C-H bond and decomposes into propene and a hydrogen atom, while n-propyl preferentially follows a C-C cleavage in the β position, forming methyl radical and ethene [76,77]. The methyl radical reacts then with a second propane molecule forming methane and regenerating the propyl radical. The hydrogen atom also reacts with another propane molecule generating a propyl radical, and H_2. The four described reactions are presented below:

$$\text{i-}C_3H_7 \cdot \rightarrow C_3H_6 + H \cdot \tag{1}$$

$$\text{n-}C_3H_7 \cdot \rightarrow C_2H_4 + CH_3 \cdot \tag{2}$$

$$CH_3 \cdot + C_3H_8 \rightarrow CH_4 + C_3H_7 \cdot \tag{3}$$

$$H \cdot + C_3H_8 \rightarrow H_2 + C_3H_7 \cdot \tag{4}$$

From the kinetic models of the radical chemistry in the oxidative pyrolysis and combustion literature it appears that in the propagation steps, i-propyl and n-propyl radicals are produced with comparable rates [78-80]. Consequently rates of reactions (1) and (2) should be similar, and the same follows for rates of reactions (3) and (4). Thus, formally the probability of C-C and C-H bond breakage is comparable. This would result in similar amount of propene, ethene, methane and hydrogen, which agrees well with our experimental observations at very low oxygen partial pressures (points at 0 bars oxygen in Figure 5.2 and Figure 5.4). Similar ratios between the products were also observed in thermal cracking (without oxygen) at low conversions [78,81].

5.4.4 Mechanism in the presence of oxygen

The presence of oxygen has two important effects. First, we discuss the influence of oxygen on the homogeneous chemistry that takes place. Second, we will discuss the effect of oxygen on the catalyst.

The enhancement seen by the oxygen addition can also be explained with the proposed radical chemistry [41]. The introduction of oxygen, even in small amounts, increases the number and the concentration of the chain carrier radicals. When oxygen is not present H · and CH_3 · radicals are the main chain propagators according to reactions (1)-(4). In the presence of oxygen the i-propyl radical reacts fast with the oxygen molecule forming a hydroperoxyl (HO_2 ·) radical and propene. The hydroperoxyl radical further reacts with a new propane molecule forming H_2O_2, which by decomposition gives two hydroxyl radicals (OH ·). OH · becomes the main chain propagator [82] and it forms water by reacting with a propane molecule. This is perfectly in line with the fact that hydrogen combustion did not occur selectively in our reactor. Thus, we conclude that water is mainly formed in the above described process. The similarity of the influence of small amount of oxygen on the propane conversion in the absence and presence of catalyst confirms the proposal that O_2 mainly influences the gas-phase radical propagation reactions, independent of the origin of radical initiation.

The CH_3 · radical is the precursor for CO and CH_4 in the presence of oxygen. When ethene is formed through reaction (2) a methyl radical is produced that can react further either to methane or CO. If this methyl radical reacts with a propane molecule, methane is formed. If it reacts with oxygen an oxygenated intermediate is formed, which is subsequently transformed into CO and further to CO_2. Because the same numbers of CH_3 · radicals and

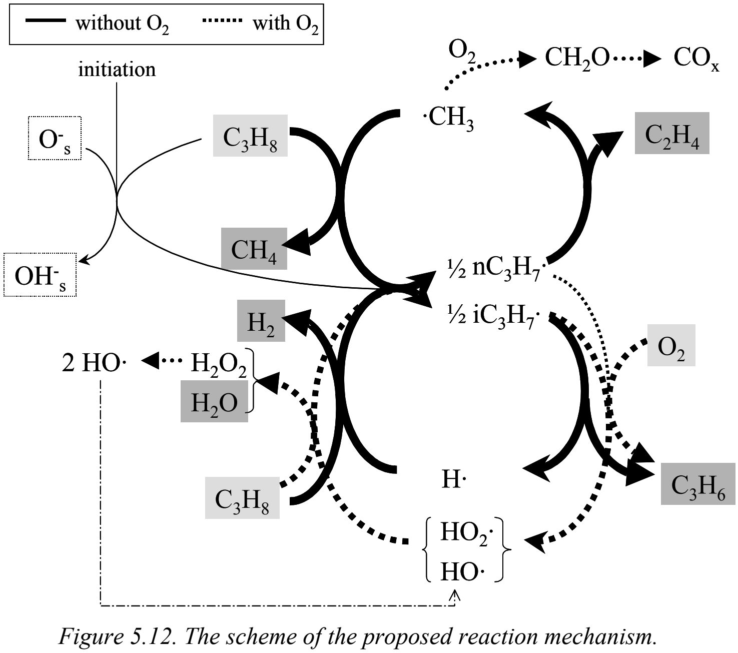

Figure 5.12. The scheme of the proposed reaction mechanism.

ethene molecules are formed in reaction (2) the sum of the formation rates of CH_4 and CO equals the formation rate of ethene over the whole range of partial pressures of both propane and oxygen (see Figure 5.1 and Figure 5.2). In the empty reactor the sum of the rates of CO and CH_4 formation does not match the ethene formation rate. We speculate therefore that a stable oxygen-containing C_1 intermediate is formed (formaldehyde, for example) which is quantitatively converted to CO over the catalyst, but is stable in the gas-phase. Analysis of oxygenates was not performed, but the small gap in the carbon balance (2-3%) makes this hypothesis feasible, since mechanistic models of homogeneous alkane oxidation predict the formation of formaldehyde [50,82].

So far we have dealt with hydrocarbon activation and gas-phase reaction steps. The proposed reaction mechanism is schematically represented in Figure 5.12. Assuming the proposed initiation on the catalyst by hydrogen abstraction, the question arises, as to how the catalytic sequence is closed by regeneration of the active site, *i.e.,* how hydrogen is removed from the active oxygen.

In the methane oxidative coupling literature primarily Li/MgO dehydroxylation was proposed as the regeneration step [45]. However, this step requires an energetically demanding removal of lattice oxygen. Regeneration of the active site is possible without dehydroxylation with the help of O_2. Recently a new mechanism has been proposed that does not require the highly energetic removal of lattice oxygen, based on computation of energetic state of various surface intermediates [43]. A sequence of reactions has been proposed by Sinev *et.al.* [44,83]. The four reactions proposed are presented below:

$$O_2 + OH^-_s \rightarrow O^-_s + HO_2 \cdot \qquad (5)$$

$$HO_2 \cdot + OH^-_s \rightarrow O^-_s + H_2O_2 \qquad (6)$$

$$H_2O_2 \rightarrow 2\,OH \cdot \qquad (7)$$

$$OH \cdot + OH^-_s \rightarrow O^-_s + H_2O \qquad (8)$$

The overall reaction equation of the regeneration is the same as in the mechanism proposed by Ito *et al.* [45] but it does not require or suggest the removal of lattice oxygen. The experimental demonstration of this mechanism at 650°C showed that OH^-_s is decomposed upon admission of oxygen to the reactor while water is formed [44,83]. It was also shown that dehydroxylation can occur as well especially at high temperatures as a parallel regeneration route [84]. Analysis of the literature data on redox mode methane coupling suggests that at intermediate temperatures (600-650°C) regeneration must occur without lattice oxygen removal, while at high temperatures (>700°C) lattice oxygen removal is the most feasible route [85,86]. In addition to water elimination by dehydroxylation, some dihydrogen elimination from the Li/MgO catalyst was also reported above 600°C [87]. The prevailing route under our conditions is, therefore, speculated to be the mechanism described in equations (5) to (8).

5.4.5 *Effects of byproducts on the catalytic performance*

CO_2 inhibits the reaction by adsorbing at the active Li^+O^- site. It has been shown in Chapter 4, that these types of catalysts strongly adsorb CO_2. TPD of carbon dioxide suggested that Li_2CO_3 forms under reaction conditions. The fact that selectivities do not change upon CO_2 addition (Figure 5.6) is in agreement with the hypothesis that the conversion of propyl radicals to propene, ethene and methane is controlled by gas-phase reactions, which are not influenced by CO_2. Fitting the rate data (only the catalytic contribution) results in a –1 order in CO_2 partial pressure. It is speculated that Li_2CO_3 is not formed directly, as that would result in –0.5 order, but possibly a stable precursor is formed initially. Adsorbing CO_2 on the Li^+O^- site results in $Li^+CO_3^-$ [88], which has been identified by ESR [89]. Adsorbed CO_2 was also detected by *in situ* IR spectroscopy, and it was suggested that CO_3^- formed is precursor for carbonate formation [75]. An alternative, though related explanation is based on the suggestion that under reaction conditions most of the active O^- sites exist in the form of (HO^-) [49]. Reaction of Li^+OH^- with CO_2 would result in lithium bicarbonate, accounting for the –1 order.

The small inhibiting effect of CO is tentatively explained by slow transformation of CO to CO_2 which subsequently blocks the active site possibly without desorption.

5.4.6 Importance of secondary reactions

It has been shown in Chapter 3 that the rate of conversion of propene was a factor 3 lower than the corresponding rate of propane conversion under the same conditions when catalyst was used. Propene appears to be even more stable in the gas-phase, because propene conversion was 40 times lower than propane conversion under similar conditions, when an empty reactor was used. Thus, we conclude that propene converts on the catalyst. This is also in agreement with the observation that CO_2 inhibits the conversion of propene (Figure 5.9). Moreover, the CO_2 inhibition also suggests that the catalytic site for propene activation must be the same Li^+O^- active center as for propane activation.

The remarkable stability of propene in the gas-phase can be explained by the stability of the allyl ($C_3H_5\cdot$) radical, which is formed upon activation of propene. The part of reaction pathways, which occurs in the gas-phase, depends on the reactivity of the radicals released upon activation. Allyl radicals do not have a fast decomposition route in the gas-phase, unlike the propyl radicals that are considerably more reactive. Therefore, the efficiency of propagation steps is greatly reduced; consequently, propane conversion due to radical chain propagation reactions is higher than that of propene [90].

CO_x forms on the catalyst in analogous mode from propane and propene, as follows. CO is formed from propane only through catalytic activation pointed out by the first order in propane for the whole partial pressure range (Figure 5.1) and no CO in the empty reactor (below 0.3 bar, Figure 5.3), while CO formation was rate limited in oxygen (0.5 order in Figure 5.2). Similarly, Figure 5.7 and Figure 5.8 show that the conversion of propene to CO and CO_2 is first order both in propene and oxygen. This suggests a rate-determining step involving both propene and oxygen. Note, that the rate of CO_x formation is comparable from both hydrocarbons, thus the total oxidation of propane at low conversions, during differential measurements in this chapter, does not occur *via* the consecutive reaction of propene.

The presence of propane does not seem to influence the conversion of propene significantly, but the conversion of propane is reduced if propene is present, probably by "quenching" of the radicals by the propene molecule while forming slow reacting allyl radical.

The enhancement of propene conversion upon addition of hydrogen can be explained by the fact that hydrogen removes the carbonate from the surface of the catalyst, as we observed some CO evolution when hydrogen was fed over the catalyst in the absence of any significant hydrogen conversion. In this manner hydrogen increases the availability of active sites, and thus contributes to the enhancement of the reaction.

5.5 Conclusions

In this chapter the main features of the reaction kinetics of the oxidation of propane and propene over Li/Dy/MgO catalysts have been described. A mechanism that qualitatively explains these kinetic results is proposed in terms of mixed heterogeneous-homogeneous radical reaction routes.

Propane activation is rate determining for all reaction products and rates are first order in propane up to 0.3 bars. At high propane partial pressures (>0.3 bars) the reaction order increases for all hydrocarbon products. This has been attributed to contributions from homogeneous activation of propane.

The presence of gas phase oxygen appears to be crucial for propane conversion. The influence of oxygen on the reaction rates has been attributed to the interaction of oxygen molecules with the chain carrier radicals, independent of the formation route of those radicals, either on the catalyst or in the gas-phase. A second function of oxygen is to regenerate the catalyst *via* removal of hydrogen from the catalyst in order to restore the activity of the catalyst for generation of radicals.

Carbon-dioxide strongly suppresses the activity of the catalyst for all products. The apparent order is –1, which his is attributed to blocking of active sites by forming $Li^+CO_3^-$ on the active site, which is possibly a precursor in the formation of lithium carbonate. Reactions in the gas-phase were not influenced by CO_2.

Consecutive reactions of propene give almost exclusively carbon oxides and proceeds mainly on the catalyst. The rate of conversion is low compared to the rate of conversion of propane due to the relative stability of the intermediate allyl radical compared to the propyl radical under reaction conditions.

Acknowledgement

Dipl.-Ing. U. Kürten for helpful discussions regarding the mechanism.

Chapter 6

6 Factors that influence catalytic activation, hetero-homogeneous reactions and the selectivity of C-C bond *vs.* C-H bond scission during the oxidative conversion of lower alkanes to olefins

Abstract

Activation of propane over Li/MgO catalyst has been investigated. It is shown that Li/MgO catalyst is able to undergo deoxygenation/ reoxygenation cycles. Catalytic activity shown by Li/MgO has a strong correlation to the amount of oxygen that is removable. It is proposed that the sites containing removable oxygen are responsible for the activation of propane. While one such oxygen was consumed, in the absence of gas-phase oxygen, about 70 propane molecules were converted, implying a mechanism in which propane molecules are activated on the catalyst resulting in propyl radicals that are released to the gas phase where they undergo chain propagation reactions to result in products observed.

Thus the oxidative conversion of propane over Li/MgO catalysts follows a mixed heterogeneous-homogeneous radical chemistry where the catalyst acts as an initiator. At low propane partial pressures (0.1 bar), the surface to volume ratio of the catalytic reactor does not influence the chain length in the propagation step. At higher propane partial pressures (>0.3 bar), that are favorable to extensive gas phase reactions, the catalyst has also a role to provide for quenching and chain termination, thus affecting activity and selectivity.

6.1 Introduction

Although there are only a few studies of propane oxidative conversion, propane oxidation appears to produce better olefin selectivities non-catalytically than over redox or non-redox type catalysts. It is unclear from literature whether non-catalytic contributions are important during catalytic propane conversion, unlike in methane oxidative coupling where the role of catalytic and homogeneous reactions is well established [29]. Some authors explain their results of propane conversion to olefins only in terms of catalytic reactions not affected by homogeneous gas-phase contribution [30-32], while others describe their results in terms of radical reactions in the gas-phase initiated on the catalyst, and radical-surface interactions [33,34]. Furthermore, Burch and Crabb [35] compared catalytic and non-catalytic reactions of propane and concluded that the combination of heterogeneous and homogeneous reactions offers better opportunity for obtaining commercially acceptable yields of olefins than a purely catalytic reaction.

In Chapter 5 a reaction mechanism is suggested which involves a sequence of propane activation on the [$Li^{+}O^{-}$] active sites of Li/MgO catalysts and gas-phase chain propagation reaction routes; the conditions when catalytic activation prevails over homogeneous activation were also rigorously defined; the role of heterogeneous and homogeneous reactions was established. It was observed that at low propane partial pressures catalytic activation prevails, while at high partial pressures of propane (typically above 0.3 bars) homogeneous activation of propane contributes to the overall performance. Heterogeneously initiated radical chain propagation reactions explained the product spectrum. Quenching role has been attributed to the catalyst at very high partial pressures of propane (>0.4 bars). The catalytic activation of propane has been proposed as the initiation step of the radical chemistry, when oxygen of the active site abstracts a hydrogen atom from propane and results in the formation of n- or iso- propyl radicals depending on whether the hydrogen was bonded to a primary or secondary carbon atom. These radicals are released into the gas phase where they first undergo decomposition reactions. The two propyl radicals have different decomposition routes: iso-propyl gives propene and $H\cdot$, n-propyl gives ethene and $CH_3\cdot$. The radicals that result from the decomposition continue the chain propagation reactions, by activating new propane molecules resulting in an equal distribution of iso- and n-propyl radicals. In the presence of oxygen the concentration of radicals increases because oxygen reacts fast with the propyl radicals to form propene and a new chain-carrier radical, $HO_2\cdot$. A C_1 compound is formed as result of $CH_3\cdot$ reaction, and depending on the partial pressure of oxygen it is methane or CO.

The effect of the catalyst constituents and the role of chlorine in a Mg-Li-Dy-Cl-O complex catalyst are reported in Chapter 3 and 4. It was concluded that only Li is crucial for the catalyst activity and selectivity, moreover chlorine introduced stability problems.

The aim of this chapter is to characterize the active sites of Li promoted magnesia catalysts that are responsible for the catalytic activation of propane, and to discuss the role of Li in creating the active sites. We also report on the role of factors that influence selectivity towards the main products and discuss the relative rate of occurrence of a C-C or a C-H bond cleavage. All measurements reported here were carried out under conditions unfavorable to purely homogeneous reactions (low propane partial pressure: 0.1 bar), unless otherwise noted.

6.2 Experimental

Catalysts containing varying amounts of Li, studied in this chapter, were prepared from MgO (Merck, assay 99.6%, high surface area magnesia: Ube Mat. Ind. 99.98%), $LiNO_3$ (Merck, >98.0%) and for dysprosia containing catalyst Dy_2O_3 (Fluka, 99.9%), according to the wet impregnation method described in detail in Chapter 2. The Li content and the impurity level of the samples were evaluated in the bulk and on the surface by elemental analysis using XRF (Philips PW1480) and XPS (Physical Instruments Φ Quantum 2000) techniques, respectively. The composition and surface area of the catalysts studied are presented in Table 6.1.

Sorption measurements were carried out on a Mettler-Toledo TGA-SDTA apparatus. Argon was used as the carrier gas. Sample weight ranged between 50 to 100 mg, gas flow rate used was 50 ml/min, and a 70μl alumina crucible used as sample holder. The samples were activated at 750°C in Ar until no weight change was noted. Gas composition was made up from 90% Ar and 10% reactive gas, being one of CO_2, O_2, H_2 or propane.

Table 6.1. Chemical compositions and specific surface areas of the catalysts used

Catalyst	Composition	MgO (wt%)	Li_2O (wt%)	Dy_2O_3 (wt%)	BET (m^2/g)
MgO	MgO	100	-	-	75.1
MgO (high surface)	MgO	100	-	-	110
1%Li_2O/MgO	$MgLi_{0.007}O_x$	99.0	1.0	-	11.4
3%Li_2O/MgO	$MgLi_{0.08}O_x$	97.0	3.0	-	2.9
3%Li_2O/MgO(hs)	$MgLi_{0.08}O_x$	97.0	3.0	-	6.2
7%Li_2O/MgO	$MgLi_{0.2}O_x$	93.0	7.0	-	1.3
12%Li_2O/MgO	$MgLi_{0.37}O_x$	88.0	12.0	-	<1
Li/Dy/MgO	$MgLi_{0.2}Dy_{0.02}O_x$	85	7.7	7.3	1.3
Li/Dy/MgO(hs)	$MgLi_{0.2}Dy_{0.02}O_x$	85	7.7	7.3	6

Details involved in the kinetic measurements are given in Chapter 2. During transient catalytic measurements samples were collected with multiport valve in sample storage system. During pulse measurements the reactor effluent was directly connected *via* Porapack Q column to the TCD detector.

In order to check impurities in the catalyst to which redox capacity could be attributed, the impurity level of all the Li/MgO catalysts and the starting materials used for the preparation of catalysts was evaluated by the XRF technique (only elements heavier than Na can be detected). The following compounds and elements were detected (maximum amount in wt% in parenthesis): SiO_2 (0.2), S (0.06), Cl (0.05), K_2O (0.002), CaO (0.04), Fe_2O_3 (0.007), Cs_2O (0.0002), BaO (0.003). MgO was the source of sulfur impurity, while iron was present in both MgO and $LiNO_3$. XPS measurements showed no impurity accumulation on the surface; the only elements detected on the surface were: Mg, O, C and Li.

6.3 Results

6.3.1 Catalytic performance of Li/MgO catalysts with varying Li content

In Chapter 3 it is shown that from a complex catalyst composition [Li-Cl-Dy-Mg-O] proposed in the patent literature [18] lithium was the only crucial component for a well performing catalyst. Here we present a detailed study on how the Li content of the Li/MgO catalyst influences the activity and selectivity to the various products.

Table 6.2 presents the catalytic performance data for the catalysts with varying amount of Li at several temperatures. Conversion was the highest for the 1 wt% Li_2O containing catalyst at all temperatures. Selectivities to olefins generally increased with Li content but at

600°C the selectivity for propene increased the most remarkably, from 25% to 40% when Li content increased from 0 to 7 wt% Li_2O.

Table 6.2. Performance of Li/MgO catalysts. Conditions: 10% propane, 8% oxygen in He, 100 mg catalyst, $WHSV_{propane}$:0.9 h^{-1}, total flow rate: 10 ml/min.

Catalyst	T(°C)	Conversion (%)	Selectivity (%)			
			C_3H_6	C_2H_4	CH_4	CO_x
MgO	550	4.3	14.0	13.9	0.7	71.4
	600	11.1	24.7	26.8	2.5	46.0
	650	43.3	34.6	32.9	11.7	20.3
1%Li_2O/MgO	550	7.6	22.2	18.0	0.6	59.2
	600	33.2	25.2	31.2	3.0	39.7
	650	64.1	19.7	36.2	7.6	32.5
3%Li_2O/MgO	550	5.4	23.5	19.5	0.7	56.2
	600	25.1	30.2	31.5	3.2	34.2
	650	58.8	23.2	36.5	7.2	28.7
7%Li_2O/MgO	550	1.2	28.4	28.2	2.2	41.0
	600	8.7	39.9	32.9	5.5	20.4
	650	33.1	34.9	36.7	8.1	16.6
12%Li_2O/MgO	550	1.1	30.2	22.6	1.6	45.6
	600	7	43	32	5.3	18
	650	26.2	37.6	38.0	9.1	10.5

The activity of 1%Li_2O/MgO catalyst was higher than the activity of MgO though the surface area of MgO was reduced considerably by Li addition (see Table 6.1). Addition of more Li further reduced the surface area paralleled by decrease of the catalytic activity. Addition of Li to MgO had the most significant effect on activity at 600°C, i.e. conversion increased 3 fold by adding 1 wt% Li_2O. Therefore, 600°C has been chosen for more detailed studies.

Rate of propane conversion, at 600°C, expressed in mol per gram catalyst per second (Figure 6.1) showed an optimum at 1 wt% Li_2O content. When the conversion rate of propane was expressed in mol per m^2 catalyst per second, the rate increased with Li_2O content up to 3 wt% where it leveled off.

In Figure 6.2 the effect of Li content on the selectivities to the main products is shown for a fixed temperature (600°C) at the same level of conversion (10%) achieved by space velocity variation. Propene selectivity increased continuously up to 7 wt% Li_2O and remained constant up to 12 wt% Li_2O. Ethene selectivity appeared to be constant for all the catalysts containing Li, and it was higher than that over pure MgO. Selectivities to CO and CO_2 were decreased strongly by increasing the Li content, whereas methane selectivity was slightly increased. All selectivities were similar for the catalysts containing 7 and 12 wt% Li_2O.

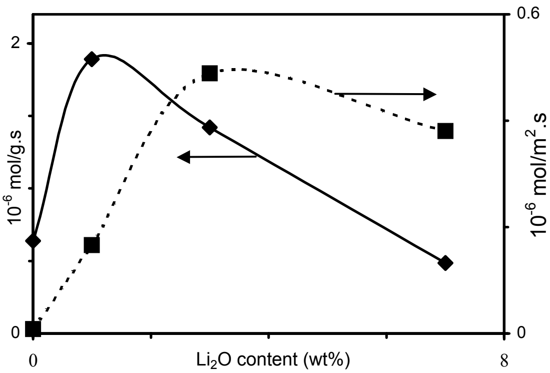

Figure 6.1. Rate of conversion of propane over Li/MgO catalysts as a function of the Li content expressed as rates normalized to the catalyst weight and specific surface area, respectively. Conditions: 10% propane and 8% oxygen in He; T: 600°C; total flow 10-80 ml/min.

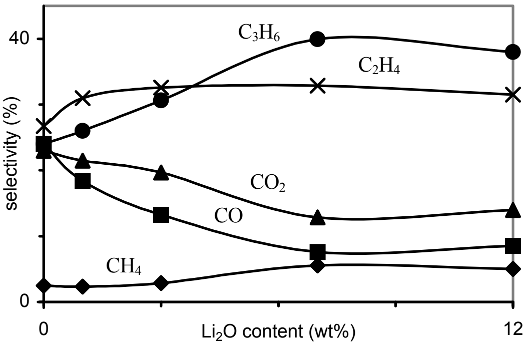

Figure 6.2. Selectivities towards the main products over Li/MgO catalyst as a function of the Li content at 10% conversion. Conditions: 10% propane and 8% oxygen in He; T: 600°C; total flow 10-80 ml/min.

6.3.2 Interaction of reactants and products on Li/MgO

Interaction of H_2, O_2, propane and CO_2 with the Li/MgO catalysts was studied by sorption/desorption experiments in a TGA apparatus under reaction conditions (600°C).

Sorption of hydrogen could not be detected at 600°C. Instead, it was observed that treating the samples in hydrogen for at least one hour resulted in a considerable weight loss. After purging in Ar and admission of oxygen over the sample, the original weight of the sample was recovered instantaneously. It was concluded that oxygen from the sample was removed by hydrogen treatment and replenished upon oxygen treatment. The results of the measurements are presented in Table 6.3. The degree of deoxygenation, expressed as percent of bulk oxygen, first increased and then decreased with increasing Li content. When we express the amount of removed oxygen as percent of the total surface oxygen (calculated using the BET surface area and assuming (001) MgO surface) the deoxygenation degree increased with Li content up to 3 wt% Li_2O where it leveled off with further increase of the Li content.

No propane adsorption was detected at the reaction temperature i.e., 600°C.

Sorption/desorption of CO_2 was studied since the strong influence of CO_2 on the catalytic activity, known from Chapter 5, makes CO_2 a suitable probe molecule for our catalysts. Switching CO_2 containing inert gas (Ar) to the samples in the TGA chamber resulted in weight increase (Sorption curves in Figure 6.3). At 700°C sorption reached equilibrium during measurement time, whereas at lower temperatures equilibrium was not achieved. Switching off CO_2 from the gas stream resulted in weight decrease of the samples, i.e. partial CO_2 desorption occurred (Desorption curves in Figure 6.3). At 700°C desorption did not reach equilibrium, the catalyst continued to desorb CO_2.

Table 6.3. The degree of deoxygenation of the Li/MgO catalysts measured by the weight loss during 1 hour H_2 treatment and the weight gain upon subsequent oxygen admission; the amount of CO_2 sorbed and desorbed at 600°C. Percent of removed oxygen are calculated relative to the total oxygen in the samples and total surface oxygen assuming the (001) face of the MgO.

Sample	removed O expressed as			mol CO_2 desorbed/m^2 of catalyst	mol Li_2O/g of catalyst	mol CO_2 sorbed./g of catalyst
	% of bulk oxygen	% of surface oxygen	mol/m^2 of catalyst			
MgO	0.02	0.48	7.46E-08	-	-	-
1%Li_2O/MgO	0.10	14	2.24E-06	1.8E-06	3.3E-04	1.7E-04
3%Li_2O/MgO	0.12	68	1.06E-05	7.9E-06	1.0E-03	6.4E-04
7%Li_2O/MgO	0.05	62	9.70E-06	7.3E-06	2.3E-03	1.0E-03

At 600°C CO_2 sorption/desorption measurements were performed with samples containing varying amount of Li. The results of these measurements are reported in Table 6.3. The quantity of sorbed CO_2 amounted roughly to half the amount of Li_2O in mols, present in the catalyst. It has to be noted, that equilibrium was not reached during sorption measurements. It was further observed that the amount (in mols) of CO_2 that can be desorbed when switching from CO_2 to inert gas at 600°C was in the same range as the number of mols of oxygen that can be removed with H_2.

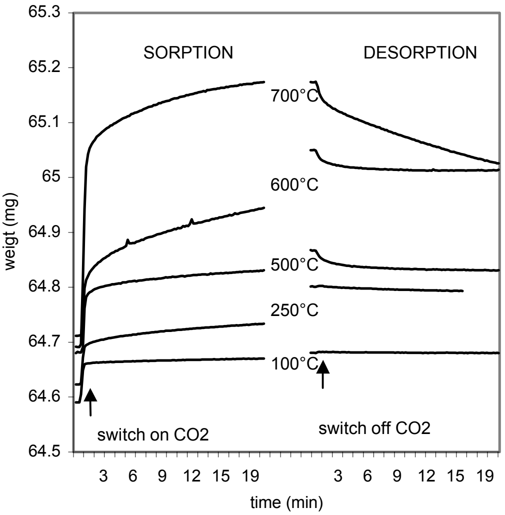

Figure 6.3. Sorption and desorption curves measured in the TGA on the 1%Li_2O/MgO catalyst. Conditions: 10% CO_2 in Ar, total flow: 50 ml/min.

6.3.3 Influence of the deoxygenation degree in hydrocarbon activation

In order to investigate how the degree of deoxygenation influences the activity of the catalyst, two measurements were carried out using the same catalyst bed in a microreactor flow system at 600°C. In the first measurement the catalyst was treated in 10% hydrogen for 1 hour then purged for 10 minutes and finally a feed consisting of 10% propane in He was switched to the reactor. Immediately after the switch, samples were taken from the effluent stream and analyzed by GC. In the second measurement the sample was treated in hydrogen for 1 hour followed by a brief oxygen treatment. After purging in He, 10% propane containing feed was admitted to the reactor. Samples were taken immediately after the switch to the propane feed and analyzed. Figure 6.4 presents the conversion of propane obtained in these two experiments. The oxygen treated catalyst produced 5 times higher conversions than the catalyst treated only in hydrogen. The oxygenated sample lost 80% of its original activity in one hour.

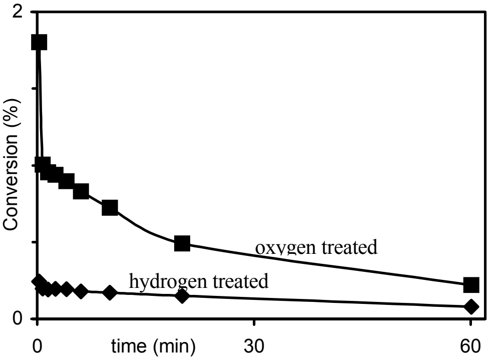

Figure 6.4. Conversion of propane in the absence of oxygen over the oxygen treated and hydrogen treated catalyst. Conditions: 10% propane in He; total flow: 100 ml/min; T: 600°C.

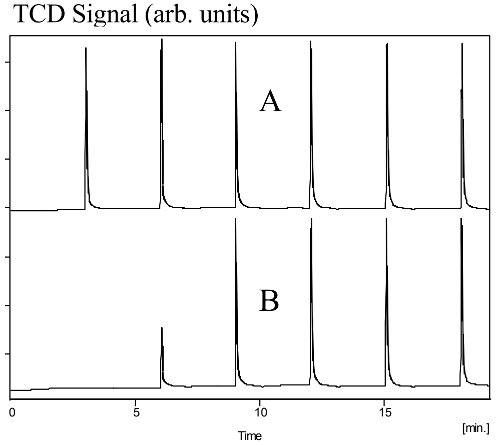

Figure 6.5. TCD signal during oxygen pulsing of pretreated 1%Li_2O/MgO catalyst at 600°C. A: pretreatment in 10% propane, 1 hour, 600°C; B: pretreatment in 10% H_2, 1 hour, 600°C. Carrier (He) flow: 50 ml/min.

In order to separate the propane reaction into redox reaction steps, reduction-oxidation cycles were attempted in pulse mode in the flow system at 600°C. In the first experiment the catalyst bed was treated with 10% propane in He for 1 hour. After purging in He for 10 minutes, pulses containing 10% oxygen in He were sent through the catalyst. The pulses in the effluent stream were detected by thermal conductivity detector (TCD). The signal of the TCD in this experiment shown in Figure 6.5A indicates no significant oxygen uptake after propane treatment. In the second experiment the catalyst was treated in hydrogen, then the oxygen containing pulses were sent through the reactor. The result of this experiment is presented in Figure 6.5B. In contrast to the propane treated catalyst, the catalyst treated in hydrogen consumed almost all oxygen from the first two pulses (~10^{-6} moles O/ m^2 catalyst).

6.3.4 Influence of the surface area on catalytic performance

In order to study the influence of surface area, high surface area MgO precursor was used to prepare catalysts with the same composition but higher surface area. The catalytic performances are presented in Table 6.4 for the 3%Li_2O/MgO catalyst together with the BET surface areas and the deoxygenation degree. Increasing surface area from 3 to 6 m^2/g had only marginal influence on the rate of conversion. However, selectivities to various products changed significantly from 3 to 6 m^2/g. As a general trend, higher surface area resulted in lower olefin products selectivities and higher CO, CO_2 selectivities. Rate of propane conversion calculated as mol per m^2 catalyst per second, obviously resulted in a decrease of the activity by a factor of two.

Table 6.4. Dependence of conversion and selectivities on surface area for Li/MgO catalyst. Conditions: 600°C, WHSV$_{propane}$: 4.8 h^{-1}, 10% propane and 8% O_2 in He, total flow: 40 ml/min; 100 mg catalyst.

catalyst	3%Li_2O/MgO	
BET (m^2/g)	3	6
conversion (%)	10	10
rate (10^{-6} mol.g^{-1}.s^{-1})	2.8	3.0
(10^{-6} mol.m^{-2}.s^{-1})	0.9	0.5
[Li^+O^-] (10^{-6} mol/m^2)	11	5
	Selectivity (%)	
CH_4	2.9	2.3
CO	13.3	20.9
CO_2	19.7	21.1
C_2H_4	32.6	29.0
C_3H_6	30.7	26.3

Catalysts with the same composition but different surface areas were prepared by modifications of the preparation method (see Chapter 3 for details). Note, that these catalysts also include small amounts of dysprosia, however presence of dysprosia does not influence the product spectrum significantly. Rate of propane conversion as a function of propane partial pressure measured under differential conditions (for details of measurement see Chapter 5) over two catalysts having the same composition but different surface areas is presented in Figure 6.6. In the same figure the rate obtained with an empty reactor is also shown. At low propane partial pressures (<0.2 bars) the two catalysts converted propane at similar rate, whereas at high partial pressures of propane (>0.3 bars) propane converted two times faster over the catalyst having lower surface area.

6.3.5 Influence of temperature on catalytic activity and selectivity

The influence of temperature on the catalytic activity of Li/MgO catalyst was studied in order to find the optimum temperature interval for the propane conversion reaction. Figure 6.7 shows how the selectivities and propane conversion evolve with temperature over 7 wt% Li_2O promoted magnesia catalyst under constant space velocity. Propene was the main product over the whole temperature range except at 700°C. The selectivity to ethene continuously increased and above 650°C it became larger than selectivity to propene. Both the selectivities to CO and CO_2 decreased between 500-600°C, while between 600-700°C they remained fairly constant. Methane selectivity increased continuously.

It is important to note that the above selectivity data were obtained at differing conversion levels. In order to check how the conversion level affected selectivities, space velocity variation was performed in order to vary the conversion at constant temperature. Figure 6.8 shows the selectivities at varying conversion, at 600°C. From the figure it is obvious that selectivities were hardly influenced by the increasing conversion. The relatively stable selectivities at varying conversion were characteristic for all Li promoted magnesia catalysts.

6.3.6 Influence of the reactant on the product distribution

In Figure 6.9 the selectivities to the main products are shown while using n-butane, propane or ethane as feed under similar conditions. While the conversion level decreased with decreasing carbon chain length of the hydrocarbon, selectivity to total olefins was in the same range in all cases, i.e., between 60-70%. Distribution of olefins was rather similar when n-butane and propane was the feed, i.e., ethene and propene were produced with similar selectivities, the exception being the small selectivity of butenes from n-butane. In the case of ethane the only olefin observed was ethene, as expected. Carbon oxide selectivities were in the same range for all the hydrocarbons.

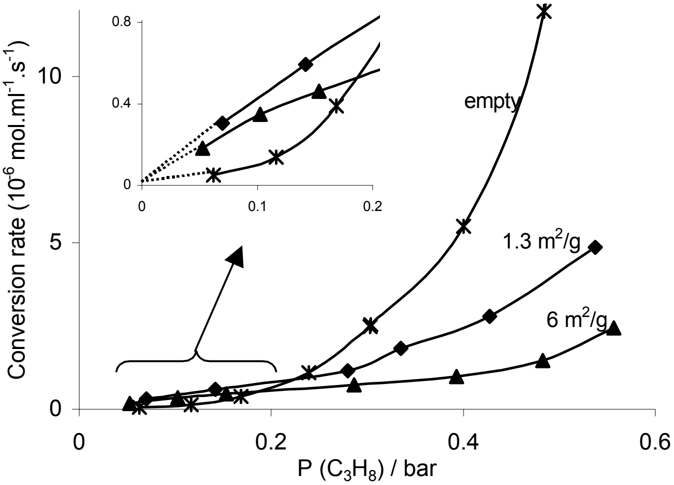

Figure 6.6. Reaction rate of propane conversion vs. *propane partial pressure over two different catalyst with the same composition (Li/Dy/MgO) but different surface area. Conditions: P(CO_2): 20 mbar; P(O_2): 140 mbar; T: 600°C; total flow: 100 ml/min.*

6.4 Discussion

First, the role of Li in creating the active site will be discussed, and then the propane reaction mechanism will be detailed. Activation over the site created by Li and further reactions will be discussed in the framework of C-C *vs.* C-H bond splitting. Formation of ethene from propane requires a C-C bond cleavage, while formation of propene can be the result of only C-H bond splitting, therefore in our analysis the relative selectivities to propene and ethene (or the ratio between these selectivities) will be the measure of the C-H *vs.* C-C bond breaking.

6.4.1 Role of Li in creating the active site and the removable oxygen

From observations on CO_2 inhibition over reaction rates and CO_2 TPD measurements it was concluded that Li is part of the active site (Chapters 3 and 4). It was proposed that [Li^+O^-] type active sites, as defects on the MgO surface, are responsible for catalytic activity, similarly to the methane oxidative coupling [42,45]. Furthermore, in the kinetic analysis of propane conversion, a strong correlation between catalytic activity and CO_2 concentration

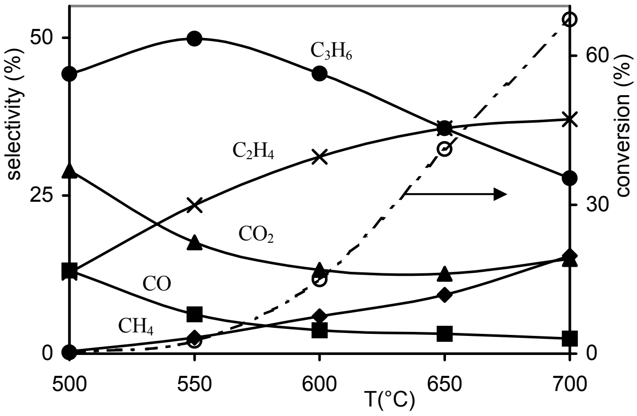

Figure 6.7. Conversion of propane and selectivities for various products vs. *temperature over Li/MgO catalyst. Conditions: 10% propane and 8% oxygen in He; total flow 10 ml/min.*

was found, whereas CO_2 did not influence gas-phase reactions; the inhibition of the rates showed -1 order in CO_2, from where it was proposed that $[Li^+CO_3^-]$ is formed on the $[Li^+O^-]$ active site, in order to account for the -1 reaction order (see Chapter 5). The activity and selectivity increase by Li addition (Table 6.2 and Figure 6.2) further supports the crucial role of Li in creating the active site: addition of up to 3 wt% Li_2O onto magnesia increases the rate of propane conversion normalized to catalyst surface area (Figure 6.1).

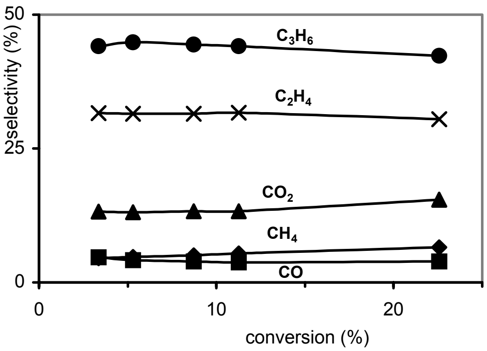

Figure 6.8. Selectivities for various products vs. *propane conversion at 600°C over Li/MgO catalyst. Conditions: 10% propane and 8% oxygen in He; total flow 4-80 ml/min.*

An important question pertains to the location of the $[Li^+O^-]$ active site. It was proposed in the literature that the Li_2O phase is the active phase present in clusters on the magnesia surface [64]. This is in agreement with our experimental observations since increasing Li content increased the rates related to the surface area Figure 6.1. In contrast, if the Li phase would cover the surface of MgO uniformly, just 1 wt% of Li_2O would be enough for 4 monolayers, and further increase of Li-content would have no influence on the surface normalized rates.

However, clusters of Li_2O on Li/MgO catalysts are not expected to show “red-ox” capacity, as observed here. The presence of Li_2O_2 under reaction conditions could, in principle, explain the release of oxygen and form Li_2O, as suggested in the literature [91,92]. However, the presence of such an unstable phase as Li_2O_2 is arguable under the reaction conditions used, as it already decomposes below 200°C. In the references mentioned the presence of Li_2O_2 was proposed based mainly on XRD data, but not unambiguously

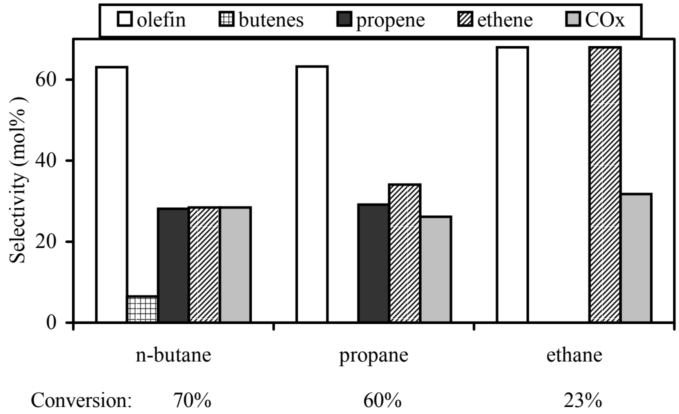

Figure 6.9. Selectivities of the main products and hydrocarbon conversion over the Li/Dy/MgO catalyst. Conditions: 6-8% hydrocarbon and 10% oxygen in He; WHSV: 0.8-1/h; T: 650°C.

identified against other Li containing but more stable phases that can be present, e.g. LiOH, LiOH.H_2O and Li_2CO_3. Futher, Bothe-Almquist *et al.* [91] used EPR evidence to argue for the presence of Li_2O_2, in spite of the fact that O_2^{2-} in the peroxide is diamagnetic. Therefore, the presence of Li_2O_2 is questionable, so is the role of this phase in the catalytic activity. The oxygen removal/ reoxygenation is more conceivable in the case of a $[Li^+O^-]$ defect on the MgO surface. This defect oxygen has peculiar properties, different from the rest of the lattice oxygen; it has, for example, EPR activity [88], and it was suggested to be removable (see for example [84-86]).

We attempt to quantify the concentration of $[Li^+O^-]$ active sites by two methods. The first method consisted of removal of the active oxygen from the active site and subsequent reoxygenation. The second method involved the decomposition of the unstable $[Li^+CO_3^-]$, as follows. In CO_2 containing atmosphere most of the $[Li^+O^-]$ sites adsorb a CO_2 molecule to form $[Li^+CO_3^-]$, while the Li_2O phase forms bulk Li_2CO_3. In inert atmosphere the majority of $[Li^+CO_3^-]$ decomposes while desorbing CO_2, whereas the bulk Li_2CO_3 phase does not decompose at 600°C. This follows from the observation that the number of mols of desorbed CO_2, as the result of $[Li^+CO_3^-]$ decomposition, is similar to the number of mols of removable oxygen at every Li content (Table 6.3). This implies that reversible adsorption of CO_2 at 600°C takes place on the same sites that can be reduced with H_2 at 600°C. Significant decomposition of the bulk Li_2CO_3 phase is noted only at 700°C (Figure 6.3). We consider therefore the surface concentration of removable oxygen as being the density of $[Li^+O^-]$ active sites. The concentration of $[Li^+O^-]$ species increases proportionally with the Li content up to 3 wt% Li_2O, however only a small fraction of the available Li forms an active site (see Figure 6.10A).

Catalytic activity is attributed to the removable oxygen present on the catalyst surface in the form of $[Li^+O^-]$. This removable oxygen activates propane as demonstrated by the correlation of the reaction rates with the density of $[Li^+O^-]$ sites, the latter measured by the degree of deoxygenation of the catalysts and by the amount of CO_2 that are desorbed due to the decomposition of the unstable $[Li^+CO_3^-]$ (Figure 6.10B). Further support for the claim that [Li^+O^-] activates propane is given by the low propane activation capacity of the deoxygenated catalyst (oxygen of the active site removed) compared to the fully oxygenated catalyst (Figure 6.4).

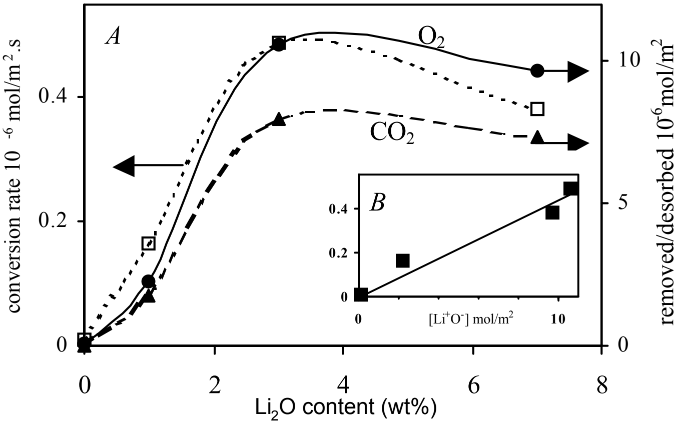

Figure 6.10. Conversion rates related to the surface area (data from Figure 6.1), deoxygenation degree (circles) and total CO_2 desorbed (triangles) related to the surface (data from Table 6.3), for the Li/MgO catalysts vs. *the Li content at 600°C (A); correlation of the activity with the density of active sites as measured by surface concentration of removable oxygen (B).*

It has to be emphasized that none of the impurities present in the catalysts can account for the weight change by redox capacity. The sulfur present as sulfate could account for max. 0.03 wt% oxygen exchange while reducing to sulfite, provided all the sulfate is on the surface. However, none of the possible sulfites is stable above 450°C, moreover, there was no sulfur found on the surface by XPS. The iron-oxide present could account for max. 0.0007 wt% change due to reduction to iron(II)-oxide. In comparison, from the measured samples MgO lost 0.01 wt%; the weight change was between 0.05-0.07 wt% for the Li/MgO catalysts in the reduction-oxidation cycles.

6.4.2 Reaction mechanism of propane activation

It was shown in Chapter 5 that the first propane molecule is activated on the catalyst and a propyl radical is released to the gas phase where it undergoes radical chain propagation reactions. Activation of propane on the [Li^+O^-] active site takes place by splitting one C-H bond in propane while forming [Li^+OH^-] and a propyl radical that is released into the gas-phase. The removable oxygen of the active site is not lost during the activation of propane, nor it is eliminated in a subsequent dehydroxylation step. This follows from the experiments presented in Figure 6.5 where propane treatment did not result in oxygen removal from the catalyst. Product hydrogen concentration is too low (0.04 vol%) to be effective in oxygen removal. Regeneration of the [Li^+OH^-] sites was proposed to occur upon oxygen admission, without the removal of the O^- of the active site (Chapter 5). However, under the pulsing conditions shown in Figure 6.5A the reaction of oxygen with [Li^+OH^-] is probably not sufficiently fast [93] to produce a noticeable oxygen uptake, neither could be water evolution confirmed due to detection difficulties.

Importantly, the amount of propane converted over the time on stream as shown in Figure 6.4 is 70 times higher than the number of removable oxygen sites. This fact supports a radical chain mechanism proposed in Chapter 5, in which one propane molecule is activated on the active site resulting in propyl radical which undergoes chain propagation reactions in the gas-phase. The number 70 is a typical chain propagation length in homogeneous chemistry [50,94].

The chain lengths of the radical chain reaction at low propane partial pressures are not influenced by the surface area of the catalyst. This follows from the data in Table 6.4; two catalysts with the same number of active sites per gram show identical catalytic activity. Assuming that the activity per site is constant, despite the difference in the density of active sites in both catalysts, it follows that the rates of formation of radicals are identical. As the conversion rate did not change either, it must be concluded that the chain length is also constant. This is also supported by the low partial pressure data in Figure 6.6 where catalysts with the same composition but differing surface area show similar activities. Further support is the fact that the activity per active site is constant for catalysts with varying surface areas induced by variation of Li loading, resulting in a linear relationship in Figure 6.10B.

On the other hand from Figure 6.6 it is observed that at high propane partial pressures the conversion rate of propane decreases with increased surface area. According to the proposed mechanism, with increasing the partial pressure of propane the concentration of radicals in the gas-phase is expected to increase. When the concentration of radicals is higher, radical quenching is more efficient on the high surface area catalyst, thus, conversion is significantly decreased.

Increased CO_x selectivity with increased surface area (Table 6.4) indicates reaction pathways on the non-promoted, unselective magnesia surface, probably crystal defects like edges, corners, etc. Contribution to the increased CO_x selectivity could come from secondary reactions of olefins and more efficient transformation of not detectable oxygenated hydrocarbons to carbon-oxides over the catalyst surface.

Selectivity and activity decrease due to interactions of radical intermediates with the catalyst surface was also reported earlier in the alkane oxidation literature [33,95,96] which agrees well with our suggestion. Simulations of surface initiated gas phase reactions were also attempted, however modeling surface initiated gas-phase reactions is still in its infancy [49,50]

6.4.3 C-C vs. C-H bond breaking

The mechanism proposed in Chapter 5 describes the conversion of propane as a heterogeneously initiated chain propagation reactions in the gas phase. Initiation over the catalyst prevails as long as the propane partial pressure is below typically 0.3 bars. In this mechanism the product distribution is mainly determined by the gas-phase propagation steps. New experimental evidence in this chapter provides additional support for this hypothesis.

For the case of propane conversion, Figure 6.7 shows that dehydrogenation selectivity decreases while cracking selectivity increases with temperature over Li/MgO. This is explained by the higher activation energy of formation of the primary alkyl radicals in the propagation reactions [50]. The primary radicals preferably follow a decomposition route involving C-C bond breakage.

C-H bond dissociation data of the radical chemistry can explain why activity observed for ethane is significantly different from that for propane and butane (Figure 6.9). The bond energy of a secondary C-H bond is the weakest in propane and butane (98.5 and 98.2 kcal/mol, respectively) and almost the same, while a primary C-H bond energy is somewhat higher (101.1 kcal/mol) [97,98]. Since ethane possesses only primary C-H bonds, its' activity is significantly different from propane and butane. These data support the proposition that the rate-determining step is hydrogen abstraction, *i.e.* a C-H bond breakage, both during catalytic initiation and gas-phase propagation.

The distribution of olefins formed from ethane, propane and butane can be explained by the decomposition routes of the radicals according to the homogeneous radical chemistry [50,94]. A primary radical, whether propyl or butyl, leads preferentially to C-C bond cleavage in β position resulting in cracked products, except for the ethyl radical which can only brake a C-H bond in β position. A secondary propyl radical can only break a C-H bond resulting propene, while a secondary butyl radical can lead to either C-C or C-H bond cleavage, resulting in propene or butene production. It follows that more cracked products are expected from butane than from propane, and hardly any cracking from ethane, which is indeed observed experimentally (Figure 6.9).

Secondary reactions of propene proceed with a much lower rate than the primary reactions. This follows from the observation that the conversion level of propane does not influence the selectivities (Figure 6.8), unlike in the case of typical redox catalysts such as vanadia [12,99]. This is in line with observations from Chapter 3 that propene conversion is a factor of 3 lower than that of propane under similar conditions, and is attributed to the relatively low reactivity of allyl radicals in the gas-phase.

6.5 Conclusions

It was confirmed that the removable oxygen sites created by Li defects on MgO (noted as $[Li^+O^-]$) activate the propane molecule *via* H · abstraction, based on the correlation between catalytic activity and active site density. The concentration of $[Li^+O^-]$ sites was measured independently by O^- removal with H_2 as well as by reversible CO_2 adsorption at 600°C.

The chain length of propagation reactions initiated on the catalyst is ~70 in the absence of oxygen at 600°C. During the initiation reactions the $[Li^+O^-]$ site is transformed to $[Li^+OH^-]$. Regeneration of the active site does not require the oxygen removal by dehydroxylation. The surface area of the Li/MgO catalysts influences the chain length of the propagation reactions at high propane partial pressures only, due to quenching.

The conversion trends of ethane, propane and butane confirm that hydrogen abstraction from the alkane is the rate-determining step. Gas-phase radical chemistry determines largely the selectivity pattern.

Acknowledgements

Heike Borchardt for help in catalyst preparation and catalytic measurements and Dr. I. Babich for help in TGA measurements.

Chapter 7

7 General discussion and recommendations: criteria for oxidative conversion of alkanes to olefins

7.1 The relative importance of catalytic and gas-phase reactions

After comparing all the kinetic data measured with and without the catalyst, highlighted especially in Chapters 5 and 6, the pragmatic reader might ask something like this: is the catalyst necessary at all? Or after a superficial look on the data one might ask: does the catalyst do anything (catalytic) at all? These questions have their raison d'être: the maximum propane conversion rate among all the measurements was measured in an empty reactor. In order to treat the question rigorously, we need to separate the discussion in two: first we discuss whether the catalyst does something significant, and second we discuss whether the catalyst is necessary for oxidative conversion of alkanes to olefins.

The catalyst *does* have a significant influence, and this is visible if we compare the reaction rates under comparable conditions. Such comparisons were already made in ch. 5 and 6, and it is clear that under certain conditions (low propane partial pressure, low residence time) the activity of the reactor in the presence of the catalyst is higher than the activity of the sole empty reactor. Secondly, CO_2 had a strong inhibiting effect in the presence of catalyst while no effect was noted in the empty reactor, implying the involvement of catalytic active sites that are susceptible to blocking by carbon-dioxide. Thirdly, the shape of the rate curves *vs.* propane partial pressure variation and conversion *vs.* residence time showed clear differences for the two cases. It is beyond doubt that the catalyst has a significant influence.

The question whether it is useful to use a catalyst still remains, as under industry friendly conditions (high propane partial pressures) the empty reactor produced higher conversions. Moreover, high propane conversion was achieved at lower residence time in the empty reactor than in the reactor with catalyst, while selectivity was virtually the same for both cases. To carefully analyze the usefulness of the catalyst we need to take into account all the small details in our measurements, and the genuine characteristics of the homogeneous reactions *vs.* those of catalysis. Homogeneous reactions are characterized by an induction time (the time necessary to form sufficient radicals to maintain chain propagation), after which, in a sufficiently large reactor, the reaction will runaway until complete oxygen conversion, and if the local temperatures in the hot spots (depending on the amount of oxygen added) are not too high, it slows down to stop. It appears that the amount of oxygen can regulate the final temperature, but if one wants to achieve reasonable conversions, considerable amounts of oxygen are necessary. This can have the consequence that the temperatures will increase locally too high for the olefins to be able to survive the still oxidizing atmosphere, that results in total oxidation. In other words, once we introduced the alkane and oxygen in the reactor we have no further control of what is going to occur.

On the other hand the introduction of a catalyst allows us to have control over the radical reactions. The catalysts developed in this thesis and operated in a fixed bed under plug flow conditions showed a balancing character. At low partial pressures of propane, where radical generation in the gas-phase is limited, the catalyst becomes a prominent radical initiator. At high propane partial pressures, when the gas-phase radical generation is facilitated, the catalyst exhibits a quenching role, too. However, even at the highest propane concentration in our experiments (54%) when the catalyst was present, about half of the initiation was generated by the catalyst. The quenching role is important in limiting very high radical concentrations that can cause local runaways.

The catalyst is also able to convert oxygenated intermediates into carbon oxides and adsorb significant amount of carbon-dioxide, thus in a cyclic operation the catalyst can be used as CO_2 removing/ separating agent. All in all, the presence of the catalyst provides us the opportunity to control radical reactions efficiently, while without it we are left with the increased chance of local runaways and a product distribution that depends only on the process conditions, similar to steam cracking.

7.2 Active site and mechanism

In the following section the configuration of the active site and the mechanism of hydrocarbon activation will be discussed.

It has been long discussed in the literature about the active sites of Li promoted magnesia catalysts, especially because they had excellent activity towards methane oxidative coupling. It is widely accepted that an activated oxygen is the center where the first hydrogen is abstracted whether by homolytic or heterolytic C-H bond splitting. However, there is less consensus as to where that active oxygen is located. The most accepted proposition is oxygen next to a cation defect caused by Li defect in the magnesia structure, while active crystalline phases were also suggested. In all these suggestions the activity of the catalyst was attempted to be correlated with experimental evidence of the active oxygen by means of EPR, XPS, IR, Raman, isotope tracing, computation, etc. In this thesis we used TGA measurements of oxygen removal and replenishment as well as CO_2 desorption for the same purpose. The lack of promotion by Na ions on the MgO and the low activity of pure Li-containing phases is a valid argument for the role of substitutional Li defects against a particular crystalline active phase. Still, these evidences cannot completely rule out one of the possibilities, whether the active oxygen is present on the magnesia surface or on a Li-containing phase.

On the other hand, there is much more known about the properties of the active oxygen and its role in the hydrocarbon activation mechanism. Computational studies showed that heterolytic C-H bond cleavage is not feasible. Homolytic splitting of the most active C-H bond leads to hydrocarbon radicals that can be released into the gas-phase. Kinetic analysis in this thesis and also in the literature has shown that some of the kinetic features can only be explained by assuming contribution of homogeneous reactions in the gas-phase. Gas phase radicals have also been detected by matrix isolation ESR and TAP techniques. However, detection of propyl radicals appears to be difficult as they have very fast decomposition routes to either propene and H · or ethene and CH_3 ·. Regeneration of the catalyst is possible with the help of oxygen without the necessity to remove the active oxygen involved in the hydrogen abstraction.

7.3 Catalyst criteria for alkane conversion to olefins

Let us define some criteria for the use of Li promoted magnesia catalysts in light alkane conversion to olefins. First, the criteria of an active and selective catalyst will be detailed and secondly, the operating conditions for maximum olefin yield will be recommended.

The most important criterion of the catalyst is the existence of an active site that is able to split and stabilize the most labile hydrogen from the hydrocarbon molecule. It is important that the hydrocarbon fragment after the activation does not have a strong stabilization on the catalyst surface, as it becomes susceptible to further degradation either by attack of the gas-phase oxygen or reactions on the surface. Metallic catalysts have strong stabilization of the hydrocarbon on their surface, hence in the presence of oxygen they lead to full combustion. Vanadia based redox catalyst have moderate stabilization of the hydrocarbon fragment if the vanadia phase is present in optimum concentration; these catalyst lead to narrow product spectrum as they are able to release the hydrocarbon chain intact from their active site, forming always the corresponding olefin. However, these catalysts give high selectivities to olefins only at low conversions. At high conversions secondary reactions of the olefins will dominate and the maximum yields are thus limited. Finally, Li/MgO catalysts probably do not stabilize the hydrocarbon fragment on their surface as all attempts to identify surface intermediates have failed. Instead, hydrocarbon fragments are released into the gas-phase where they decompose and undergo radical chain propagation reactions. Because of the nature of radical formation and decomposition these catalysts produce a mixture of olefins (both from dehydrogenation and cracking). Nevertheless, due to the low stabilization of hydrocarbon fragments on the surface, secondary conversion of olefins is hindered, as the radical fragments formed from olefins are more stable in the gas-phase, they do not have a facile decomposition route, comparable to the alkanes. The ideal catalyst would have active site that releases radicals into the gas-phase under conditions where chain propagation reactions are limited. For example if only i-propyl radicals are released into the gas phase, that decompose into propene, H · is released. If the H · resulted from the decomposition will not pursue chain propagation, at least not with a rate comparable to the (catalytic) termination of radicals, propene will be selectively produced. In principle this could be possible at lower temperature than those used in this thesis with a more active catalyst, as C-C bond breaking selectivity was lower at low temperatures. Another option is to quench the H · radicals selectively.

To be selective is also necessary that the catalyst does not form stronger C-O bonds than the bonding of active oxygen on the catalyst, in order not to remove the active oxygen and form carbon-oxides. This implies that the bonding of the active oxygen should be sufficiently high, certainly higher than for most of the redox-type catalysts, which can release oxygen fairly well while changing the oxidation state of the metal.

The active site (oxygen or other) must be sufficiently basic to easily abstract the hydrogen from the hydrocarbon, however, CO_2 adsorption on the active site should be preferably avoided. This seems to be a difficult task as the C-H bond activation and CO_2 adsorption appear to be strongly interrelated. Addition of chlorine appeared to tackle the CO_2 inhibition problem because most probably Cl^- has taken the same role as O^-, being able to split the hydrogen from the hydrocarbon. It may as well be that Cl activates the hydrocarbon in the gas phase, if under reaction conditions Cl atoms are released from the catalyst. One way or another HCl is formed and the Cl from the catalyst is slowly lost, i.e. washed out with the reaction gas stream, causing stability and contamination problems at the same time. Therefore our recommendation is to avoid the use of Cl in the catalyst.

For the reaction to occur, i.e. the activation of hydrocarbon to proceed, there is need only for one type of relatively strongly bound oxygen. Weakly bound active oxygen is likely to favor combustion. Therefore the use of other oxides in the composition, i.e. rare earth oxides (REO) is questionable. REO have the tendency to show redox properties, they are also more acidic than alkaline earth oxides such as magnesia. REO by themselves show very high activity, but low selectivity. They can be used as ignitor similarly to metals such as Pt, in the typical process that is operated under oxygen limiting conditions, i.e. first the available oxygen burns part of the hydrocarbon while producing heat, then the rest of the hydrocarbon feed undergoes thermal cracking. The REO are present in most catalyst compositions in the methane coupling and ethane dehydrogenation literature for activity reasons. In our experiments, however, the use of REO has not proven to be useful. Moreover, Dy_2O_3 for example, forms mixed oxide with Li, which is probably inactive, thereby blocking part of the Li. The conclusion is that the catalyst should be simple, and there should be only one type of active oxygen present. The use of multiple oxides is to be avoided, as they all present different types of oxygen on the surface.

7.4 Process conditions criteria

Let us now discuss the criteria regarding the operating conditions. It is obvious from the thesis that temperature increases activity and interestingly also the olefin product selectivity between 500-600°C. Further increase of the temperature decreases propene selectivity but ethene selectivity increases further. Decrease of CO_x selectivity with increasing conversion when increasing temperature seems to indicate the beneficial effect of gas-phase reactions. Increase of temperature between 500-600°C increases the chain propagation rates significantly, therefore the ratio of homogeneous *vs.* heterogeneous reactions of the chain carrier radicals is increased. Due to the same reason, the ratio of ethene to propene is also increasing with the temperature, thus the temperature can be a tool to control the olefin distribution. However, there is a lower limit in the temperature since at temperatures lower than 450-500°C the addition of O_2 molecules to the gas phase radicals while forming peroxy radicals becomes increasingly important. Hydrocarbon peroxy radicals react further to oxygenates and to CO_x.

The propane concentration influences mainly the activity. High propane concentrations mean high conversions and are also preferred by the industrial operations. When using basically pure propane feed with oxygen or air addition, the oxygen content will set the conversion level. When oxygen is consumed the reaction basically stops, so for activity reasons some oxygen always needs to be present. Moreover, the oxygen content has influence over the selectivities; on the activity it has not very important influence as long as it is present. Further, the oxygen content has strong influence on the secondary reactions of propene. Rates of formation with propene partial pressure show that the conversion of propene is first order both in propene and oxygen. This suggests a rate-determining step involving both propene and oxygen. As the main products of reaction are carbon oxides, minimizing oxygen partial pressure is another option preventing secondary conversion of propene. However, low oxygen content reduces propene formation rates in the primary reaction, and exhaustion of O_2 leads to a detrimental decrease of the reaction rates. It has to be noted that secondary reactions of propene proceed with the help of the catalyst an order of magnitude faster than in the gas phase. Attention should be directed therefore, towards minimizing catalytic secondary reactions of propene in order to reach high propene yields.

7.5 Concluding remarks

In conclusion, the information from this thesis allows us to set the criteria for a successful olefin production, as follows. The catalyst should be a basic material with one type of active oxygen that is able to split a carbon-hydrogen bond of the hydrocarbons, but it does not stabilize the resulted hydrocarbon fragment. The catalyst should be used in a reactor where the advantages of gas phase reactions can be utilized (fluidized bed for example). Operation in autothermal mode would be preferred. Propane concentration should preferably be high and a low oxygen concentration maintained over the whole reactor by e.g. distributed oxygen.

Of course the present catalyst is not the best one can have. It suffers from disadvantages that need to be tackled in the future. The presence of Li brings two major disadvantages: volatility (long term instability especially at temperature above 700°C), and carbonate formation. A good replacement for Li would be thus desirable. Our attempts of preparing a good catalyst with other alkali and MgO were unsuccessful, as apparently only Li fits well with the magnesia lattice. It is reasonable to think that another combination of dopant/support can be found.

Furthermore, there is need for more knowledge over the properties and the location of the active site in order to define the nature of the needed properties very explicitly. Once the requirements for an active and selective site are settled in basic chemical terms, the *"ab initio"* design of a catalyst can start. Future work is also required on the field of kinetic modeling in order to assess the feasibility of a process based on this catalyst and, to find out whether there is a way to influence gas-phase radical reactions in order to improve the selectivity.

8 References

1. *European Chemical News* **April, 1995**, 3-9.
2. Zehnder, S. *Hydrocarb. Process.* **1998**, *77*(2), 59-65.
3. Petrochemistry Activity Review http://www.cefic.org, 1999-2000.
4. Cavani, F.; Trifiro, F. *Catal.Today* **1995**, *24*(3), 307-313.
5. Kung, H. H. *Adv.Catal.* **1994**, *40*1-38.
6. Mazzocchia, C.; Aboumrad, C.; Diagne, C.; Tempesti, E.; Herrmann, J. M.; Thomas, G. *Catal. Lett.* **1991**, *10*(3-4), 181-91 .
7. Lemonidou, A. A.; Tjatjopoulos, G. J.; Vasalos, I. A. *Catal. Today* **1998**, *45*(1-4), 65-71.
8. Michalakos, P. M.; Kung, M. C.; Jahan, I.; Kung, H. H. *J. Catal.* **1993**, *140*(1), 226-242.
9. Chaar, M. A.; Patel, D.; Kung, M. C.; Kung, H. H. *J. Catal.* **1987**, *105*(2), 483-98 .
10. Kung, H. H.; Chaar, M. A. U.S. US. 4777319. A. 881011, 1988.
11. Chaar, M. A.; Patel, D.; Kung, H. H. *J. Catal.* **1988**, *109*(2), 463-7 .
12. Kung, H. H.; Kung, M. C. *Appl.Catal.* **1997**, *A, 157*(1-2), 105-116.
13. Watling, T. C.; Deo, G.; Seshan, K.; Wachs, I. E.; Lercher, J. A. *Catal. Today* **1996**, *28*(1-2), 139-145 .
14. Conway, S. J.; Wang, D. J.; Lunsford, J. H. *Appl.Catal.A* **1991**, *79*(1), L1-L5.
15. Conway, S. J.; Lunsford, J. H. *J. Catal.* **1991**, *131*(2), 513-522.
16. Xu, M.; Lunsford, J. H. *React.Kinet.Catal.Lett.* **1996**, *57*(1), 3-11.
17. Landau, M. V.; Kaliya, M. L.; Herskowitz, M.; van den Oosterkamp, P. F.; Bocque, P. S. G. *Chemtech* **1996**, *26*(2), 24-29.
18. Herskowitz, M.; Landau, M.; Kaliya, M. PCT Int. Appl. WO. 9622161. A1. 960725, 1996.
19. Conway, S. J.; Wang, D. J.; Lunsford, J. H. *Appl.Catal.A* **1991**, *79*(1), L1-L5.
20. *Ullmann's Encyclopedia of Industrial Chemistry;* Sixth ed. Wiley-VCH : Weinheim, 2002.
21. *Kirk-Othmer Encyclopedia of Chemical Technology ;* ONLINE ed. Wiley-VCH : Weinheim, 2002.
22. Bhasin, M. M.; Mccain, J. H.; Vora, B. V.; Imai, T.; Pujado, P. R. *Appl. Catal. A-Gen.* **2001**, *221*(1-2), 397-419.
23. Ranzi, E.; Faravelli, T.; Gaffuri, P.; Pennati, G. C.; Sogaro, A. *Combust. Sci. Technol.* **1994**, *100*(1-6), 299-330.
24. Cavani, F.; Trifiro, F. *Catal. Today* **1999**, *51*(3-4), 561-580.
25. Baerns, M.; Buyevskaya, O. *Catal. Today* **1998**, *45*(1-4), 13-22.
26. Grasselli, R. K.; Stern, D. L.; Tsikoyiannis, J. G. *Appl. Catal. A-Gen.* **1999**, *189*(1), 9-14.
27. Grasselli, R. K.; Stern, D. L.; Tsikoyiannis, J. G. *Appl. Catal. A-Gen.* **1999**, *189*(1), 1-8.
28. Hinson, P. G.; Clearfield, A.; Lunsford, J. H. *J. Chem. Soc.-Chem. Commun.* **1991**, (20), 1430-1432.
29. Hatano, M.; Hinson, P. G.; Vines, K. S.; Lunsford, J. H. *J. Catal.* **1990**, *124*, 557-561.

30. Buyevskaya, O. V.; Baerns, M. *Catal. Today* **1998**, *42*(3), 315-323.
31. Zhang, W. D.; Zhou, X. P.; Tang, D. L.; Wan, H. L.; Tsai, K. *Catal. Lett.* **1994**, *23*(1-2), 103-106.
32. Ge, Q. J.; Zhaorigetu, B.; Yu, C. Y.; Li, W. Z.; Xu, H. Y. *Catal. Lett.* **2000**, *68*(1-2), 59-62.
33. Sinev, M. Y.; Margolis, L. Y.; Bychkov, V. Y.; Korchak, V. N. *Stud. Surf. Sci. Catal.* **1997**, *110*( ), 327-335.
34. Dahl, I. M.; Grande, K.; Jens, K. J.; Rytter, E.; Slagtern, A. *Appl. Cat.* **1991**, *77*(1), 163-174.
35. Burch, R.; Crabb, E. M. *Appl.Catal.* **1993**, *A, 100*(1), 111-130.
36. Schmidt, L. D.; Siddall, J.; Bearden, M. *Aiche J.* **2000**, *46*(8), 1492-1495.
37. Beretta, A.; Piovesan, L.; Forzatti, P. *J. Catal.* **1999**, *184*(2), 455-468.
38. Schmidt, L. D. *Stud. Surf. Sci. Catal.* **2000**, *130A*(International Congress on Catalysis, 2000, Pt. A), 61-81.
39. Lemonidou, A. A.; Stambouli, A. E. *Appl.Catal.* **1998**, *A, 171*(2), 325-332.
40. Ranzi, E.; Faravelli, T.; Gaffuri, P.; Garavaglia, E.; Goldaniga, A. *Ind. Eng. Chem. Res.* **1997**, *36*(8), 3336-3344.
41. Choudhary, V. R.; Rane, V. H.; Rajput, A. M. *AIChE J.* **1998**, *44*(10), 2293-2301.
42. Ito, T.; Wang, J. X.; Lin, C. H.; Lunsford, J. H. *J. Am. Chem. Soc.* **1985**, *107*5062-5068.
43. Johnson, M. A.; Stefanovich, E. V.; Truong, T. N. *J.Phys.Chem.B* **1997**, *101*(16), 3196-3201.
44. Sinev, M. Y.; Bychkov, V. Y. *Kinet.Katal.* **1993**, *34*(2), 309-313.
45. Driscoll, D. J.; Martir, W.; Wang, J. X.; Lunsford, J. H. *Adv. Catal.* **1987**, *35*, 139-185.
46. Driscoll, D. J.; Lunsford, J. H. *J. Phys. Chem.* **1985**, *89*, 4415-4418.
47. Driscoll, D. J.; Martir, W.; Wang, J. X.; Lunsford, J. H. *J. Am. Chem. Soc.* **1985**, *107*58-63.
48. Shi, C.; Hatano, M.; Lunsford, J. H. *Catal.Today* **1992**, *13*(2-3), 191-199.
49. Sinev, M. Y. *Catal. Today* **1995**, *24*(3), 389-393.
50. Mims, C. A.; Mauti, R.; Dean, A. M.; Rose, K. D. *J. Phys. Chem.* **1994**, *98*(50), 13357-13372.
51. Baranek, P.; Pinarello, G.; Pisani, C.; Dovesi, R. *Phys. Chem. Chem. Phys.* **2000**, *2*(17), 3893-3901.
52. Lichanot, A.; Larrieu, C.; Zicovich-Wilson, C.; Roetti, C.; Orlando, R.; Dovesi, R. *J. Phys. Chem. Solids* **1999**, *60*(6), 855.
53. Birkenheuer, U.; Cora, F.; Pisani, C.; Scorza, E.; Perego, G. *Surf. Sci.* **1997**, *373*(2-3), 393-408.
54. Borve, K. J.; Pettersson, L. G. M. *J. Phys. Chem.* **1991**, *95*(19), 7401-7405.
55. Orlando, R.; Cora, F.; Millini, R.; Perego, G.; Dovesi, R. *J. Chem. Phys.* **1996**, *105*(19), 8937-8943.
56. Ackermann, L.; Gale, J. D.; Catlow, C. R. A. *J.Phys.Chem.B* **1997**, *101*(48), 10028-10034.
57. D'ercole, A.; Pisani, C. *J. Chem. Phys.* **1999**, *111*(21), 9743-9753.
58. Daturi, M.; Binet, C.; Bernal, S.; Omil, J. A. P.; Lavalley, J. C. *J. Chem. Soc.-Faraday Trans.* **1998**, *94*(8), 1143-1147.
59. Hoogendam, G. C.; Seshan, K.; Van Ommen, J. G.; Ross, J. R. H. *Methane Alkane Convers.Chem. [Proc. Am. Chem. Soc. Symp.];* Plenum: New York, N. Y., 1994; pp 39-44.

60. Tanabe, K.; Okazaki, S. *Appl. Catal. A-Gen.* **1995**, *133*(2), 191-218.
61. Ross, J. R. H.; Smits, R. H. H.; Seshan, K. *Catal. Today* **1993**, *16*(3-4), 503-11 .
62. Borve, K. J. *J. Chem. Phys.* **1991**, *95*(6), 4626-4631.
63. Landau, M. V.; Kaliya, M. L.; Gutman, A.; Kogan, L. O.; Herskowitz, M.; van den Oosterkamp, P. F. *Stud.Surf.Sci.Catal.* **1997**, *110*(3rd World Congress on Oxidation Catalysis, 1997), 315-326.
64. Wang, D. J.; Rosynek, M. P.; Lunsford, J. H. *J. Catal.* **1995**, *151*(1), 155-167.
65. Batiot, C.; Cassidy, F. E.; Doyle, A. M.; Hodnett, B. K. *Stud.Surf.Sci.Catal.* **1997**, *110*(3rd World Congress on Oxidation Catalysis, 1997), 1097-1106.
66. Banares, M. A. *Catal. Today* **1999**, *51*(2), 319-348.
67. Sinev, M. Y.; Bychkov, V. Y.; Korchak, V. N.; Krylov, O. V. *Catal. Today* **1990**, *6*, 543-549.
68. Mears, D. E. *J. Catal* **1971**, *20*, 127.
69. Mears, D. E. *Chem. Eng. Sci.* **1971**, *26*, 1361.
70. Roos, J. A.; Korf, S. J.; Veehof, R. H. J.; van Ommen, J. G.; Ross, J. R. H. **1989**, *52*(1-2), 131-145.
71. Beretta, A.; Ranzi, E.; Forzatti, P. *Chem. Eng. Sci.* **2001**, *56*(3), 779-787.
72. Huff, M. C.; Androulakis, I. P.; Sinfelt, J. H.; Reyes, S. C. *J. Catal.* **2000**, *191*(1), 46-54.
73. Back, M. H.; Martin, R. *Int. J. Chem. Kin.* **1979**, *11*, 757-774.
74. Bychkov, V. Y.; Sinev, M. Y.; Korchak, V. N.; Aptekar, E. L.; Krylov, O. V. *Kinet. Catal.* **1989**, *30*(5), 989-994.
75. Bhumkar, S. C.; Lobban, L. L. *Ind.Eng.Chem.Res.* **1992**, *31*(8), 1856-1864.
76. Yamauchi, N.; Miyoshi, A.; Kosaka, K.; Koshi, M.; Matsui, N. *J. Phys. Chem. A* **1999**, *103*(15), 2723-2733.
77. Jitariu, L. C.; Wang, F.; Hillier, I. H.; Pilling, M. J. *Phys. Chem. Chem. Phys.* **2001**, *3*(12), 2459-2466.
78. Perrin, D.; Martin, R. *Int. J. Chem. Kinet.* **2000**, *32*(6), 340-364.
79. Westbrook, C. K.; Pitz, W. J. *Combust. Sci. Tech.* **1984** , *37*, 117-152.
80. Tsang, W. *J. Phys. Chem. Ref. Data* **1988**, *17*(2), 887-952.
81. Damme, P. S. v.; Narayanan, S.; Froment, G. F. *AIChE Journal* **1975**, *21*(6), 1065-1073.
82. Beretta, A.; Forzatti, P.; Ranzi, E. *J. Catal.* **1999**, *184*(2), 469-478.
83. Sinev, M. Y.; Bychkov, V. Y.; Korchak, V. N.; Aptekar, E. L.; Krylov, O. V. *Kinet. Catal.* **1989**, *30*(6), 1236-1241.
84. Sinev, M. Y.; Bychkov, V. Y. *Kinet. Catal.* **1993**, *34*(2), 272-276.
85. Choudhary, V. R.; Rane, V. H.; Chaudhari, S. T. *React. Kinet. Catal. Lett.* **1998**, *63*(2), 371-377.
86. Hoogendam, G. C. PhD Thesis, University of Twente, the Netherlands, 1996.
87. Karasuda, T.; Aika, K. *J. Catal.* **1997**, *171*(2), 439-448.
88. Che, M.; Tench, A. J. *Adv. Catal.* **1982**, *31*, 77-133.
89. Maksimov, N. G.; Selyutin, G. E.; Anshits, A. G.; Kondratenko, E. V.; Roguleva, V. G. *Catal. Today* **1998**, *42*(3), 279-281.
90. Konnov, A. A. 2000. Detailed reaction mechanism for small hydrocarbons combustion. Release 0.5. Web Page, http://homepages.vub.ac.be/~akonnov/.
91. Bothe-Almquist, C. L.; Ettireddy, R. P.; Bobst, A.; Smirniotis, P. G. *J. Catal.* **2000**, *192*(1), 174-184.
92. Landau, M. V.; Gutman, A.; Herskowitz, M.; Shuker, R.; Bitton, Y.; Mogilyansky, D. *J. Mol. Catal. A-Chem.* **2001**, *176*(1-2), 127-139.

93. Sinev, M. Y.; Bychkov, V. Y. *Kinet. Catal.* **1999**, *40*(6), 819-835.
94. Ranzi, E.; Sogaro, A.; Gaffuri, P.; Pennati, G.; Westbrook, C. K.; Pitz, W. J. *Combust. Flame* **1994**, *99*(2), 201-211.
95. Vislovskiy, V. P.; Suleimanov, T. E.; Sinev, M. Y.; Tulenin, Y. P.; Margolis, L. Y.; Corberan, V. C. *Catal. Today* **2000**, *61*(1-4), 287-293.
96. Sinev, M. Y.; Margolis, L. Y.; Korchak, V. N. *Uspekhi Khimii* **1995**, *64*(4), 373-389.
97. Poutsma, M. L. *J. Anal. Appl. Pyrolysis* **2000**, *54*(1-2), 5-35.
98. Berkowitz, J.; Ellison, G. B.; Gutman, D. *J. Phys. Chem.* **1994**, *98*(11), 2744-2765.
99. Albonetti, S.; Cavani, F.; Trifiro, F. *Catal. Rev.-Sci. Eng.* **1996**, *38*(4), 413-438.

9 Summary

Olefins are the most important building blocks in the modern petrochemical industry. Propene and ethene are the raw materials for polypropylene and polyethylene and their demand continuously increases. The majority of today's olefin capacity is provided by steam-cracking and fluid catalytic cracking (FCC). While these processes are well developed, increasing their capacity is limited due to limitations in byproduct usage. Propylene is produced as byproduct in both steam-cracking and FCC, thus the strongly increasing propylene demand can only be satisfied by dedicated processes. One such process, catalytic dehydrogenation of propane shows major disadvantages: thermodynamic limitation and coking of catalyst, consequently short catalyst lifetimes.

Conceptually, dehydrogenation in the presence of oxygen can help to overcome the limitations of catalytic dehydrogenation. *Oxidative dehydrogenation* has been recognized as new alternative olefin production method and it has been studied extensively. Despite the research efforts invested both in academia and industry, commercial application has not been realized to date, mainly due to low yields of olefins (max. achieved so far: 30%) over the catalysts employed. Transition metal oxide catalysts with pronounced redox character showed high tendency to limit the olefin yield by consecutive full oxidation. In contrast, magnesia based catalysts promoted by alkali-chloride showed high activity and selectivity in ethane oxidative dehydrogenation. This type of catalysts performed well in conversion of LPG to olefins as well.

In this thesis, alkali promoted magnesia catalysts were studied for the oxidative conversion of lower alkanes to olefins. Our research was motivated by the worldwide increase in olefin, especially propylene demand.

Yields of olefins above 50% could be obtained over Li/Cl/Dy/MgO with a product spectrum similar to that of steam-cracking. However, there are major advantages compared to steam cracking: the share of propylene is higher in the olefin yield, the reaction temperature is lower, and the heat is generated internally.

From the three supports tested in this thesis (magnesia, zirconia, and niobia) only magnesia has been seen active and selective. From the multitude of additives claimed in the patent literature only Li proved to be the essential promoter of magnesia. Addition of chloride induces small improvement in selectivity but the instability of the catalyst is also greatly increased. Therefore use of Cl-free catalysts is recommended. Catalytic performance had an optimum with both Li and Cl content of the catalysts. While the activity increase with varying Cl-content could be explained by the surface area increase caused, the activity and selectivity improvements caused by the Li addition can be explained only by the promoting effect of Li on the magnesia surface, whereby Li participates in the active site or in its creation. Addition of dysprosia limited the available Li *via* the formation of a mixed oxide, thereby causing decrease in the activity.

The kinetics of the reaction implied a reaction mechanism that involves radical initiation reactions on the catalyst surface and radical chain propagation reactions in the gas-phase. Gas-phase radical chemistry determines largely the selectivity pattern. The conversion trends of ethane, propane and butane confirm that activation by hydrogen abstraction from the alkane molecule is the rate-determining step. Above 0.3 bars propane partial pressure homogeneously initiated reactions also participate. The presence of gas-phase oxygen is crucial. Oxygen reacts with the radicals present in the gas-phase and as a result more radicals are produced that are also more reactive, thereby activity is greatly increased. The second function of oxygen is to regenerate the catalytic active site. Regeneration of the active site does not require oxygen removal by dehydroxylation, instead the hydrogen from the surface OH^- species is removed with the help of gas phase oxygen.

Carbon dioxide strongly suppresses the activity of the catalyst by blocking the active site, while forming inactive surface carbonate.

Consecutive reactions of propene give almost exclusively carbon oxides and proceed mainly on the catalyst. Olefins proved to be less reactive compared to alkanes, e.g. propene is converted with lower rate than propane, due to the relative low reactivity of the intermediate allyl radical compared to the propyl radical.

It is shown in chapter 6 that Li/MgO catalyst is able to undergo deoxygenation/ reoxygenation cycles. Catalytic activity shown by Li/MgO has a strong correlation to the amount of oxygen that is removable. The number of sites containing removable oxygen that are responsible for the activation of propane was quantified by TGA measurements following independently oxygen removal and CO_2 desorption. It was confirmed that the active sites for radical generation are active oxygen ions created by alkali defects in the magnesia surface. While one such oxygen was consumed, in the absence of gas-phase oxygen, about 70 propane molecules were converted, implying a mechanism in which propane molecules are activated on the catalyst resulting in propyl radicals that are released to the gas phase where they undergo chain propagation reactions with a chain length of ~70.

The catalyst shows a characteristic radical controlling function as it not only generates but also quenches radicals. At low propane partial pressures (0.1 bar), the surface to volume ratio of the catalytic reactor does not influence the chain length in the propagation step. However, at higher propane partial pressures (>0.3 bar), that are favorable to extensive gas phase reactions, the catalyst has also a role to provide for quenching and chain termination, thus affecting activity and selectivity.

The information from this thesis allows us to set the criteria for a successful olefin production process, as follows. The catalyst should be a basic material with one type of active oxygen that is able to split a carbon-hydrogen bond of the alkanes, but it does not stabilize the resulted hydrocarbon fragment on the surface. The catalyst should be used in a reactor where the advantages of gas phase reactions can be utilized (fluidized bed for example). Operation in autothermal mode is possible. Propane concentration should preferably be high and a low oxygen concentration maintained over the whole reactor by e.g. distributed oxygen. Kinetic modeling is required in the future for feasibility evaluation and further study on influencing radical reactions in the gas phase in order to improve the selectivity.

9.1 Samenvatting

Olefinen zijn de meest belangrijke bouwstenen in de moderne petrochemische industrie. Propeen en etheen zijn de ruwe chemicaliën voor polypropyleen en polyethyleen en de vraag hiernaar neemt nog steeds toe. De meerderheid van de olefine capaciteit van vandaag wordt geleverd door stoom kraken en katalytisch kraken (FCC). Terwijl deze processen optimaal zijn ontwikkeld, blijkt productie toename gelimiteerd door beperkingen in het gebruik van de bijproducten. Propeen wordt geproduceerd als bijproduct in zowel stoom kraken als katalytisch kraken, dus aan de sterke toename in de vraag naar propyleen kan alleen worden voldaan door specifiek hiervoor ontwikkelde processen. Een van deze processen is de katalytische propaan dehydrogenering, deze heeft echter grote nadelen: thermodynamische limitering en koolafzetting op de katalysator, en dus een korte katalysator levensduur.

Dehydrogenering in de aanwezigheid van zuurstof kan helpen om de beperkingen van de katalytische dehydrogenering te overwinnen. Oxidatieve dehydrogenering is algemeen herkend als nieuwe alternatieve methode voor de productie van olefinen en het wordt uitgebreid bestudeerd. Ondanks de onderzoeksprestaties in zowel de academische als de industriële wereld zijn commerciële toepassingen vandaag de dag nog niet gerealiseerd, voornamelijk door de lage opbrengst aan olefinen (maximum haalbare tot nu toe: 30%) over de gebruikte katalysatoren. Overgangsmetaal oxide katalysatoren met een uitgesproken redox karakter toonden een hoge tendens om de olefinen productie te beperken door daarop volgende volle oxidatie (verbranding). Daarentegen vertonen de op magnesia gebaseerde katalysatoren, gepromoteerd met alkalichloride een hoge activiteit en selectiviteit in de oxidatieve ethaan dehydrogenering. Dit type katalysator doet het ook goed in de omzetting van LPG naar olefinen.

In dit proefschrift, werden alkali gepromoteerde magnesia katalysatoren bestudeerd in de oxidatieve dehydrogenering van lagere alkanen naar olefinen. Het belang van ons onderzoek komt voornamelijk uit de toenemende wereldwijde vraag naar olefinen met name propyleen.

Opbrengsten van olefinen van meer dan 50% werden bereikt over een Li/Cl/Dy/MgO met een product spectrum vergelijkbaar met die van stoom kraken. Er zijn echter grote voordelen ten opzichte van stoom kraken: het aandeel van propyleen is hoger in de olefine opbrengst, de reactie temperatuur is lager en de reactiewarmte wordt intern opgewekt.

Van de drie geteste dragers (magnesia, zirconia en niobia) bleek alleen magnesia actief en selectief te zijn. Van het grote aantal toevoegingen die worden geclaimd in de literatuur bleek alleen Li de essentiële promotor van magnesia te zijn. Toevoeging van chloride had alleen een kleine toename in de selectiviteit tot gevolg, maar ook de onstabiliteit van de katalysator nam toe. Daarom wordt het gebruik van een Cl vrije katalysator aanbevolen. De katalytische prestaties van de katalysatoren vertoonden een optimum met zowel de Li als de Cl hoeveelheid op de katalysatoren. Terwijl de toename van activiteit met variërende Cl hoeveelheid kon worden verklaard door een toename van het katalysator oppervlak, bleek de toename van activiteit en selectiviteit met de toevoeging van Li alleen verklaard te kunnen worden door een promotie effect van Li op het magnesia oppervlak, waarbij Li in de actieve plaats of in het ontstaan daarvan deelneemt. Toevoeging van dysprosia limiteerde de hoeveelheid Li door de vorming van een mengoxide en veroorzaakte daarmee een verlaging van activiteit.

De kinetiek van de reactie impliceerde een reactie mechanisme dat radicaal initiatie reacties op het katalysator oppervlak en radicaal propagatie reacties in de gasfase omvatte. Radicaal chemie in de gasfase bepaald grotendeels het waargenomen selectiviteitspatroon. De trend in de omzetting van ethaan, propaan en butaan bevestigt dat activering door waterstof abstractie van een alkaan molecuul de snelheidsbepalende stap is. Boven een partiële druk van 0.3 bar van propaan nemen homogeen geïnitieerde reacties ook deel aan de reactie. De aanwezigheid van gasfase zuurstof is cruciaal. Zuurstof reageert met de aanwezige radicalen in de gasfase en dit heeft tot gevolg dat meer radicalen gevormd worden, welke ook veel reactiever zijn. De tweede functie van zuurstof is dat de katalytische actieve site wordt geregenereerd. Regeneratie van de actieve site behoeft geen verwijdering van zuurstof door dehydroxylatie, maar in plaats daarvan wordt de waterstof van de oppervlakte OH^- groep verwijderd met behulp van gasfase zuurstof.

Koolstofdioxide verlaagt de activiteit van de katalystor, doordat het de actieve site blokkeert door de vorming van inactieve oppervlakte carbonaat groepen. Volgreacties van propeen geven voornamelijk koolstof oxides en verlopen voornamelijk over de katalysator. Olefinen bleken minder reactief te zijn dan de overeenkomstige alkanen, bijvoorbeeld propeen wordt met een lagere snelheid omgezet dan propaan vanwege de relatieve stabiliteit van het allyl radicaal als intermediair in vergelijking tot het propyl radicaal.

In hoofdstuk 6 is getoond dat Li/MgO katalysatoren deoxygenering / reoxygenering cycli kunnen ondergaan. De katalytische activiteit waargenomen met Li/MgO vertoonde een sterke correlatie met de hoeveelheid zuurstof welke verwijderd kan worden. Het aantal sites welke zuurstof bevatten dat verwijderd kan worden en die verantwoordelijk zijn voor de activering van propaan werden kwantitatief bepaald met behulp van TGA metingen van zuurstof opname en CO_2 desorptie. Deze metingen bevestigden dat de actieve sites voor de generatie van radicalen actieve zuurstof ionen waren welke gecreëerd werden door alkali defecten in het magnesia-oppervlak. Een zo'n zuurstof ion is in staat om ongeveer 70 moleculen propaan om te zetten. Dit wijst op een mechanisme waarbij propaan moleculen geactiveerd worden op de katalysator wat resulteert in propyl radicalen, die worden losgelaten in de gasfase waar ze keten propagatie reacties met een ketenlengte van ~70 ondergaan.

De katalysator vertoont een karakteristieke controlerende functie op de radicalen, omdat het niet alleen de radicalen genereert maar ze ook weer vernietigd. Bij een lage propaan partiële druk (0.1 bar) bleek de oppervlakte tot volume verhouding van de katalytische reactor de keten lengte van de propagatie stap niet te beïnvloeden. Echter bij hogere partiële drukken van propaan (>0.3 bar), waardoor gasfase reacties gestimuleerd worden, heeft de katalysator ook de rol te vervullen van radicaalvanger en ketenstopper en zo dus de activiteit en selectiviteit te beïnvloeden.

De informatie beschreven in dit proefschrift geeft ons de mogelijkheid om een set criteria op te stellen voor een succesvol olefinen productie proces en wel als volgt. De katalysator zou een basisch materiaal moeten zijn met een type actieve zuurstof welke in staat is om een koolstof-waterstof binding te breken van de koolwaterstoffen, maar het fragment niet te stabiliseren. De katalysator zou gebruikt moeten worden in een reactor type waarbij de voordelen van de gasfase ten volste kunnen worden benut (bijvoorbeeld in een fluidized bed). Werken onder autotherme condities is mogelijk. De propaanconcentratie zou bij voorkeur hoog moeten zijn en een lage zuurstof concentratie over de gehele reactor zou behouden moeten worden door bijvoorbeeld, gedistribueerd zuurstof.

9.2 Összefoglaló

Az olefinek a modern petrolkémiai ipar legfontosabb alapanyagai. A polietilén és polipropilén gyártásának alapanyaga etén és propén, a felhasználási szükséglet pedig folyamatosan nő. A világ mai olefintermelésének túlnyomó hányadát gőzkrakkolással és fluidágyas katalitikus krakkolással (FCC) állítják elő. Habár e folyamatoknak fejlett a technológiája, az olefinkapacitás növelése korlátozva van a melléktermékek felhasználása miatt. A propén melléktermékként termelődik, úgy a gőzkrakkolásnál, mint az FCC-nél, így tehát az erősen növekvő propénigényt csak célirányos folyamattal lehet kielégíteni. Ilyen célirányos folyamat lehetne a direkt katalitikus dehidrogénezés, de ennek súlyos hátrányai a termodinamikai (egyensúlyi) korlátozottság és kormozódás miatti rövid katalizátor-élettartam.

Elméletileg, oxigén jelenlétében történő dehidrogénezés képes feloldani a termodinamikai korlátozottságot. Az *oxidatív dehidrogénezés*, mint egy lehetséges új olefin előállítási módszer lett felismerve. A kutatási erőfeszítések ellenére, ipari alkalmazása mindeddig nem valósult meg, ami főleg a használt katalizátorokon elért alacsony olefin hozamnak volt köszönhető (eddig elért maximális hozam: 30%). A gyakran használt, kiemelt redox tulajdonsággal rendelkező átmenetifém-oxid katalizátorok hajlamosak teljesen oxidálni az előállított olefint egy második reakciólépésben. Ezzel ellentétben a magnézium-oxid alapú alkáli-kloriddal módosított katalizátorok magas aktivitást és szelektivitást mutattak az etán oxidatív dehidrogénezése során. Hasonlóképpen, ezek katalizátorok az cseppfolyósított petróleum gáz (LPG) olefinekké történő konverziója során is jól szerepeltek.

Az itt olvasható tézis az alacsony szénatomszámú alkánok olefinekké való oxidatív konverzióját tanulmányozza alkálifém promotorral módosított magnéziumoxid katalizátorokon. A kutatást az egyre növekvő olefinigény (főleg propénigény) motiválta.

Li-Cl-Dy-MgO katalizátoron 50%-os olefinhozamot sikerült elérni; a termékek spektruma hasonló volt a gőzkrakkoláséhoz. A gőzkrakkoláshoz képest a folyamatnak a következő előnyei vannak: a propénhozam nagyobb, a hőmérséklet alacsonyabb, és a reakcióhoz szükséges hő belsőleg van generálva.

A három tesztelt hordozó közül (magnézium-oxid, cirkónium-oxid és nióbium-oxid) csak a magnézium-oxid mutatott elegendő aktivitást és szelektivitást. A szabadalmi irodalomban feltüntetett adalékok sokaságából csak a lítium bizonyult lényeges magnézium-oxid módosítónak. Klorid hozzáadása növeli a szelektivitást egy kissé, azonban a katalizátor instabilitása is jelentősen megnő, ezért a klórmentes katalizátorok használata ajánlott. A katalizátorok teljesítménye maximumot mutatott, úgy a lítium-, mint a klórtartalom függvényében. Amíg a klór aktivitás-növelő hatása magyarázható a katalizátor felületének - kloridhozzáadás okozta - növekedésével, addig a lítium aktivitás- és szelektivitás-javító hatása csak a lítiumnak a magnéziumoxid felületét módosító hatásával lesz érthető. Tehát a lítium vagy része az aktív centrumnak, vagy részt vesz annak létrehozásában. Diszprózium-oxid hozzáadása csökkenti a hozzáférhető lítium mennyiségét egy lítium-diszprózium vegyes oxid keletkezése révén, ezáltal csökkentve az aktivitást.

A reakció kinetikájának tanulmányozása egy olyan mechanizmushoz vezetett, amely a katalizátor felületén történő gyökös iniciálással kezdődik, és gyökös láncreakcióval folytatódik a gázfázisban. A reakciótermékek spektrumát többnyire a gázfázisú gyökös reakciók határozzák meg. Az etán, propán és bután konverziója összehasonlítva igazolja hogy a hidrogén leszakítása az alkánmolekulából a sebesség-meghatározó lépés. Amikor a propán parciális nyomása 0,3 bar fölött volt a gázfázisú iniciálás is jelen volt. A gázfázisú oxigén jelenléte nélkülözhetetlen. Oxigén, a jelenlevő gyökökkel reagálva, még több, még reaktívabb gyököt produkál, és ez az aktivitást jelentősen megnöveli. Az oxigén második funkciója a katalitikus centrum regenerálása. Ahhoz hogy az aktív centrumon levő hidrogénatomot eltávolítsuk, nem szükséges hogy az oxigén atom dehidroxilezés útján eltávozzon, ugyanis a gázfázisú oxigén segít eltávolítani a hidrogént.

A szén-dioxid erős inhibitora a katalitikus aktivitásnak azáltal, hogy az aktív centrumot blokkolja, miközben inaktív felületi karbonátot hoz létre.

A propén konszekutív reakciója szinte kizárólag szén-monoxidot és szén-dioxidot eredményez és főleg a katalizátor felületén megy végbe. Az olefinek az alkánoknál kevésbé bizonyultak reaktívnak; a propén kisebb sebességgel reagált, mint a propán, a köztes allil gyök propil gyökhöz viszonyított alacsony reaktivitása miatt.

A 6. fejezetben kimutattuk, hogy a Li/MgO katalizátor redukálható (az oxigén a katalizátor felületéből eltávolítható) és újraoxidálható. A Li/MgO katalizátor aktivitása összefüggésbe hozható az eltávolítatható oxigén mennyiségével. Az eltávolítható oxigént tartalmazó, a propán aktiválásáért felelős aktív centrumok számát gravimetriás mérésekkel határoztuk meg, külön-külön követve úgy az oxigén eltávolítását, mint a szén-dioxid deszorpcióját. Bebizonyosodott, hogy a szabadgyökök generálásáért felelős aktív centrumok nem mások, mint az alkálifémnek a magnéziumoxid felületén okozott hibái következtében létrejött oxigénionok. Egy ilyen aktív oxigén felhasználásakor - gázfázisú oxigén hiányában - 70 propán molekula aktiválódik, egy olyan mechanizmusra mutatva, amelyben a propánmolekulák a katalizátor felületén aktiválódnak propilgyököket hozva létre. Ezek a gázfázisba szabadulva 70-es lánchosszúságú gyökös láncreakciót hoznak létre.

A katalizátor egy jellegzetes szabadgyök-kontrolláló hatást mutat, ugyanis nemcsak generál, hanem ki is olt szabadgyököket. Amikor a propán parciális nyomása alacsony (0,1 bar) a reaktorban található felület nem befolyásolja a láncreakció hosszúságát. Amikor azonban a propán parciális nyomása magas (>0,3 bar) a katalizátornak szabadgyök kioltó szerepe is van, ezáltal hatást gyakorol az aktivitásra és szelektivitásra.

Az itt közölt munkában található információ elősegíti egy sikeres olefingyártó folyamat kritériumainak összeállítását. A katalizátornak egy bázikus jellegű anyagnak kell lennie, és csak egy fajta aktív oxigénnel rendelkezhet, mely képes elszakítani az alkánokban a szén-hidrogén kötést, de nem stabilizálja felületén a keletkezett szénhidrogéngyököt. A katalizátort egy olyan reaktorban kell alkalmazni, amelyben a gázfázisú reakciók előnyeit ki lehet használni (például fluidizált ágy). Autótermál módon való működtetés is lehetséges. Kedvezőbb, ha a propánkoncentráció magas, és ha alacsony oxigénkoncentrációt tartunk fenn a reaktor egészében, például szétosztás útján.

A továbbiakban kinetikai modellezésre lesz szükség, hogy egy ilyen folyamat gazdaságosságát közelebbről tudjuk vizsgálni. A gáz fázisban zajló gyökös reakciók befolyásolását célzó kutatások a jövőben lehetővé tehetik a szelektivitás kedvező eltolását.

9.3 Rezumat

Alchenele reprezintă clasa cea mai importantă din industria petrochimică modernă având ca reprezentanţi mai importanţi propena şi etena, componenţi ce stau la baza obţinerii polipropilenelor şi polietilenelor. Până în prezent necesarul de alchene a fost acoperit prin procese de tipul, reformare cu aburi sau cracare catalitică în strat fluidizat, procese ce se văd limitate în obţinerea acestei clase. Ca şi alţi produşi, propena poate fi obţinută atât prin reformare cu aburi cât şi cracare catalitică, dar odată cu creşterea necesarului de propenă în vederea obţinerii de polimeri, s-a văzut necesitatea suplimentării acesteia prin alte tipuri de procese. Un astfel de proces este dehidrogenarea catalitică a propanului, proces ce prezintă unele dezavantaje precum: limitarea termodinamică şi formarea de cox ce duce la scurtarea vieţii catalizatorului.

Ideea de baza în trecerea acestor bariere a fost cea de adăugare de oxigen, factor ce poate favoriza reacţia de dehidrogenare. Astfel, *dehidrogenarea oxidativă* a fost recunoscută ca o alternativă pentru producerea de alchene fiind pe deplin studiat în ultimii ani. În ciuda investigaţiilor făcute atât în domeniul cercetării cât şi în domeniul industrial, aplicarea acestui proces nu a fost făcută încă, datorită randamentului mic de alchene produse (maximul obţinut de aproximativ 30 %). Caracterul redox pronunţat al catalizatorilor bazaţi pe oxizii metalelor tranziţionale limitează procesul de producere a alchenelor datorită oxidării totale a acestora. În contrast cu aceştia, catalizatorii bazaţi pe oxid de magneziu promotaţi cu cloruri ai metalelor alcaline prezintă activitate şi selectivitate ridicată cu precădere în dehidrogenarea oxidativă a etanului, dar şi în obţinerea altor alchene sau a gazelor petroliere lichefiate.

În lucrarea de fată sunt prezentate studii de transformare a alcanilor inferiori în alchene, pe catalizatori bazaţi pe oxid de magneziu. Atâta vreme cât necesitatea de polimeri este în continuă creştere şi în special cea de polipropilene, s-a văzut necesară realizarea unor astfel de studii ce au în vedere suplimentarea de alchene dar mai ales de propenă.

Cu aceeaşi plajă de produşi ca şi în cracarea cu aburi, catalizatorul de tipul Li/Cl/Dy/MgO formează alchene cu un randament de peste 50%, dar spre deosebire de cracarea cu aburi randamentul de propenă este mai ridicat, temperatura de reacţie este inferioară cracării cu aburi şi în plus procesul poate decurge în regim autoterm.

Din cele trei suporturi studiaţi (magneziu, zirconiu şi niobiu), cel cu activitate şi selectivitate mai ridicată s-a dovedit a fii suportul de oxid de magneziu. Din multitudinea de aditivi prezentaţi în literatura de patente doar Li s-a arătat a fii promotorul esenţial al acestui oxid. Adaosul de cloruri duce pe de o parte la creşterea selectivităţii, dar pe de altă parte descreşte stabilitatea catalizatorului, recomandându-se astfel utilizarea de catalizatori ce nu conţin clor. S-au studiate performanţele catalizatorilor atât la adaos de litiu cât şi la adaos de clor. Creşterea activităţii datorată creşterii conţinutului de clor poate fi pusă pe seama creşterii suprafeţei specifice. Performanţa ridicată datorită creşterii conţinutului de litiu poate fi explicat numai prin acţiunea de promotare a suprafeţei de oxid de magneziu, prin participarea litiului fie în cadrul situsului catalitic fie la generarea acestuia. Limitarea disponibilităţii litiului la adaos de disprosiu se datorează formării de oxizi micşti ce cauzează descreşterea în activitate.

Cinetica de dehidrogenare oxidativă, în prezenţa oxigenului, expune un mecanism de tip radicalic în care iniţierea reacţiei se realizează la suprafaţa catalizatorului urmând ca propagarea acesteia sa aibă loc în faza gazoasă. Caracterul radicalic al mecanismului determină în mare măsura selectivitatea reacției. Creşterea conversiei în cazul etanului, propanului şi a butanului indică că etapa determinantă de viteză este abstracția unui radical de hidrogen din molecula de alcan. La presiuni parțiale ale propanului mai mari de 0.3 bari reacția este inițiată şi în faza gazoasă adițional față de inițierea pe suprafața catalizatorului. Prezența oxigenului în faza de gaz prezintă două avantaje majore: unul este formarea mai multor radicali în faza de gaz, ce pot iniția reacția, decât în faza inițială, iar cel de-al doilea de regenerare a situsului catalitic. Regenerarea situsului catalitic nu se realizează prin îndepărtarea oxigenului prin dehidroxilare, ci mai degrabă grupările HO^- sunt decompuse prin reacția acestora cu oxigenul din faza de gaz.

Dioxidul de carbon format în reacție, descreşte activitatea catalitică prin formare de carbonați inerți ce blochează situsului catalitic. Reacțiile consecutive ale propenei produc oxizi de carbon cu precădere la suprafața catalizatorului. Fată de alcani, alchenele s-au arătat mai puțin reactive datorita formării de radicali mai puțin reactivi; propena este convertită în proporție mult mai mică decât propanul datorita stabilității mai ridicate a radicalului alilic față de radicalul propil.

În capitolul 6 se prezintă capacitatea catalizatorului Li/MgO de realizare a ciclului deoxidare/ reoxidare. Activitatea catalizatorului este corelată cu capacitatea de îndepărtare a oxigenului (deoxidare). Numărul de situsuri ce conțin oxigen activ, responsabili de activarea propanului, a fost determinat prin metode gravimetrice, urmărindu-se atât prin evoluția oxigenului mobil cât şi prin desorbția de dioxid de carbon. S-a confirmat ca fiind responsabili de generarea radicalilor, oxigenii activi prezenți la suprafața oxidului de magneziu. Când un astfel de oxigen este consumat – în absența oxigenului gazos – 70 de molecule de propan sunt transformați, implicând un mecanism în care moleculele de propan sunt transformate în radicali propil pe suprafața catalizatorului, ce sunt ulterior eliberați în faza de gaz. Aceştia inițiază reacția în faza de gaz, propagând mai apoi cu un lanț de lungime de aprox. ~70. La presiuni parțiale joase ale propanului (0,1 bar) s-a arătat că raportul dintre suprafața specifică a catalizatorului nu influențează lungimea lanțului de propagare în faza gazoasă. În contrast cu acestea, la presiuni parțiale ridicate (>0,3 bar) când reacțiile în faza de gaz sunt favorizate, catalizatorul are proprietatea nu numai de inițiere, dar atât stingere cât şi terminare a reacției influențând în acest fel activitatea şi selectivitatea.

Pe baza datelor din această lucrare s-au emis atât criterii de selectare a catalizatorilor cât şi criterii de producere de alchene. Astfel un prim criteriu este cel de alegerea catalizatorului, acesta trebuie sa fie de tip bazic, să aibă un singur tip de oxigen activ care să poată fi capabil de ruperea legăturii C-H din hidrocarburi saturate şi totodată să nu aibă posibilitatea stabilizării radicalilor formați. Catalizatorul poate fi utilizat în reactoare ce dispun spații pentru reacțiile în faza de gaz (de exemplu: reactor în strat fluidizat). Menținerea unei concentrații ridicate de propan şi concentrații scăzute în oxigen pe toată lungimea reactorului ar fi de dorit (de exemplu prin redistribuirea acestuia în concentrații mici în lungul reactorului). Operarea poate fi condus în regim autoterm.

În viitor va fi nevoie de modelare cinetică, ca evaluarea economică a unui proces bazat pe catalizatoarele studiate aici, să fie posibil. Studiul influențării reacțiilor radicalice în faza de gaz ne poate aduce posibilitatea de îmbunătățire a selectivității.

Curriculum Vitae

László Leveles was born on 1st of April 1972 in Csíkkarcfalva/Cârța, Romania. He has completed his primary education at the General School of Csíkkarcfalva/Cârța. Afterwards, he went to the Márton Áron Gymnasium in Csíkszereda/Miercurea-Ciuc, where he was admitted to the biology-chemistry class. After two years he changed to the industrial chemistry class from which he majored in 1990. From 1990 to 1995 he studied at the Faculty of Chemistry and Chemical Engineering of the Babeş-Bolyai University in Kolozsvár/Cluj-Napoca, specialization chemistry. His interests lead him to Assoc. Prof. Dr. Cs. Muzsnay, where he started his scientific work in the fields of theoretical-chemistry, electrochemistry, and electroanalytical chemistry, the results of which he presented with success on many scientific events. After graduation he followed a one-year postgraduate study on applied electrochemistry at the physical-chemistry department of the same university led by Prof. Dr. doc. L. Oniciu. From 1996 to 1997 he was interim trainee teaching assistant, while he also continued research work on development of electroanalytical techniques at the Babeş-Bolyai University.

From the end of 1997 he started working as a PhD student at the University of Twente in the group of Prof. Dr. J.A. Lercher that later he continued under the guidance of Prof. Dr. Ir. L. Lefferts. The work carried out on the study of oxidative dehydrogenation and oxidative conversion of alkanes to olefins over alkali promoted magnesia is described in this thesis. At the NCCC III his work was awarded with the KNCV Poster Award.

Publications

L. Leveles, K. Seshan, J. A. Lercher and L. Lefferts, Factors that influence catalytic activation, hetero-homogeneous reactions and the selectivity of C-C bond *vs.* C-H bond scission during the oxidative conversion of lower alkanes to olefins, in preparation;

L. Leveles, K. Seshan, J. A. Lercher and L. Lefferts, Kinetics and Mechanism of the Oxidative Conversion of Propane over Lithium Promoted Magnesia Catalyst, submitted to *J. Catal.*;

L. Leveles, St. Fuchs, K. Seshan, J. A. Lercher and L. Lefferts, Oxidative conversion of light alkanes to olefins over alkali promoted oxide catalysts, *Applied Catalysis A: General*, in press;

St. Fuchs, L. Leveles, K. Seshan, L. Lefferts, A. Lemonidou, and J. A. Lercher, Oxidative dehydrogenation and cracking of alkanes over novel mixed oxides, *Topics in Catalysis*, 2001, 15(2), pp 169-174;

*Cs. Muzsnay, L. Leveles, A. Rubleczky: Magnetic field effect on practically non-polarizing electrochemical cells (in Romanian), *Analele Univ. Oradea*, 1998, Fasc. CHIM., pp 161-166;

*Cs. Muzsnay, L. Leveles, I. Török, Activation energy of electric conductivity. Aqueous solutions of bromide and iodide of bivalent cations (in Romanian), *Analele Univ. Oradea*, 1998, Fasc. CHIM., in press;

Cs. Muzsnay, L. Leveles: Complex equilibrium structure of water VIII. Temperature dependence of the main thermodynamic functions in the M2i model (in Romanian); Analele Univ. Craiova,* 1995, Ser. Chim., Nr. Spec., Vol.2, pp 233-236.

---

* not included in this thesis

Selected presentations

L. Leveles, St. Fuchs, K. Seshan, L. Lefferts and J.A. Lercher, Novel catalysts for oxidative conversion of lower alkanes to olefins, Netherlands Catalysis and Chemistry Conference NCCC III, March 4-6, 2002, Noordwijkerhout, The Netherlands (poster II-12-16, *winner of KNCV Poster Award*, pp 264)

L. Leveles, St. Fuchs, K. Seshan, L. Lefferts and J.A. Lercher, Novel catalysts for oxidative conversion of lower alkanes to olefins, 4th World Congress on Oxidation Catalysis, September 16-21, 2001, Berlin, Germany (poster 2a.19)

L. Leveles, St. Fuchs, K. Seshan, J.A. Lercher and L. Lefferts, Oxidative conversion of light alkanes to olefins over alkali promoted oxide catalysts, EUROPACAT V., the Fifth European Congress on Catalysis, September 1-7, 2001, Limerick, Ireland, (*oral presentation* 5-O-23)

L. Leveles, St. Fuchs, K. Seshan, J.A. Lercher and L. Lefferts, Oxidative Conversion of Alkanes to Olefins over Magnesia Based Catalysts, Netherlands' Catalysis and Chemistry Conference, NCCC II March 5-7 2001 Noordwijkerhout, The Netherlands, (*oral presentation*, pp 109)

L. Leveles, St. Fuchs, K. Seshan, J.A. Lercher and L. Lefferts, Magnesia based catalysts for oxidative production of low olefins, Netherlands' Catalysis and Chemistry Conference, NCCC 2000 January 2000, Lunteren, The Netherlands (poster)

[*]Cs.Muzsnay, T.Nagy and L.Leveles: New possibility of standardization in volumetry III. Precipitation titrations with electrometric end-point indications, Deauville CONFERENCE 97: 5th Symposium on Analytical Sciences (SAS), Nice, France, June 1997 (poster p502, pp 54);

[*]Cs. Muzsnay, L. Leveles: Complex Equilibrium Structure of Heavy Water IV. Numerical Evaluation of the M_{2i} Model Using Potentiometric Data; 47-th Annual Meeting of ISE, Veszprém-Balatonfüred, Hungary; September 1996. (poster P5-1b).

[*]Cs. Muzsnay, L. Leveles: Complex Equilibrium Structure of Water VI. Numerical Evaluation of the Simplified M_{3i} Model In One Single Step; 35-th IUPAC Congress, Istambul, Turkey, 14-19 August, 1995; (p.333).

---

[*] not related with this thesis